The influence of interacting stressors on soft sediment ecosystem function

A thesis

submitted in fulfilment

of the requirements for the degree

of

Doctor of Philosophy in Biological Sciences

at

The University of Waikato

by

Stephanie Mangan

THE UNIVERSITY OF
WAIKATO
Te Whare Wānanga o Waikato

2021

Abstract

Soft sediment intertidal habitats provide valuable ecosystem services to millions of people worldwide yet are under intense anthropogenic pressure. In particular, the intensification of land derived sediment and nutrient delivery has resulted in elevated water column turbidity and nutrient over-enrichment, both of which can diminish ecosystem functionality. Identifying how these stressors interact and influence benthic ecosystems is crucial to understanding the resilience of these valuable habitats and to help manage effectively to prevent shifts towards ecological tipping points. This thesis therefore investigates the response of benthic primary production and biogeochemical cycling to two pervasive stressors; increasing water column turbidity and sediment nutrient enrichment.

Water column turbidity directly restricts the availability of light to microphytobenthos (MPB), a key primary producer in soft sediment intertidal habitats. However, the degree to which turbidity may limit primary production across New Zealand was largely unknown. I recorded light availability at the seafloor over a 9-month period at 22 sites situated within 14 estuaries. Coupled with a global literature compilation of photosynthesis-irradiance curves, the proportion of time MPB were light limited during submergence ranged from a median of 55–100 %. For estuaries close to 100 % light limitation, emerged intertidal areas represent a refuge for MPB production which is vulnerable to sea-level rise. Using hypsometric curves, the intertidal area of my study estuaries was predicted to decrease by 27–94 % under a 1.4 m rise in sea-level. The combination of high light limitation during submergence and large losses of intertidal area will increase vulnerability to the loss of MPB production and the associated ecosystem services, which can push these ecosystems towards tipping points.

Anthropogenic stressors often occur concomitantly, and therefore understanding how differing degrees of water column turbidity may interact with other stressors, such as increasing nutrient enrichment and influence benthic productivity over alternating periods of submergence and emergence were investigated. A field

manipulation study was designed to enrich porewaters at three levels for 20 months, at six sites that spanned a gradient in water column turbidity. While nutrient enrichment had no detectable effect on MPB primary production, water column turbidity had a significant influence, explaining up to 40 % of the variability during tidal submergence, followed by temperature and sediment characteristics. In addition, negative net primary production (NPP) and therefore net heterotrophy for the most turbid estuaries during tidal submergence resulted in an increased reliance on production during emerged periods. This study highlights the prominent role of turbidity over porewater nutrient enrichment in moderating MPB production and supports earlier conclusions of the increasing importance of emerged periods to maintain the health and functioning of coastal habitats.

Soft sediment intertidal habitats are not only hot spots for benthic productivity, but they also play a fundamental role in biogeochemical cycling. The influence of increased nutrient availability on nitrogen and carbon cycling was investigated after 15 and 20 months of nitrogen enrichment. This study highlighted the limited capacity for denitrification, a key process in removing bioavailable nitrogen, to mitigate large increases in nitrogen availability, as evidenced through the consistent rates of net denitrification and reductions in the efficiency at which nitrogen was removed. Denitrification rate was most strongly correlated to carbon supply, trophic status and to a lesser extent, macrofaunal diversity. In addition, analysis of factor-ceiling relationships revealed the vulnerability of estuaries to increasing stressor loads. The appearance of significant nonlinearities with increasing nitrogen enrichment suggests alterations to the interactions of intrinsic dynamics and drivers which can fundamentally alter biogeochemical cycling within soft sediments and increase the likelihood of abrupt non-linear shifts.

Overall, the findings of my thesis demonstrate how the health and functioning of coastal ecosystems can be significantly diminished under increasing anthropogenic stress, and that the vulnerability of coastal ecosystems to the loss of ecosystem functionality will change in the future as global scale stressors intensify.

Preface

The main body of this thesis is comprised of three research chapters (Chapter 2 – 4). Chapters 2 and 3 have been published in peer-reviewed journals and Chapter 4 is in preparation for submission. I assumed responsibility for the field and laboratory work, data analysis and the writing of this thesis. The ideas in this thesis are my own, unless otherwise referenced. All work was produced under the supervision of Professor Conrad Pilditch at the University of Waikato, Dr Andrew Lohrer at the National Institute of Water and Atmospheric Research Ltd. (NIWA) and Professor Simon Thrush at the University of Auckland.

Chapter 2 has been published by Marine Ecology Progress Series (2020) under the title "Shady business: the darkening of estuaries constrains benthic ecosystem function" by S. Mangan, K. R. Bryan, S. F. Thrush, R. V. Gladstone-Gallagher, A.M. Lohrer and C. A. Pilditch. DOI: 10.3354/meps13410

Chapter 3 has been published by the Journal of Marine Science and Engineering (2020) under the title: "Water column turbidity not sediment nutrient enrichment moderates microphytobenthic primary production" by S. Mangan, A.M. Lohrer, S. F. Thrush and C. A. Pilditch. DOI: 10.3390/jmse8100732

Chapter 4 is currently in preparation for publication.

Acknowledgements

There are so many people who have contributed to my thesis and have made my PhD journey so enjoyable, to them all I owe innumerable thanks. First and foremost, I would like to thank Professor Conrad Pilditch. Your enthusiasm and passion for soft sediment ecology is inspiring and infectious. I feel extremely lucky to have had such a supportive and encouraging mentor and I am hugely grateful for the opportunities, guidance and patience you have shown me throughout my PhD. Thank you to my supervisors Dr Drew Lohrer and Professor Simon Thrush for all of the discussions and opportunities you have created. Drew, your expertise and guidance has been invaluable throughout the development of research ideas, and Simon thank you for your insightful feedback and analytical support. To Professor Karin Bryan, thank you for taking the time to share some of your unbelievable MATLAB knowledge with me, your patience and support is greatly appreciated. Thank you to Dr Rebecca Gladstone-Gallagher for your input, guidance and feedback, but also for teaching me everything there is to know about benthic chamber fieldwork and your willingness to always help with any task, you truly made every aspect of my PhD so much easier. And to Dr Joanne Ellis, thank you for your advice, feedback and help with my statistical analysis.

So much of this work would not have been possible without such a supportive technical team both in the field and in the lab. Professor Ian Hawes, Dean Sandwell, Bex Gibson, Peter Jarman, Grant Tempero, Lee Laboyrie and Warrick Powrie, thank you for your technical assistance and sharing your expertise, it is very much appreciated. To Sarah Hailes, thank you for taking the time to teach me how to ID macrofauna, you made such a challenging prospect so enjoyable. Thank you to Cheryl Ward for making thesis formatting so painless. To all of my fieldwork volunteers, thank you for making it so much fun, working in all weather conditions and for helping me core nearly 13,000 holes! A special mention to my regulars: Galilee Miles, Rebecca Gladstone-Gallagher, Bex Gibson, Alice Morrison, Roger Colquhoun, Chris Dixon, Vera Rullens, Georgina Flowers, Kit Squires, Kate Rodgers, Emily Douglas, Grady Peterson and Jack Hamilton.

A big thank you to all my colleagues in the benthic ecology team and the wider coastal marine group. Entering such a welcoming and friendly group made moving 18,000 km a whole lot easier. A special mention to Bérengère, Vera, Emily, Rebecca, Tarn, Georgina, Kit, Kate, Peter, Erik and Jon for the many laughs and tea breaks. Thank you to my office mates, Dr Emily Douglas, Kate Rodgers and Steph Watson, for sharing your knowledge and bringing a welcome distraction when needed, it has been so much fun. Thank you to Professor David Schiel and Mareike Babuder for hosting me during my final few months, providing some much needed sanity and welcoming me into the MERG group.

I would also like to thank Dr Ceri Lewis, if it wasn't for your ardent support, encouragement and enthusiastic passion for marine biology that persuaded me to complete a masters I'm not sure I'd be here today. I will always be so grateful.

To my parents, Marina and John, my many years at university would not have been possible without your unconditional love, generosity, support and hard work. Thank you for always telling me to follow my dreams and then doing everything possible to make sure that was realised, I am the luckiest person in the world. To my sisters, Kim and Laura, thank you for being my role models, my best friends and cheerleaders. To my nan, Ruby, thank you for my many care packages (including an endless supply of tea), supportive skypes and encouraging words, you are the best. To my best friend and partner Andy, I am so lucky that I could share this journey with you. Thank you for being everything I needed and more.

I would like to thank the Sustainable Seas Science Challenge, Dynamic Seas Program, Tipping Points project (4.2.1), funded by the Ministry of Business, Innovation and Employment (C01X1515) for supporting me throughout this PhD project. Attendance to an oversees conference was made possible with support from the New Zealand Marine Sciences Society First Overseas Conference Travel Fund. I would also like to thank Dr Joanna Norkko, Professor Alf Norkko and Dr Johanna Gammal for facilitating my visit and hosting me at the Tvärminne Zoological Station, University of Helsinki, Finland.

Table of Contents

List of Figures

List of Tables

Chapter One: General Introduction

1.1 Background

Coastal ecosystems are ecologically, economically, and culturally important. In particular, soft sediment habitats which are characterised by interstitial complexity and high light availability are global hotspots for primary and secondary productivity, nutrient cycling and the filtering of terrestrial derived sediments (Levin et al., 2001). The importance of these habitats is therefore often derived from processes within the benthos, where biological interactions and biogeochemical transformations drive dynamic exchanges of nutrients, mass and energy (Griffiths et al., 2017). The ecosystem functions provided culminate into human centric benefits, often termed ecosystem services, which include, but are not limited to, food provision, water filtration, climate regulation and shoreline protection (Snelgrove et al., 2014).

The diversity and importance of the services provided has contributed to the substantial development of human populations in coastal areas, and the consequential increase in anthropogenic pressures, such as nutrient and sediment loading, habitat modification, chemical contamination and intense fishing activity (Airoldi and Beck, 2007, Halpern et al., 2008). Anthropogenic impacts additionally extend to global scale stressors, which include global warming, increases in the intensity and severity of storm events and sea level rise (Seneviratne et al., 2012). Both local and global scale stressors interact, cumulatively degrading the health and functioning of coastal habitats and are therefore threatening the continued delivery of the ecosystem functions and services upon which humanity relies.

Estuarine ecosystems are particularly susceptible to multiple pressures, being the intermediately between terrestrial, freshwater and marine ecosystems. Globally, two of the most pervasive pressures within estuarine environments are increases in land-derived sediment and nutrient inputs, both of which can alter physical, biological and biogeochemical properties and processes (Nixon, 1995, Levin et al., 2001, Valiela and Bowen, 2002). Despite the relatively recent arrival of humans

(ca. 700–800 years ago) (McWethy et al., 2010), New Zealand is no exception to these prevalent pressures. For example, the recent expansion and intensification of agriculture and coastal development (Swales et al., 2002, Thrush et al., 2004, Moller et al., 2008) has resulted in an estimated 200 million tons of soil being lost from the land and transported to the oceans each year, a contribution of up to 2 % of total global sediment delivery (Hicks et al., 2011). This is coupled with New Zealand having the highest percentage increase in nitrogen (N) balance of any OECD (Organisation for Economic Co-operation and Development) country, with an estimated net input of 680 000 tonnes of N per year (OECD, 2020). Both sediment and nutrient inputs are likely to continue to increase, which will be exacerbated by increases in the frequency and intensity of storm events under global climatic change (Seneviratne et al., 2012, Hewitt et al., 2016).

Consistently high sedimentation rates have the potential to alter physical, chemical and biological properties of both the water column and the benthos. In the short-term, increases in suspended sediment concentrations increase the attenuation of light through the water column (i.e. elevating turbidity), reducing the availability of light for benthic phototrophs (Cloern, 1987). In addition, fine sediments can directly interfere with suspension feeding benthic fauna, reducing both physiological condition and recruitment (Ellis et al., 2002, Hewitt and Norkko, 2007). In the long-term, the continued resuspension and deposition of fine sediments (grain size <63 μm) can result in persistently elevated water column turbidity and increases in sediment mud content. This can further alter sediment properties, influencing permeability and therefore affecting solute and particle transport and thus local biogeochemistry (Billerbeck et al., 2007). While our understanding of the influence of increasing mud content on benthic ecosystem functioning has increased considerably, it is still largely unknown what degree of water column turbidity persists across New Zealand's coastal habitats and how this is influencing the dominant primary producers and thus ecosystem functioning.

Increased sedimentation often occurs concomitantly with increased nutrient inputs. In particular, an increase in N availability can fuel increases in pelagic production, further increasing the attenuation of light to the benthos (Rabalais et al., 2005). Any reductions in benthic productivity reduces the availability of labile carbon for secondary consumers, while increases in phyto-detritus can increase organic loading and thus carbon decomposition and oxygen consumption (Kemp et al., 1990). In addition, changes in the ability to process and remove N can result in an increase in the amount of bioavailable N recycled back to the water column, further fuelling pelagic production (Nielsen et al., 2002). Ultimately, if N enrichment exceeds the capacity for assimilated-enhanced benthic production and/or removal (via denitrification), then a system can be push beyond a tipping point whereby coastal eutrophication persists (Cooper and Brush, 1993, Scheffer and Carpenter, 2003). A state of eutrophication not only shifts a system to pelagic dominated primary production, but can also result in oxygen depletion, global acidification and the loss of biodiversity (Gruber and Galloway, 2008). While these alterations to biogeochemical cycling have been quantified in heavily impacted and eutrophic systems, the response of low-nutrient systems characterised by tight benthic-pelagic coupling to increasing N enrichment is less well known (Vieillard et al., 2020). The aim of this thesis was therefore to investigate the impacts of sedimentation and nutrient inputs on benthic primary productivity and nutrient processing within multiple New Zealand estuaries.

1.1.1 Benthic primary production

Coastal regions are often dominated by benthic primary production owing to sufficient light availability in shallow waters (Ackleson, 2003). This includes vascular plants (such as seagrass), macroalgae and microalgae or microphytobenthos, hereafter MPB. MPB communities are a combination of cyanobacteria, unicellular eukaryotic algae and euglenoids which inhabit the sediment surface (MacIntyre et al., 1996). MPB are integral constituents of unvegetated habitats, substantially contributing to total marine carbon fixation (Borum and Sand-Jensen, 1996) and through the supply of high-quality labile

carbon, often underpin coastal food webs (Christianen et al., 2017). In addition to their central role as a food source, MPB alter biogeochemical gradients within the sediment and thus can alter the transformation and recycling of nutrients (Sundbäck et al., 2004, Hochard et al., 2010). MPB additionally enhance sediment stability through the secretion of extracellular polymeric substances, reducing erosion and the suspension of sediments as well as providing an additional source of organic material to bacteria (Tobias et al., 2003, Tolhurst et al., 2008). MPB are therefore integral to regulating ecosystem service delivery, and consequently any reductions in MPB productivity will have cascading implications for entire coastal ecosystems.

Productivity by MPB is primarily regulated by the availability of light, temperature, nutrients and hydrodynamic conditions (Kromkamp et al., 1995, Perkins et al., 2001). Of particular importance during submerged tidal periods is light availability (Ackleson, 2003, Gattuso et al., 2006). In coastal waters, the underwater light field is a product of water depth, properties of the ocean floor and suspended material. However, temporal variability of light is principally a consequence of the latter (Kirk, 1994). While phytoplankton biomass can contribute to increased water column turbidity, up to 80 % of light variations are accounted for by suspended sediments (Anthony et al., 2004). High turbidity restricts the amount of light reaching the seafloor and thus can directly diminish benthic primary production. Not only does this influence food web dynamics and global carbon budgets (Duarte et al., 2005) but the consequential reduced uptake of nutrients and reductions in sediment oxygenation can alter sediment biogeochemical processes such as microbial nitrification (Thornton et al., 1999, Longphuirt et al., 2009) as well as alter the distributions of functionally important macrofauna species (Van der Wal et al., 2008). Furthermore, high turbidity is often positively correlated with sediment mud content, which in turn has been linked to a reduction in MPB biomass (measured as sediment chlorophyll *a* content) (Cahoon et al., 1999) and reduced gross primary production (corrected by MPB biomass) (Pratt et al., 2014). The necessity of understanding light availability is therefore compelling, as alterations in light climate can have a cascading influence throughout estuarine

ecosystems dominated by MPB (Figure 1.1). However, relatively few studies have aimed to increase our understanding of the functional relationship between MPB and light, limiting our ability to extrapolate productivity measurements over larger spatial and temporal scales and to estimate the ecological consequences to persistent water column turbidity.

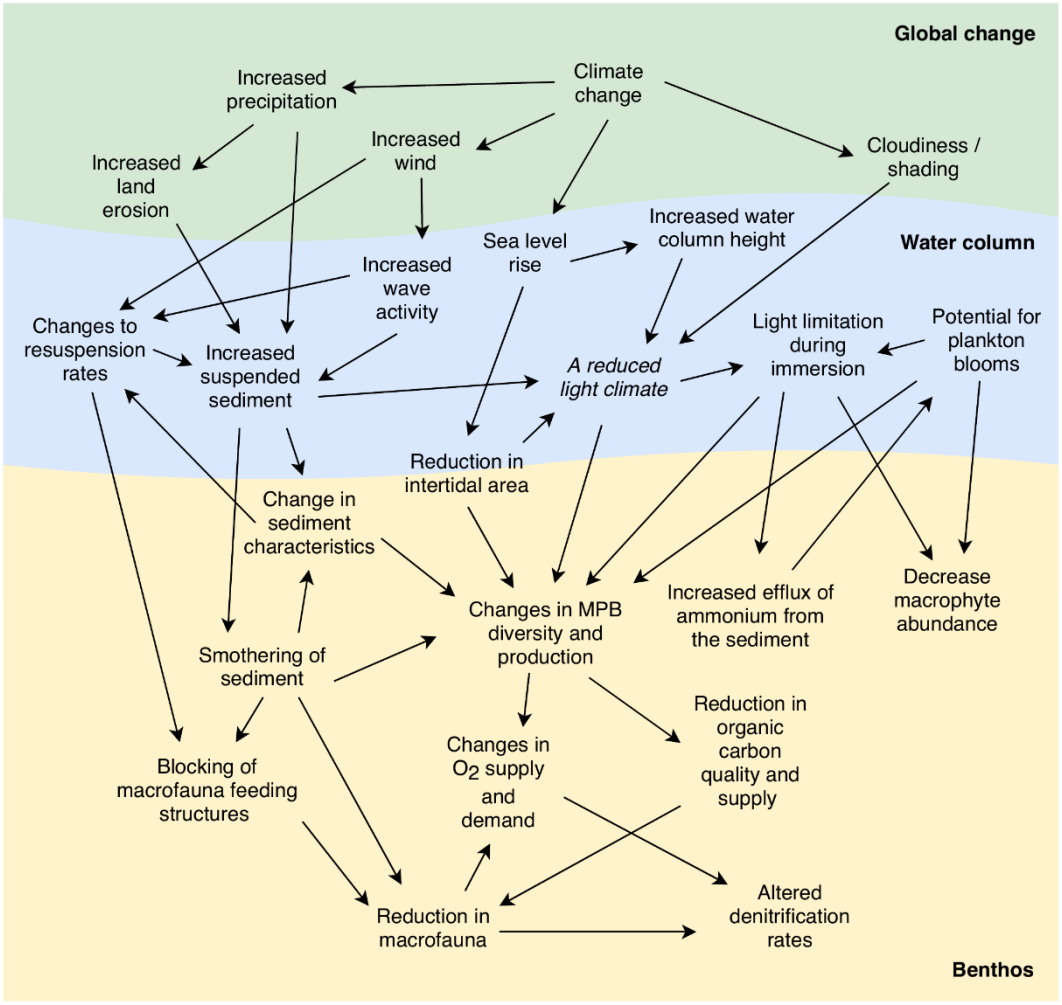

Figure 1.1: The main pathways which alter water column light climate and the subsequent alterations to ecosystem functioning and service delivery in intertidal habitats dominated by MPB. Adapted from Thrush et al. (2004).

Within intertidal environments, however, high turbidity is a temporally displaced stressor as the tide recedes and exposes the sediment surface (Drylie et al., 2018). Therefore, exposure during low tide periods may provide some resilience to any restrictions of MPB production during submerged periods. This has been

demonstrated in many estuaries throughout the world, especially in Europe, where primary productivity is often reported to be limited to low tide periods (Guarini et al., 2002, Migné et al., 2004, Spilmont et al., 2006, Migné et al., 2018). However, in the majority of studies, focus has been placed on heavily impacted and highly turbid estuaries where submerged productivity is assumed to be lost, limiting our ability to understand the ecological implications to the loss of submerged production. Nevertheless, it may be expected that the dependence on emerged exposure periods would be tightly coupled to water column turbidity (Drylie et al., 2018). Despite this crucial link, few studies have directly compared emerged and submerged primary production in response to increasing water column turbidity.

Despite being released from light limitation, low tide periods can provide other challenges which can impede productivity. Therefore, MPB employ multiple techniques to prevent exposure to unfavourable conditions and thrive in an unstable and challenging environment. In particular, MPB are able to vertically migrate up to 2 and 12 centimetres in muddy and sandy sediments, respectively (Kingston, 1999, Middelburg et al., 2000). The migration lower into the sediment is predicted to reduce photoinhibition, desiccation and grazing stress, while also increasing access to nutrients within oligotrophic systems (Underwood et al., 2005). In addition, different taxa within the MPB community can display differences in photoadaptations, and thus can increase photosynthetic capacity under varying light conditions (Underwood and Kromkamp, 1999, Underwood et al., 2005). While multiple approaches can at least partially compensate any reductions in productivity during emerged tidal periods, other ecosystem services are still likely to be diminished (in particular nutrient processing), increasing the vulnerability of coastal ecosystems to further anthropogenic stress.

Within estuarine ecosystems, increased nutrient loading can accompany sedimentation inputs and therefore these two stressors often occur simultaneously. While it is widely acknowledged that nutrient enrichment can lead to increases in phytoplankton and filamentous benthic macroalgae (Duarte, 1995,

Cloern, 2001), much less is known about the response of MPB production. It has been suggested however that N inputs can directly stimulate MPB productivity (Hillebrand et al., 2000) resulting in both a bottom-up cascade through increases in the abundance and biomass of grazing populations (Lever and Valiela, 2005) and a top-down influence through alterations in macrofaunal densities as a result of changes in oxygen profiles, sediment biogeochemistry and organic matter availability (Hillebrand et al., 2000, Douglas et al., 2017). While most studies focus on one phase of a tidal cycle and the individual influences of different anthropogenic stressors, the differences in MPB response to increasing nutrient enrichment is likely to be closely coupled to light availability (Stutes et al., 2006). For example, nutrient enrichment stimulated MPB production within a low turbidity system (Hillebrand et al., 2000) but not in a highly turbid but also nutrient rich estuary (Meyercordt and Meyer-Reil, 1999). Conversely, during tidal emergence, N was not limiting in a high nutrient system and therefore did not stimulate MPB productivity (de Jonge et al., 2012), while in low-nutrient systems the response of MPB is largely unknown. To disentangle the influence of light availability and nutrient enrichment, experiments which include comparisons across full tidal cycles in addition to encompassing the interactions of multiple stressors over large environmental gradients are essential.

Further complicating the effects of multiple stressors at a local scale will be the interacting effects with global stressors associated with climate change. For example, changes in sediment supply and nutrient delivery are likely to increase in response to altered storm frequency and intensity, further exacerbating water column turbidity and nutrient enrichment in coastal areas (Seneviratne et al., 2012). Simultaneously, sea-level rise will begin to inundate coastal areas (Nicholls and Cazenave, 2010), increasing the demand for flood and erosion protection, further driving intertidal habitat loss (Airoldi and Beck, 2007). Therefore, the resilience provided by intertidal areas will begin to erode at a crucial period where water column turbidity will be increasing. Consequently, it is becoming increasingly more important to understand the vulnerability of intertidal habitats to the loss of benthic primary production before these valuable ecosystems are

pushed even closer towards tipping points (Scheffer and Carpenter, 2003, Thrush et al., 2014).

1.1.2 Nitrogen and carbon cycling

Estuarine sediments play a fundamental role in the transport, processing and recycling of nutrients (particularly N), and are therefore often described as filters (Crossland et al., 2005). Sediment N is transformed or recycled via microbially-mediated redox reactions between more oxidised forms (nitrate and nitrite) and more reduced forms (ammonium, amino acids and organic N compounds), with gaseous products of dinitrogen gas, nitrous oxide and nitric oxide (Devol, 2015). These reactions are often highly coupled and therefore for each given N species there are several competing pathways, depending on the physical, biological, and chemical conditions of the sediment (Figure 1.2).

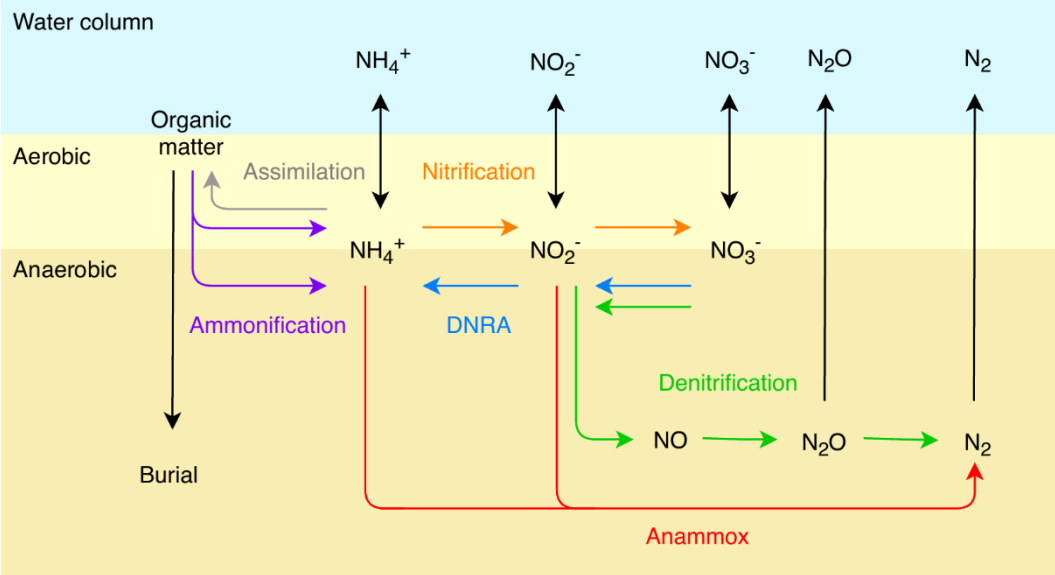

Figure 1.2: Simplified nitrogen cycling pathways within estuarine sediments, showing aerobic and anaerobic processes. DNRA: dissimilatory nitrate reduction to ammonium; Anammox: anaerobic ammonium oxidation. Adapted from Stief (2013).

The energy required to drive the redox reactions shown in Figure 1.2, either directly or indirectly, is derived from organic matter oxidation (Eyre et al., 2013). Therefore, sedimentary N and carbon (C) cycles are intrinsically linked. Through

the decomposition of organic matter, organic N compounds are remineralised to ammonium, initially via aerobic pathways, before continuing anaerobically via dissimilatory nitrate reduction (DNRA) or canonical denitrification (Devol, 2015). Canonical denitrification is a process whereby nitrate is used by predominantly facultative anaerobic bacteria as the terminal electron acceptor to oxidise organic matter and produce dinitrogen (N_2) gas (Knowles 1982). N_2 can additionally be produced during anaerobic ammonium oxidation (anammox), a chemoautotrophic process where ammonium is oxidised using nitrite (Dalsgaard et al., 2005). Both processes can co-occur, with the contribution of anammox to total denitrification ranging from 0 – 80 % in marine sediments (Dalsgaard et al., 2005). It is, however, difficult to distinguish between these two pathways and therefore the production of N_2 gas will be collectively referred to as denitrification.

Denitrification is an important mechanism in estuarine ecosystems, especially those receiving significant inputs of land-derived nutrients (Seitzinger et al., 2006). This is exemplified in soft sediment ecosystems where up to 50 % of terrestrial N can be denitrified (Seitzinger, 1988). Through regulating the availability of N to primary producers and for microbial assimilation, denitrification can act to increase the resilience of an ecosystem by reducing shifts towards eutrophication (Teixeira et al., 2010). However, quantification of denitrification rates are often restricted to highly degraded and enriched ecosystems (Vieillard et al., 2020), with fewer studies investigating the potential for denitrification to mitigate increases of nutrient enrichment across stressor gradients or over multiple temporal and spatial scales. This can restrict our ability to manage and mitigate the ecological consequences associated with increasing N enrichment.

Denitrification requires a source of organic matter to proceed and therefore the supply of organic matter can exert significant control over rates of denitrification (Maher and Eyre, 2012, Eyre et al., 2013). In particular, positive relationships between denitrification rates in the absence of photosynthesis and the quantity of organic matter oxidation, measured as sediment oxygen consumption, has regularly been identified in soft sediment habitats (Oakes et al., 2011, Piehler and

Smyth, 2011, Eyre et al., 2013). However, both the quality and quantity of organic matter can modify rates of organic matter oxidation, which in turn can alter the efficiency at which denitrification can remove N as N_2 (Fulweiler et al., 2008, Eyre and Ferguson, 2009, Piehler and Smyth, 2011). In oligotrophic systems, competition for N by heterotrophs processing organic matter can suppress denitrification (Risgaard-Petersen et al., 2004b), highlighting the complex interaction between carbon supply and N availability, and the importance of incorporating measures of C processing when investigating N cycling within estuarine sediments.

In addition to the supply of organic matter, denitrification rate is primarily controlled by oxygen and nitrate concentrations, both in the sediment and in the overlying water column (Seitzinger et al., 2006). Within eutrophic estuaries, high water column nitrate concentrations can supply that needed for direct denitrification (Dong et al., 2000, Magalhães et al., 2005). However, within oligotrophic estuaries where nitrate concentrations are low, nitrification often supplies the majority of nitrate needed for denitrification (Jenkins and Kemp, 1984), termed coupled nitrification-denitrification. Nitrification involves the oxidation of ammonium to nitrite and then nitrate, and thus increases the availability of electron acceptors for denitrification (Figure 1.2). The preceding ammonium is often a product of ammonification during the mineralisation of organic matter (in addition to excretion products from benthic macrofauna), hence the primary controls for denitrification are inherently coupled (Devol, 2015).

The coupling between nitrification and denitrification is strongly regulated by the boundary between oxic and sub-oxic sediment layers because of the contrasting oxygen requirements necessary for nitrification (oxic layers) and denitrification (sub-oxic <0.2 mg O_2 L^{-1} (Seitzinger et al., 2006)). Oxygen concentrations within the sediment are influenced by various factors including sediment permeability, concentrations within the overlying water column, macrofaunal activities and MPB activities (Rysgaard et al., 1995, Middelburg et al., 1996, Aller and Aller, 1998).

MPB productivity and the oxygenation of the surface sediment can enhance nitrification rate and thus facilitate coupled nitrification-dentification within nutrient rich systems when the surface sediment is sub-oxic (such as in organic rich sediments) (An and Joye, 2001). However, oxygenation can additionally inhibit denitrification through the increased depth of the oxic zone and thus the lengthening of diffusive pathways for solutes (such as nitrate) (Risgaard-Petersen, 2003). MPB additionally directly compete against nitrifying and denitrifying bacteria for ammonium and nitrate, which can ultimately supresses rates of denitrification (Risgaard-Petersen et al., 2004a, Risgaard-Petersen et al., 2004b). Therefore, the regulation of MPB on coupled nitrification-denitrification may be largely regulated by the availability of N and thus may change with increasing nutrient enrichment as the system becomes increasingly decoupled.

The role of MPB extends to regulating benthic-pelagic coupling through the modification of sediment-water fluxes. Within net heterotrophic systems, which are often characterised by high water column turbidity, productivity by MPB is reduced, leading to increases in the efflux of ammonium into the water column (Pratt et al., 2014). However, when the system is net autotrophic, MPB can reduce (or reverse, e.g. uptake) the flux of remineralised nutrients (ammonium) from the sediments to the overlying water column (Sundbäck et al., 2000, Eyre and Ferguson, 2002). This can effectively decouple N remineralisation within the sediment from primary production within the water column (by both phytoplankton and macroalgae), limiting any shifts towards eutrophication.

Sediment-water column fluxes and benthic nutrient recycling are further influenced by macrofaunal communities through bioturbation, feeding activities and burrow construction (Aller and Aller, 1998). Throughout New Zealand's North Island, intertidal habitats are dominated by the suspension feeling bivalve *Austrovenus stutchburyi* and the deposit feeling bivalve *Macomona liliana* (Hewitt et al., 1996). Bioturbation activity (such as that from *A. stutchburyi*) can increase the effective area of oxic-anoxic interfaces and the vertical distribution of solutes, particles and water, directly contributing to the spatial and temporal

heterogeneity of sedimentary redox zones (Woodin et al., 2016). This in turn influences microbial activities such as organic matter mineralisation, respiration, nitrification, denitrification and DNRA (Welsh, 2003, Jones et al., 2011). In addition, surface deposit feeding by *M. liliana* can alter the rate of solute exchange and create porewater pressure gradients through their hydraulic pumping behaviour, influencing both MPB biomass and biogeochemical processes (Woodin et al., 2010, Volkenborn et al., 2012). Furthermore, faecal casting and excretion by benthic macrofauna can increase dissolved inorganic N concentrations which may be regenerated and transported deeper into the sediment or released into the water column via active pumping and ventilation activities (Sandwell et al., 2009, Woodin et al., 2016).

The moderation of denitrification rate and nutrient processing by macrofaunal communities is, however, likely to be reduced if communities are deleteriously affected by increasing nitrogen enrichment (Douglas et al., 2017). This can occur as a consequence of ammonium toxicity, the formation of hydrogen sulphide and/or increased anoxia within the sediment (Fenchel and Riedl, 1970, Posey et al., 2006). The response of macrofaunal communities to sediment N enrichment is largely species and location dependent (Morris and Keough, 2003, Posey et al., 2006). However, enrichment of sediment porewaters within respect to ammonium has been shown to reduce the abundance of bioturbating macrofauna, which suppressed denitrification activity (Douglas et al., 2017). While during moderate enrichment, macrofaunal biodiversity mitigated the effects of increased nutrient enrichment and thus allowed the maintenance of ecosystem functioning. This may be a consequence of changes in species compositions and functions which can potentially provide resilience against increasing stress (Rice et al., 2012). Understanding the response of key macrofaunal species is therefore likely to be a crucial component in understanding any alterations in coastal biogeochemical cycling.

It is evident that both C and N cycling within estuarine sediments are both tightly coupled and embedded within a complex network of ecosystem interactions,

involving both direct and indirect feedbacks that consist of biological, physical and chemical processes. However, increasing nitrogen inputs are altering ecosystem interactions which can collectively increase the likelihood of nonlinear responses, reducing the ability of an ecosystem to adapt to further stress (Kemp et al., 2005, Howarth and Marino, 2006). Relatively few studies have examined the relationship between both N and C cycling in addition to changes in macrofaunal communities to increasing nutrient enrichment, especially in combination and across large spatial scales. Therefore, studies incorporating significant spatial and temporal heterogeneity within multiple estuaries are critical to understanding changing nutrient dynamics to increasing N inputs and are essential to inform management approaches within all estuarine environments.

1.2 Rationale

Anthropogenic pressure within coastal ecosystems is intensifying, having considerable impacts on ecosystem functionality and the delivery of ecosystem services. Improving our understanding of how different stressors may interact over multiple temporal and spatial scales and influence benthic productivity and biogeochemical cycling is therefore essential when trying to understand the resilience of these valuable habitats and to help manage effectively to prevent shifts towards ecological tipping points. In addition, periods of tidal emergence are largely overlooked when assessing benthic productivity, despite the potential for these habitats to be disproportionately important under increasing water column turbidity, climate change scenarios and land reclamation practices. The aim of my thesis was therefore to understand the degree at which water column turbidity may inhibit benthic primary production within multiple estuaries throughout New Zealand, and the associated vulnerability of these estuaries to the loss of intertidal area under future sea-level rise projections. I then aimed to assess the role of water column turbidity and long-term nutrient enrichment on the productivity of intertidal habitats over a full tidal cycle and their influence on nutrient processing.

1.3 Thesis overview

The main body of this thesis is comprised of three research chapters which collectively aim to further our understanding of the effects of increasing water column turbidity and nutrient enrichment on estuarine ecosystem functioning. To achieve this, light availability across multiple New Zealand estuaries was characterised before their relative vulnerability to future climatic change was explored (Chapter 2). In addition, a field manipulation experiment where sediment porewaters were enriched with nitrogen at multiple sites situated along a large natural gradient in water column turbidity was used to investigate the influence of water column turbidity and nutrient enrichment on benthic primary production (Chapter 3) and nutrient processing (Chapter 4).

1.3.1 Chapter 2

To understand the extent of water column turbidity across New Zealand estuaries, light sensors were deployed at 22 sites situated within 14 estuaries, chosen to encompass a gradient of anthropogenic disturbance. These sensors recorded light availability reaching the sediment surface (and thus MPB) for a total of 9 months. A global summary of MPB productivity-light relationships was then used to estimate how often light would limit MPB productivity. These estimations of light limitation were then coupled with future sea-level rise scenarios to determine the vulnerability of each site to the loss of intertidal area predicted for the end of the century.

Objectives:

1. To characterise light availability reaching MPB across 14 New Zealand estuaries.
2. To present a global literature summary of *in situ* MPB photosynthesis-irradiance relationships and to use these to estimate the proportion of time MPB are light limited across submerged and emerged tidal periods.

3. To estimate the vulnerability of each estuary to increasing sea-level rise and the consequential loss of intertidal area.

1.3.2 Chapter 3

The aim of Chapter 3 was to experimentally investigate the interactive effects of water column turbidity and increases in nutrient enrichment on benthic primary production. Six sites situated along a gradient of water column turbidity (as confirmed in Chapter 2), were experimentally enriched with nitrogen. After 8, 15 and 20 months of enrichment, the effects on sediment properties, macrofaunal communities and solute fluxes were derived using benthic incubation chambers. This study enabled me to characterise and compare benthic primary production estimates across different seasons and during both submerged and emerged tidal periods in response to two pervasive coastal pressures.

Objectives:

1. To investigate how water column turbidity may influence both submerged and emerged MPB primary production, and if this is modified by sediment nutrient enrichment.
2. To determine if these responses are temporally variable.

1.3.3 Chapter 4

Data collection for Chapter 4 took place alongside Chapter 3 to examine the effects of sediment nutrient enrichment on nitrogen and carbon cycling within multiple estuaries. During the benthic incubation measurements, additional solute and gas samples were taken to identify any alterations in nitrogen processing, while carbon quality and quantity measurements were used to assess the regulation and influence of carbon on nutrient processing. The nature of the response of environmental variables and macrofaunal communities to increasing nutrient enrichment was then explored to determine potential non-linearities and/or step

changes in ecosystem interactions which could lead to functional shifts within estuarine systems.

Objectives:

1. To investigate the effects of sediment nutrient enrichment on nitrogen and carbon cycling within multiple estuaries.
2. To examine alterations in biodiversity-ecosystem relationships to increasing nutrient enrichment and their influence on nutrient processing.

Chapter Two: Shady business: the darkening of estuaries constrains benthic ecosystem function

2.1 Introduction

Soft sediment intertidal habitats are among the most extensive coastal ecosystems, supporting millions of people worldwide through the ecosystem services they provide (e.g., food production, storm protection and shoreline stabilisation) (MEA 2005, Field et al., 2014). Many of these services are underpinned by light, which sustains ecosystem functionality by fuelling benthic primary production and the associated modification of biogeochemical processes that are critical for the structure of the ecosystem's interaction network (Thrush et al., 2012, Pivato et al., 2019). However, as coastal ecosystems are situated at the transition between land and sea, they are affected by a multitude of pressures, such as coastal development, sea level rise (SLR) and increases in nutrient and sediment supply from terrestrial run-off (MEA 2005, Arkema et al., 2013, Passeri et al., 2015). These pressures act in concert to modify the seafloor light climate by changing water column optical properties and/or depth, which, through changes in benthic primary production, can have detrimental implications for coastal ecosystems and the vital ecosystem services they provide.

Benthic primary production is moderated by a number of factors including temperature, nutrient availability, sediment resuspension and grazing pressure (Cebrián, 2004, Howarth and Marino, 2006, Kwon et al., 2018). However, without sufficient light (specifically photosynthetically active radiation [PAR]: the amount of light available for photosynthesis ranging between 400 – 700 nm), photosynthesis is not possible and its availability can limit coastal primary production by vascular plants (e.g. seagrass), macroalgae, and microalgae (phytoplankton and microphytobenthos). Microphytobenthos (MPB) refers to the photosynthetic eukaryotic algae and cyanobacteria (MacIntyre et al., 1996) found in soft sediment habitats from the intertidal zone to depths of ~200 m (Cahoon,

1999). In coastal areas, MPB production is a significant contributor to total marine carbon fixation (Borum and Sand-Jensen, 1996) and thus fuels nearshore food webs (Christianen et al., 2017, Jones et al., 2017). In addition to the central role MPB play in carbon flow, they also contribute to a multitude of other ecological functions, which through complex ecosystem interactions, can regulate ecosystem service delivery (Hope et al., 2020). This includes vital services such as the transformation and recycling of nutrients, sediment stabilisation, climate regulation, support of benthic biodiversity, improvement of water quality, and numerous cultural services (e.g. Sundbäck et al., 2006, Kowalski et al., 2009, Joensuu et al., 2018, Hope et al., 2020). Therefore, any process that results in a decline in MPB production will not only alter food web dynamics but, through changes in the other functions they provide, will have cascading effects on coastal ecosystems.

Atmospheric conditions, tides and water column properties combine to make light highly variable within estuaries (Kirk, 1994, Gattuso et al., 2006), but up to 80 % of this variability can be driven by water column turbidity alone (Anthony et al., 2004). Water column turbidity is in part a consequence of eutrophication, where an oversupply of nutrients can result in increases of phytoplankton. In addition, the intensification of terrestrial soil erosion can act to elevate concentrations of suspended inorganic material (sediment) (Rabalais et al., 2005). Both eutrophication and suspended sediment concentrations are significant global stressors, which are continuing to increase worldwide (Airoldi, 2003, Thrush et al., 2004, Rabalais et al., 2009, Hewitt et al., 2016, Halpern et al., 2019, Carrier-Belleau et al., 2021), resulting in less sunlight reaching MPB on the seafloor. When light is persistently limiting to MPB, benthic primary productivity can be lost, shifting a system to one dominated by pelagic primary production (Cooper and Brush, 1993). Most obviously, this reduction or loss in MPB primary production diminishes the availability of labile organic material to benthic food webs, but it also changes nutrient transformation and recycling pathways (Sundbäck et al., 2000, Pratt et al., 2014). These changes have been documented across the globe and can have

detrimental impacts to these multifaceted ecosystems (e.g., by accelerating eutrophication and promoting hypoxia).

In shallow estuaries, extensive intertidal areas provide some resilience to highly turbid coastal waters through the maintenance of MPB production, as the water shallows and drains off the intertidal flats (Drylie et al., 2018). The restriction of primary production to periods of emersion has been reported from turbid estuaries globally (Guarini et al., 2002, Migné et al., 2004, Yamochi et al., 2017, Drylie et al., 2018). To better understand the potential compensatory dynamics involving water depth, availability of PAR and potential MPB production, we need to know how intertidal light climate varies spatially and temporally, and how this variability influences the amount of time MPB are light limited. In estuaries with extensive intertidal and shallow sublittoral flats, this will indicate an estuary's vulnerability to increased turbidity or loss of intertidal area and susceptibility to tipping points associated with a loss of MPB productivity (Thrush et al., 2012, Thrush et al., 2014).

Conducting research across natural turbidity gradients is a useful method to explore the sensitivity of an estuary to the loss of MPB production, and this kind of research is critical for improving the understanding of how these ecosystems will respond to future changes under both local (e.g., turbidity) and global stressors (e.g., climate). New Zealand's estuaries offer an ideal natural laboratory, with clear gradients in water column turbidity owing to the relatively recent arrival of humans that has created spatial variability in anthropogenic pressures across the country (McWethy et al., 2010). In this study, the light climate reaching MPB was measured at 22 intertidal sites situated within 14 estuaries across New Zealand. Our study was conducted over a 9 mo period, with the estuaries chosen to encompass a gradient of anthropogenic disturbance. This unique data set was combined with a global literature summary of MPB photosynthesis–irradiance (P–I) curves to estimate how often MPB production within these intertidal areas was potentially light limited and therefore the relative dependence of each estuary on periods of emersion. By coupling these measurements with estimates of future

sea-level rise scenarios, we were able to determine the sensitivity of each estuary to the loss of intertidal area predicted by the end of the century.

2.2 Materials and Methods

2.2.1 Study sites

Fourteen estuaries throughout New Zealand were chosen to encompass a range of anthropogenic influence and water clarity (Figure 2.1). The estuaries were predominantly shallow (<10 m), barrier enclosed coastal lagoons with extensive intertidal areas, characteristic of many New Zealand estuaries (Hume et al., 2007) and up to 22 % of the global coastline (Dame, 2008, Dürr et al., 2011). Catchment, estuarine and tidal properties are described in Table 2.1, and the GPS coordinates of the sensor deployment locations are given in Table A1.1. Within each estuary, 1 – 3 study sites (22 in total) were chosen in the mid-intertidal. All had predominantly sandy sediments, and semi-diurnal tides (Table 2.1).

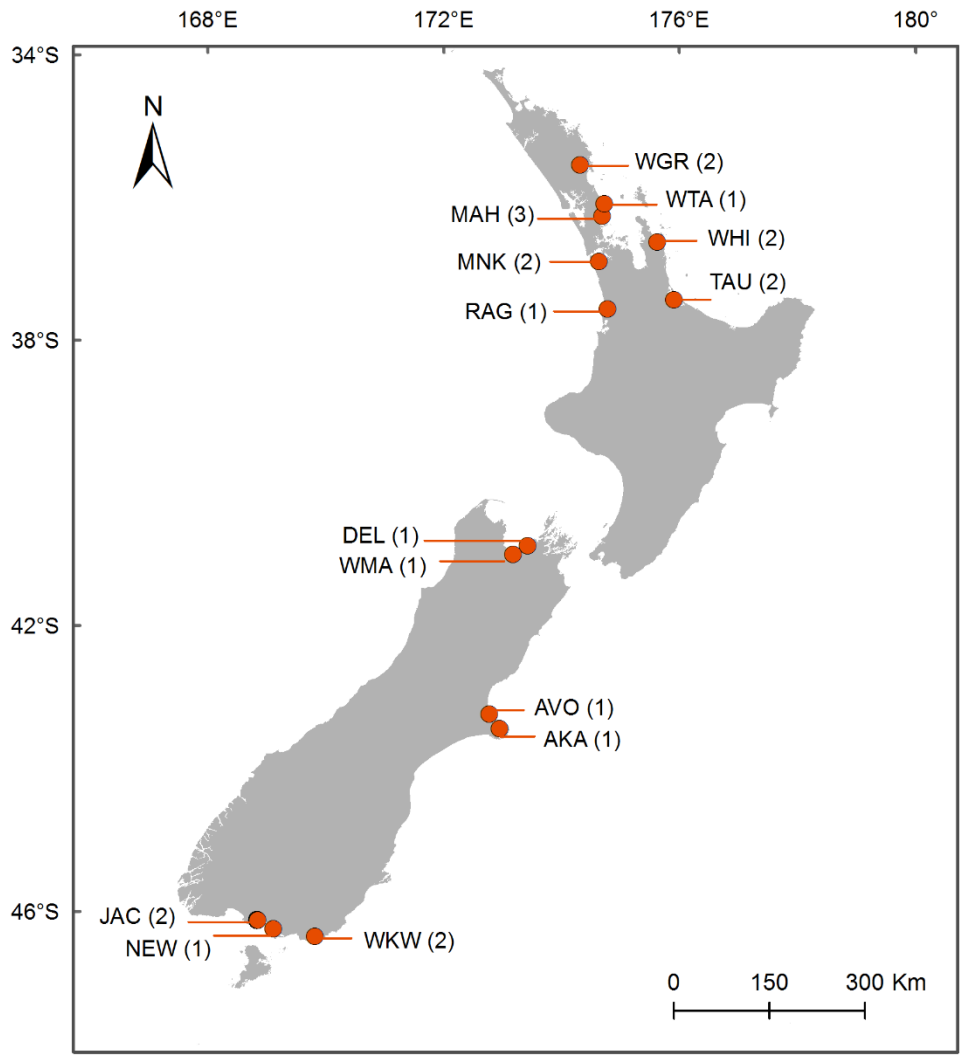

Figure 2.1: Location of estuaries where light sensors were deployed. The number of sites within each estuary is shown in parentheses. Site abbreviations are defined in Table 2.1. For site-specific GPS locations, see Table A1.1.

At each site, PAR levels were measured 10 cm above the seabed by deploying Odyssey PAR loggers (Dataflow Systems). Measurements were recorded every 10 min for 201 – 260 d between March and November 2017. Each sensor was checked monthly for fouling and cleaned, although, data screening and monthly checks revealed no obvious fouling or sediment deposition throughout the deployment period.

Table 2.1: Estuarine characteristics and site sediment properties ordered by latitude from north to south. Estuary Environment Classification (EEC) from Hume et al. (2007). Hydrological, C: river flow dominated; E: dominated by ocean forcing with high flushing and wind–wave sediment resuspension, extensive intertidal area; F: complex shoreline with numerous arms off basin, dominated by ocean forcing and high flushing, extensive intertidal area. Geological, AI: alluvium; HS: hard sedimentary; M: miscellaneous; SS: soft sedimentary; VS: volcanic strong; VW: volcanic weak. Land cover, N: natural; P: pastoral; U: urban. DW: dry weight. All sediment data are estuary/site mean ± SD (n = 6–18). For site-specific GPS locations, see Table A1.1 in the Supplement.

Estuary	Code	Total area (km^2)[a]	Intertidal area (%)[a]	Mean tidal range (m)[a]	Mean estuary depth (m)[a]	Land catchment area (km^2)[a]	EEC Hydro-logical	EEC Geo-logical	EEC Land cover	Grain size median (µm)[b]	Mud content (% <63 µm)[b]	Sediment organic content (%)[b]	Sediment chl *a* (DW µg g^{-1})[b]
Whangārei	WGR	104	58	1.72	4.42	297	F	HS	P	169 ± 56	3.6 ± 2.6	1.5 ± 0.2	8.4 ± 2.1
Whangateau	WTA	7.5	85	2.79	1.56	42	F	SS	P	255 ± 8	3.4 ± 0.9	1.4 ± 0.1	7.7 ± 0.9
Mahurangi	MAH	25	51	2.11	2.74	122	F	SS	P	263 ± 40	3.6 ± 1.7	2.3 ± 0.3	5.4 ± 2.3
Whitianga	WHI	16	72	1.91	0.84	450	F	VS	P	177 ± 27	17.3 ± 7.5	4.3 ± 0.8	11.0 ± 6.0
Manukau	MNK	366	62	2.20	6.06	1023	F	VW	P	200 ± 6	5.3 ± 4.7	1.6 ± 0.5	11.6 ± 4.5
Tauranga	TAU	200	77	1.50	2.12	1300	F	VW	P	179 ± 23	9.3 ± 5.4	2.0 ± 0.6	12.5 ± 2.8
Raglan	RAG	33	69	2.28	2.24	523	F	VW	P	130 ± 4	16.5 ± 2.1	3.8 ± 0.2	17.1 ± 4.6
Delaware	DEL	3.1	93	2.69	2.02	93	E	HS	P	103 ± 9	16.1 ± 4.7	2.7 ± 0.3	4.2 ± 0.5
Waimea	WMA	29	59	1.51	3.40	933	F	SS	P	151 ± 2	0.4 ± 0.7	1.3 ± 0.0	2.7 ± 0.5
Avon-Heathcote	AVO	7.5	67	1.68	1.87	211	F	M	U	190 ± 9	1.0 ± 1.5	1.3 ± 0.2	5.6 ± 2.4
Akaroa	AKA	43	3	1.62	10.60	127	E	M	P	84 ± 1	23.2 ± 1.4	1.4 ± 0.1	4.5 ± 0.2
Jacobs River	JAC	6.7	66	1.86	2.19	1570	F	AI	P	196 ± 61	3.8 ± 1.7	1.5 ± 0.2	4.1 ± 1.3
New River	NEW	0.2	42	2.03	4.56	3948	C	SS	N	171 ± 3	0.0 ± 0.0	0.7 ± 0.0	1.5 ± 0.4
Waikawa	WKW	6.4	82	1.73	1.53	241	E	SS	P	201 ± 24	6.6 ± 6.1	1.5 ± 0.4	8.4 ± 2.6

[a]Data from EEC database

[b]Unpublished data measured at the end of the photosynthetically active radiation sensor deployment

2.2.2 PAR calculations

Each Odyssey sensor was calibrated prior to deployment with a LI-COR PAR sensor, with the calibration regression used to convert all count measurements to PAR in µmol m^{-2} s^{-1}. Data were then partitioned into either immersed or emerged periods, defined by the time of high or low tide ±2 h. This ensured a distinct separation of tidal state at all sites and therefore a 4 h period, wherein the sensor was either completely covered by the water column, including the time of maximum water depth (immersed), or was uncovered when the tide receded (emerged). Night-time were excluded by removing times where PAR measured 0 µmol m^{-2} s^{-1}.

2.2.3 Calculation of MPB light saturation

Changes in light climate become ecologically important to marine sediments when phototrophic organisms become light limited. Light saturation is highly variable in both time and space, which limits the ability to extrapolate single, one-off estimations (Cahoon, 2006, Kwon et al., 2018). To overcome this issue and determine potential periods of light limitation for MPB (the main primary producers on intertidal flats) across a large spatial gradient, we used estimates of light saturation levels obtained from an extensive literature search that incorporated a variety of different contexts. Estimates of light saturation were obtained from studies of P–I curves for MPB, with a focus on natural, intact communities that integrated effects of environmental and behavioural responses, such as MPB vertical migration (Consalvey et al., 2004, Jesus et al., 2006). Therefore, studies conducted on suspended, cultured or sieved communities were omitted from this analysis (a summary of suspended MPB P–I curves can be found in Cahoon (2006)). In addition, studies using pulse-amplitude modulated (PAM) fluorometry were also excluded because they are conducted at the surface sediment and are not readily comparable with primary production estimates via gas fluxes (O_2, CO_2) which dominate the literature (Consalvey et al., 2005).

Studies were divided into either subtidal or intertidal habitats. The majority of studies reporting P–I curves came from intertidal habitats (14 of 18) and most of these were conducted on emerged sediment only (11 of 14, a reflection of the high

turbidity in many northern hemisphere estuaries), with only 3 including immersion periods (see Appendix Table A1.2 for details). Therefore, it was not possible to distinguish between immersed and emerged periods in estimates of light saturation point. Maximum gross community production rates were also obtained from the P–I curves and where necessary were converted from mg O_2 m^{-2} h^{-1} to mg C m^{-2} h^{-1} using a conversion factor of 1.2 (Mills and Wilkinson, 1986).

The median global light saturation value of all intertidal P–I curves (42 in total) was used to estimate light saturation in this study and thus we defined light limitation as the amount of time during the day when PAR was below 258 µmol m^{-2} s^{-1}. A daily proportion of light limitation was then calculated for immersed and emerged periods separately. To determine the robustness of these results to variations in choice of light saturation, we also calculated daily light limitation for the middle 50 % of literature saturation values at 170 and 424 µmol m^{-2} s^{-1}, which correspond to the 25th and 75th percentile respectively. An overall estimate (over the entire 9 mo period) summarising the proportion of time benthic primary production was not light limited (i.e. saturated) within each estuary over the 2 daily tidal phases was then calculated using the proportion of time during which PAR was greater than 258 µmol m^{-2} s^{-1}. After testing for normality, a linear regression was used to test the relationship between the calculated daily proportions and latitude using the R stats package (v 3.6.2) in R Studio.

2.3 Results

2.3.1 Spatial and temporal variability in light climate

Across all 22 sites, intertidal light climate was highly variable over the 9 mo period such that the interquartile range during emerged and immersed periods of the tide varied from 239 – 1060 and 71 – 554 µmol m^{-2} s^{-1}, respectively (Figure 2.2). Additionally, high spatial variability occurred within estuaries; for example, within WHI estuary (see Table 2.1 and Figure 2.1 for all site codes and locations, respectively), the interquartile range during immersion was 258 µmol m^{-2} s^{-1} at WHI-2 compared to 419 µmol m^{-2} s^{-1} at WHI-1 and, during emersion, it was 798 and 1019 µmol m^{-2} s^{-1}, respectively.

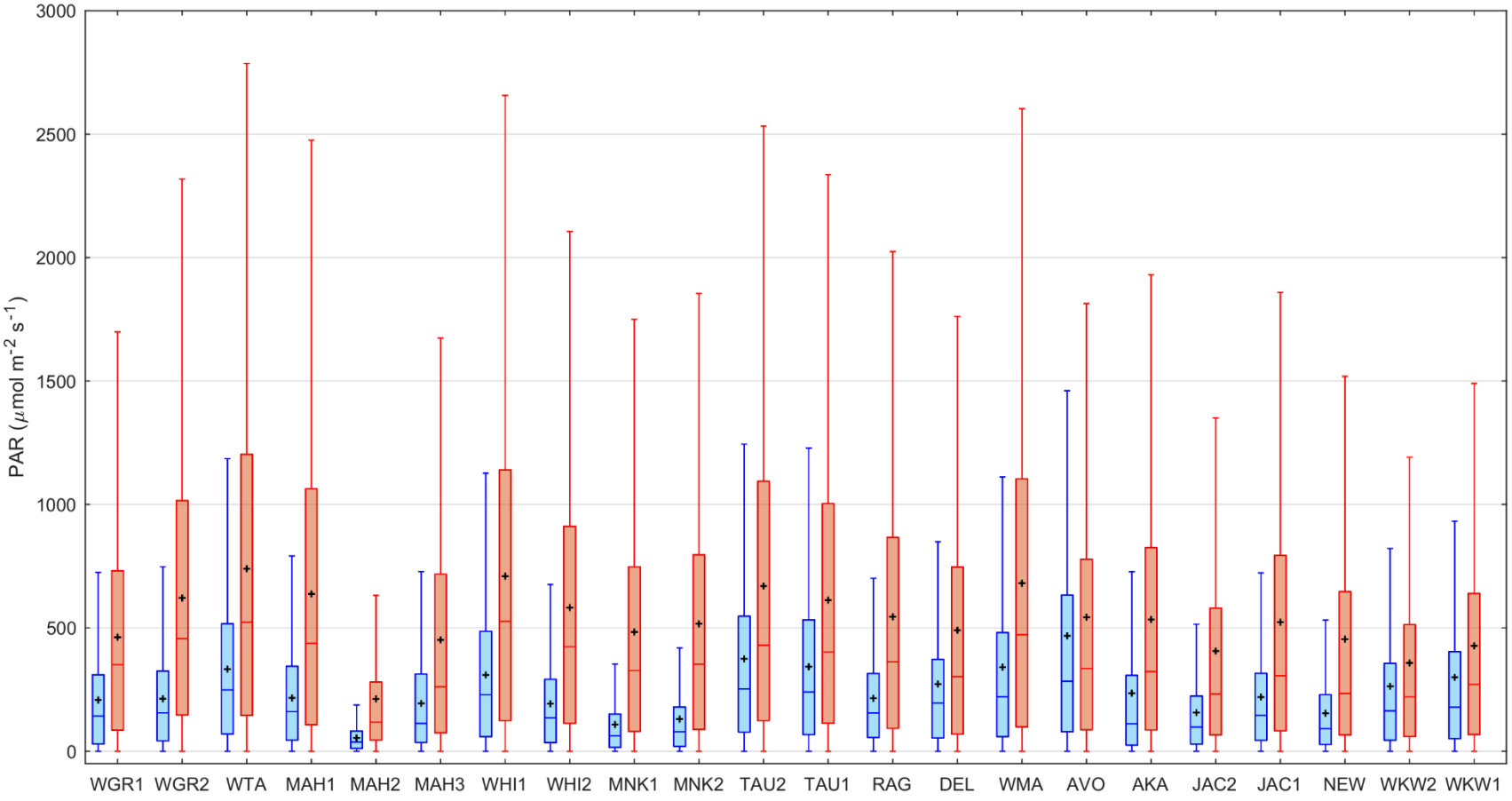

Figure 2.2: Variability in daytime photosynthetically active radiation (PAR) during immersion (blue) and emersion (red) between March and November 2017, with sites ordered by latitude from north to south. Data are comprised of 10 min measurements over a 9 mo period. Boxes represent the 25th and 75th percentiles, and whiskers are the 5th and 95th percentiles. A solid line and black cross within each box denote median and mean, respectively. Site abbreviations are defined in Table 2.1.

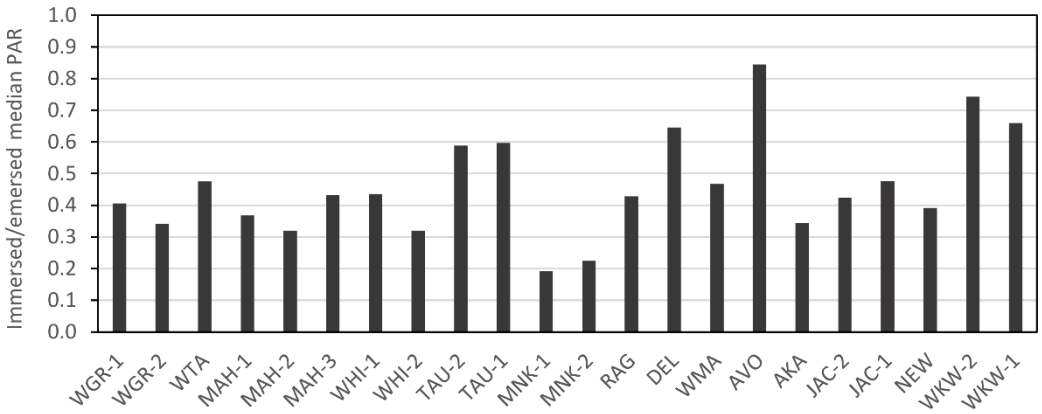

Figure 2.3: Ratio of immersed to emerged median photosynthetically active radiation (PAR) between sites, ordered by latitude from north to south. A value close to 0 represents a greater dissimilarity between immersed and emerged PAR (i.e. greater influence of water column properties). Site abbreviations are defined in Table 2.1.

Immersed tidal periods resulted in a reduction of seafloor light levels compared to emerged periods at each site (the difference in emerged and immersed median PAR for each site ranged from 118 – 526 µmol m^{-2} s^{-1}). The degree of water column influence on light climate is illustrated in Figure 2.3 using a calculated ratio of median immersed to emerged PAR (hereafter the immersed:emerged ratio). Values close to 0 indicate that light was heavily influenced by tidal state (i.e., water column properties) (e.g., 0.12 at site MNK-1), whilst other sites showed little variation between immersion and emersion (e.g., 0.84 at AVO). Within an estuary, there was both dissimilarity (e.g., WHI-1 and WHI-2: 0.44 and 0.32, respectively) and similarity (e.g., 0.59 and 0.60 for TAU-2 and TAU-1, and 0.19 and 0.22 for MNK-1 and MNK-2) in the immersed:emerged ratio between sites.

2.3.2 Impacts on benthic primary production

Literature derived intertidal MPB light saturation values were predictably variable, with an interquartile range of 254 µmol m^{-2} s^{-1} and a median of 258 µmol m^{-2} s^{-1} (Table A1.2). Using this median value of light saturation, the proportion of each day spent below 258 µmol m^{-2} s^{-1} was calculated for both immersed and emerged tidal periods (Figure 2.4). The proportion of each day spent light limited during emersion varied from a median of 32 % (WGR-2, WHI-1 and WTA) to 64 % (WKW-2) and was correlated to latitude (R^2 = 0.65, $p < 0.001$) such that lower latitudes

received more light. The only exception was MAH-2 in the north of New Zealand, which was characterised by low light availability (88 % median light limitation) and was excluded from the above calculation. Here, steep, high cliffs to the north and east shadowed the small intertidal bay, reducing the quantity of light reaching the sediment surface. During immersion however, the correlation of light limitation to latitude disappeared ($R^2 = 0.04$, $p = 0.39$) and sites varied from 55 % (AVO) to 100 % light limitation (MAH-2, MNK-1, MNK-2, NEW and JAC-2).

These estimates of light limitation predictably change depending on the value of light saturation used, as demonstrated using the 25th, 50th (median) and 75th percentile of literature values (Figure 2.5). A lower light saturation value inevitably results in a reduced proportion of each day estimated to be light limited, and vice versa. For example, the median proportion of time that AVO was estimated to be light limited during immersion using the 25th, 50th and 75th percentile of light saturation was 39 %, 55 % and 75 %, respectively. However, the changes in light limitation estimates are less pronounced for highly turbid estuaries (e.g., MNK, MAH-2). Despite the change in absolute proportion of time spent light limited, overall patterns are conserved such that the relative differences between estuaries remain constant regardless of choice of light limitation value. For example, the difference between light limitation estimates for AVO and WMA are 1, 5 and 5 % when using the 25th, 50th and 75th percentile, respectively (Figure 2.5).

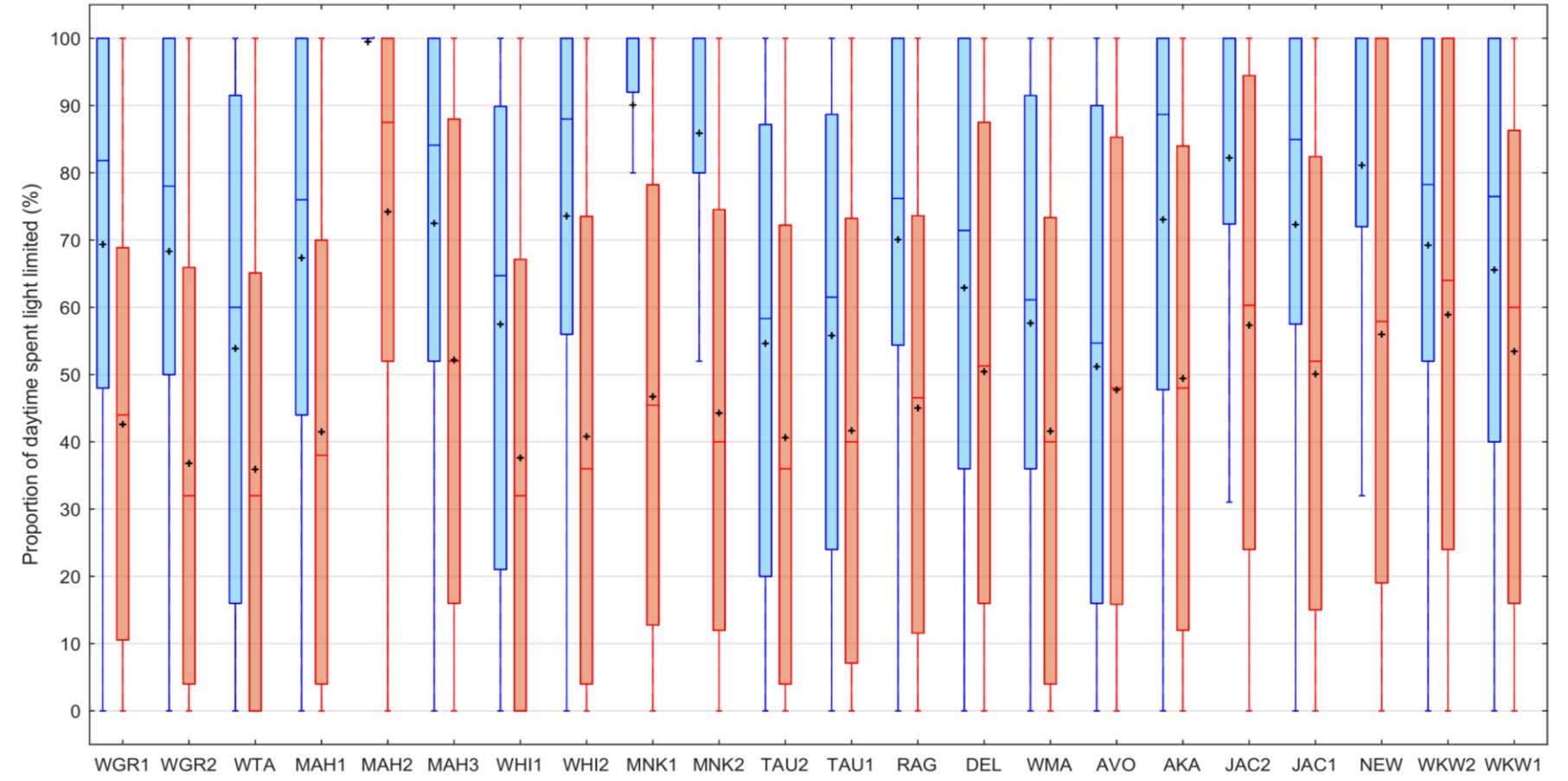

Figure 2.4: Estimated proportion of each day over 9 mo that microphytobenthic production was light limited during immersion (blue) and emersion (red) assuming a light saturation value of 258 µmol m^{-2} s^{-1} (see Section 2.2.3 for details). Boxes represent the 25th and 75th percentiles, and whiskers are the 5th and 95th percentiles. A solid line and black cross within each box denote median and mean, respectively. Sites are ordered by latitude from north to south. Site abbreviations are defined in Table 2.1.

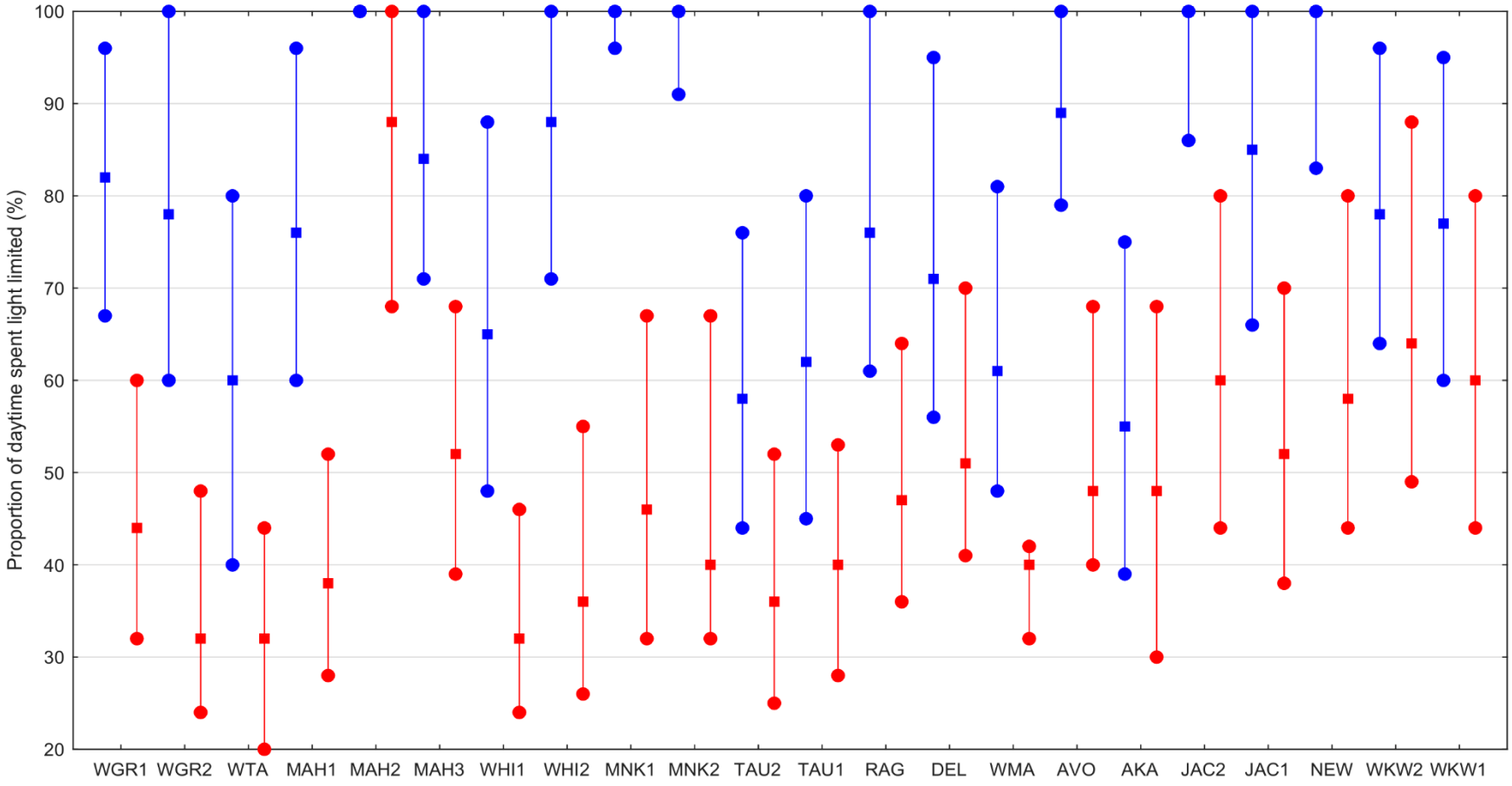

Figure 2.5: Variation in the median proportion of the daytime that each estuary was light limited, assuming a light saturation value of 170 (lower point in each line), 258 (centre point) and 424 µmol m^{-2} s^{-1} (upper point). These values correspond to the 25th, 50th and 75th percentiles of literature light saturation values. Blue and red represent submerged and emerged data, respectively, and sites are ordered by latitude from north to south. Site abbreviations are defined in Table 2.1.

When light reaching the sediment surface during tidal inundation is reduced, the dependence on periods of exposure will become increasingly more important for maintaining benthic primary production. Therefore, we estimated the proportion of time over the entire 9 mo where light was saturating to benthic primary production (using an estimated median light saturation literature value of 258 µmol m m^{-2} s^{-1}) during both immersion and emersion (Figure 2.6). During immersion, the total proportion of time that light was saturated to MPB production ranged from 0 – 26 %, with two thirds of the estuaries below 20 % saturation. Excluding MAH-2 because of topographic shading, during emersion, the amount of time light was saturating to MPB production increased to 23 – 33 %, resulting in cumulative proportions (emersion + immersion) of 34 % (MNK-1) to 57 % (WTA) light saturation.

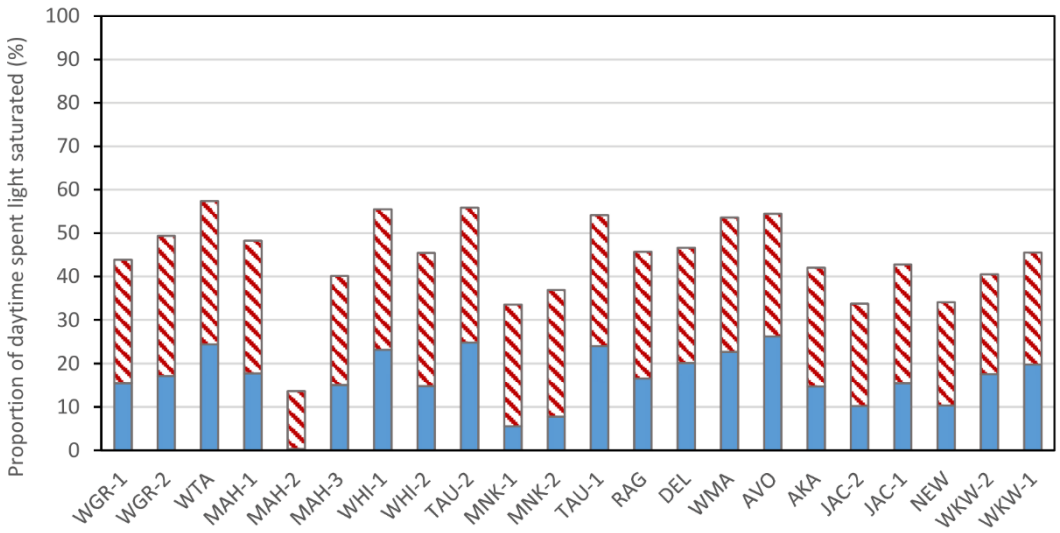

Figure 2.6: Proportion of time over 9 mo where benthic primary production was light saturated (based on a light saturation value of 258 µmol m^{-2} s^{-1}; see Section 2.2.3 for details). Daytime is divided into 2 tidal periods: immersion (solid blue bars) and emersion (hashed red bars). Sites are ordered by latitude from north to south. Site abbreviations are defined in Table 2.1.

2.4 Discussion

The large variability in light climate measured over an extensive spatial and temporal sampling domain can be attributed to numerous factors, most of which differ depending on tidal state (Figure 2.2). During periods of emersion, latitudinal

and geographic characteristics (e.g., shading from topography) influence light availability. Previous studies have additionally reported significant effects of atmospheric conditions (Kirk, 1994, Anthony et al., 2004); however, further analysis of light limitation over 4 h of midday tidal emergence found 0 % light limitation for the 9 mo period at all but 1 site (which was limited 10 % of the time due to topographic shading). This suggests that the atmospheric effects on MPB production are unlikely to be a contributing source of light limitation because of the high measured irradiance relative to MPB saturation values even on cloudy, low sun-angle days (e.g., in winter).

Assuming the differences in atmospheric conditions between high and low tide are likely to be negligible over large temporal scales, and that the correlation of light to latitude diminished during immersion, the observed reduction in light availability from emerged to immersed periods is an indicator of the role played by water column optical properties at each site (Figure 2.2). These properties are likely to be governed by the suspended organic and inorganic material because of the relatively shallow nature of these intertidal zones (site mean tidal range from 1.50 – 2.79 m) (Kirk, 1994, Cussioli et al., 2019). Water clarity across the 22 sites was variable, including sites that remained relatively clear during immersion (immersed:emerged ratio close to 1, Figure 2.3) while others were highly turbid (immersed:emerged ratio close to 0). In addition, the high temporal variability in water clarity within some sites (e.g., TAU), may be attributed to variability in meteorological events (e.g., storms) that can increase fine sediment inputs from the land and/or resuspend sediments off the seabed. The resulting gradient in water column turbidity provides an opportunity to estimate the proportion of time MPB production is light limited across large spatial and temporal scales.

Despite the significance of light availability within coastal ecosystems (Ackleson, 2003), our literature search shows the limited knowledge of the functional relationship between light and *in situ* MPB production (only 18 studies identified). Based on a median light saturation value of 258 μmol m^{-2} s^{-1}, MPB production was light limited between 55 and 100 % of the day during tidal immersion (Figure 2.4). These estimates will shift depending on the light saturation value used and the

inclusion of different data periods (e.g., the omission of a summer period in our data, which would introduce differences in day length, sun angle and cloud clover). However, using the 25th or 75th percentile of the literature values (instead of the median) results in light limitation shifting to 39 – 100 % and 75 – 100 % of the time, respectively (Figure 2.5), with little effect on overall patterns between estuaries. The maintenance of high light limitation under various saturation value scenarios and in all 14 estuaries that span a latitudinal gradient (and therefore a gradient in daylength and sun angle) demonstrates the substantial impact of light limitation irrespective of the exact value used, and the environmental or temporal context. Therefore, although choosing one light saturation value from the literature is an imperfect measure of light limitation, it does allow the novel examination of broad-scale patterns across large spatial and temporal gradients as well as comparisons with estuaries globally.

The literature-derived P–I curves are valuable not only for estimating the onset of light limitation, but also for gaining insight into maximum potential rates of primary production. Our literature review revealed that light saturation was notably lower for subtidal compared to intertidal environments (median 79 vs. 258 µmol m^{-2} s^{-1}), which corresponded to a lower rate of maximum gross community production (median 25 and 52 mg C m^{-2} s^{-1}, respectively). Moreover, light saturation and maximum gross community production observed in the literature data are positively correlated (Pearson's $r = 0.7$, $p < 0.001$; Figure S1). Thus, a lower saturation value, while resulting in a decreased percentage of time being light limited, is more likely to correspond to lower maximal rates of primary production; the 2 effects compensate for each other.

Reductions in primary production, as evident in this study, have direct implications for the ecosystem functions delivered by MPB. For highly turbid estuaries, the persistent inhibition of production (those close to 100 % light limitation, Figure 2.4) is likely to directly modify the transfer of labile organic carbon and thus the transfer of energy within and across ecosystems (MacIntyre et al., 1996), having direct implications for global carbon budgets (Duarte et al., 2005, Bauer et al., 2013). In addition, decreasing light availability is closely coupled to increasing

effluxes of ammonium (NH_4^+) (Pratt et al., 2014), which, in synergy with other modifications to nutrient recycling and transformation (e.g. changes in denitrification rate), can lead to an exacerbation of the eutrophication cycle (Sundbäck et al., 2006) and further reductions in light climate over the longer term. Increasing attenuation of light will therefore have the effect of breaking down closely linked ecosystem processes as MPB photosynthesis becomes inhibited during tidal inundation. While there are many other factors when considering modifications to primary production estimates and comparisons across large spatial gradients (e.g., temperature and nutrient availability), our study highlights the profound impact of high light limitation (as occurs at MAH-2 and MNK). The resulting ecological consequences extend not only to direct effects on primary production, but have cascading ecological impacts in these coastal marine ecosystems, to the point where systems are pushed beyond tipping points (Kemp et al., 2005, Jickells et al., 2016, Christianen et al., 2017).

When light attenuation in the water column inhibits benthic production, intertidal areas can become a refuge for MPB through emerged periods at low tide (Migné et al., 2004). We estimate this may already occur at site MAH-2, where over the 9 mo period, light conditions during immersion were almost continuously below our estimated saturation threshold (Figure 2.6), suggesting that MPB within this area are relying on periods of emergence at low tide. Similarly, light only became saturating within MNK-1 and MNK-2 for 6 and 8 % of immersion periods, respectively, also suggesting that low tide periods may be contributing significantly to the maintenance of MPB production. This reliance on emersion is already evident for turbid estuaries globally, where low tide production can support and sustain MPB communities (e.g. Guarini et al., 2002, Migné et al., 2004, Yamochi et al., 2017, Drylie et al., 2018). In addition, this light saturated emerged period can result in intertidal habitats being frequently more productive than their subtidal counterparts (Charpy-Roubaud and Sournia, 1990) as supported by our review of literature-based P–I curves (see above). Although productivity can be sustained during emersion, other ecosystem functions are lost (e.g. modification to nutrient recycling through effluxes of ammonium with decreasing light availability; (Pratt et al., 2014)) and so ecosystem service delivery will still be

reduced. Our currently limited knowledge of MPB is impeding our understanding of this compensatory dynamic in relation to other ecosystem services.

The dependence on low tide emergence in estuaries within this study and globally are likely to strengthen if light limitation and water column turbidity continue to increase. In addition, there has already been a 16 % decline in worldwide intertidal habitats over the last 30 yr (Murray et al., 2019), a consequence primarily attributed to coastal development and land reclamation (MEA 2005, Blum and Roberts, 2009, Field et al., 2014), an inevitable outcome of growing coastal populations worldwide (Airoldi and Beck, 2007). Intertidal areas are disproportionately impacted such that many countries have already lost over half of their intertidal habitats (Perkins et al., 2015). Climatic changes will exacerbate these effects, as sea-level rise and stormier seas begin to inundate coastal areas (Nicholls and Cazenave, 2010). The most extreme sea-level rise scenario of the Intergovernmental Panel on Climate Change (RCP8.5) predicts a 0.6 – 1.1 m increase by 2100 (Pörtner et al., 2019), with other estimates of up to 1.4 m (Rahmstorf, 2007, Turner et al., 2009, NRC 2012) and exceeding 2 m (Kopp et al., 2017). This in turn will increase the demand for flood and erosion protection (Hallegatte et al., 2013), further driving habitat loss and alterations (Airoldi and Beck, 2007). For example, sea defences constrict the ability of the intertidal to shift with SLR, ultimately resulting in the squeezing and reduction of intertidal areas. These significant alterations of important physical, chemical and biological processes unique to intertidal habitats have detrimental implications to benthic community structure and the associated ecosystem functions derived from these habitats (Perkins et al., 2015).

Despite the fact SLR has been described as one of the greatest potential causes of ecosystem disruption and global species extinctions (Noss, 2011), we know very little of the ecological implications on intertidal areas. To provide a first-order estimation of the loss of intertidal area with SLR on our study estuaries, we used hypsometry curves (Figure 2.7) to determine their sensitivity. Hypsometry curves are calculated using bathymetric grids, and compare the cumulative distribution of surface area with respect to elevation (for more details see Text A1.1), with the

shape of the curve influenced by the curvature of the shoreline, tidal range, net sediment transport and wind-waves (Friedrichs and Aubrey, 1996). The change in intertidal area (defined as the area between mean high/low water spring tide) following SLR scenarios from 0.2 – 1.4 m (Rahmstorf, 2007, Turner et al., 2009, NRC 2012, Pörtner et al., 2019) were then calculated (Figure 2.8). Assuming the intertidal area does not migrate landward (either restricted due to flood and coastal defences or occurs so rapidly there is a long hysteresis in ecological/morphological recovery), the resulting loss of intertidal area in our focal estuaries would range from 27 – 94 % (Figure 2.8). The difference in calculated estimates stems from the slope of the hypsometry curve, such that those estuaries with the most gradual slopes result in the largest losses of intertidal area. This is exemplified within TAU (Figure 2.8) where a relatively small increase in sea level can disproportionately result in a large loss of intertidal area. In addition, MAH highlights the non-linear rate of change observed in several estuaries, where a 0.2 m increase in sea level from 0.6 to 0.8 m produced an abrupt (18 %) loss of intertidal area. It should be noted that these estimates of intertidal loss are an over-simplification of highly complex and dynamic systems with both landward and seaward influences. For example, it discounts the role of changes to sedimentation rates and biomorphodynamic feedbacks which can build new land (D'Alpaos et al., 2007) and potential changes to sediment supply due to altered storm frequencies and intensities (Seneviratne et al., 2012). Despite its limitations, this analysis does provide a framework to examine the relative extent of intertidal area lost which is likely to have far-reaching ecological consequences for coastal ecosystems.

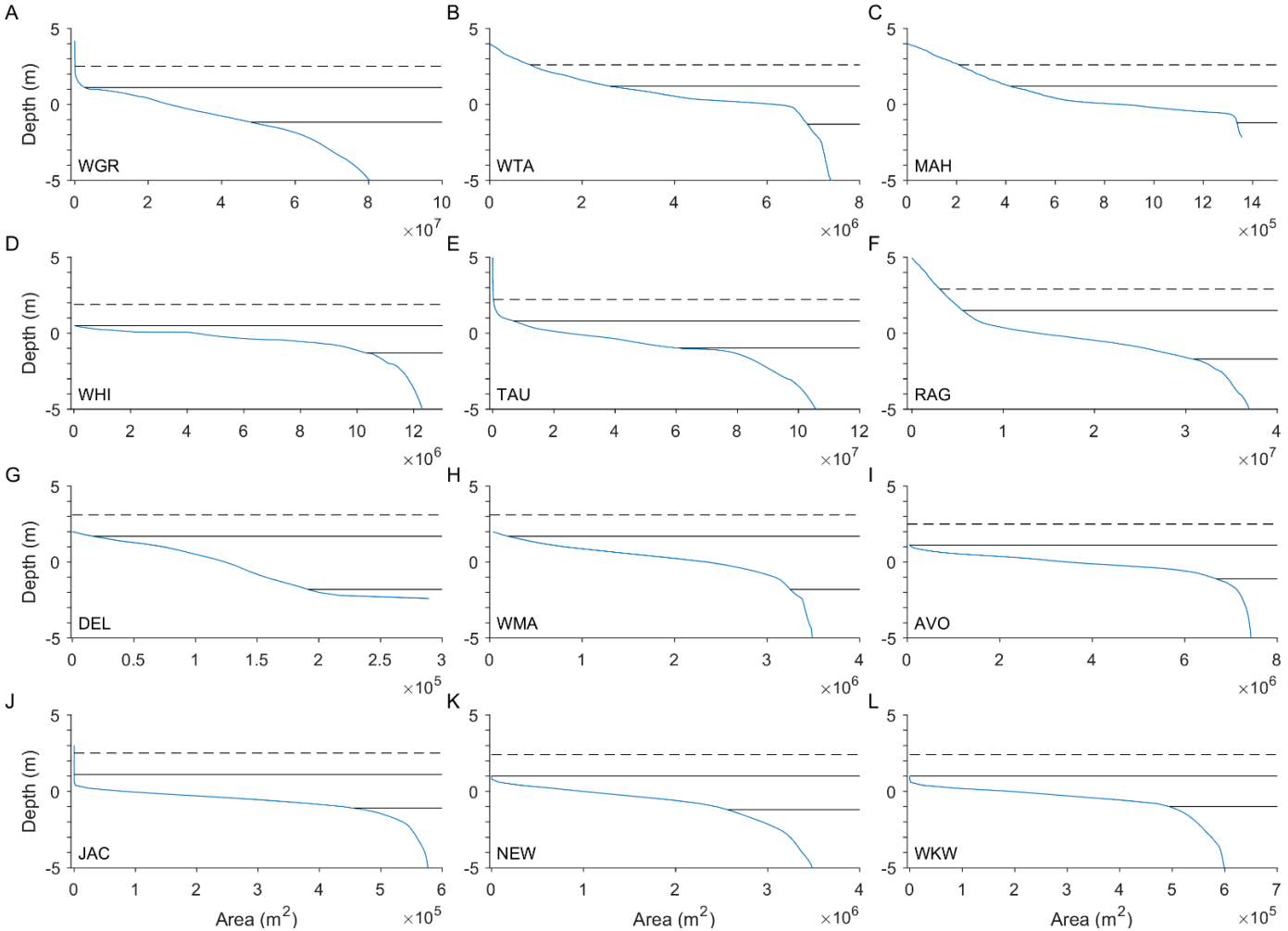

Figure 2.7: Estuary hypsometric curves (see Text A1.1) ordered by latitude (north to south: A–L). The upper and lower solid black lines represent the water level at high and low tide during a spring tide, respectively, and the dashed black line represents a 1.4 m increase in sea level. For locations of each estuary, see Figure 2.1. Site abbreviations are defined in Table 2.1.

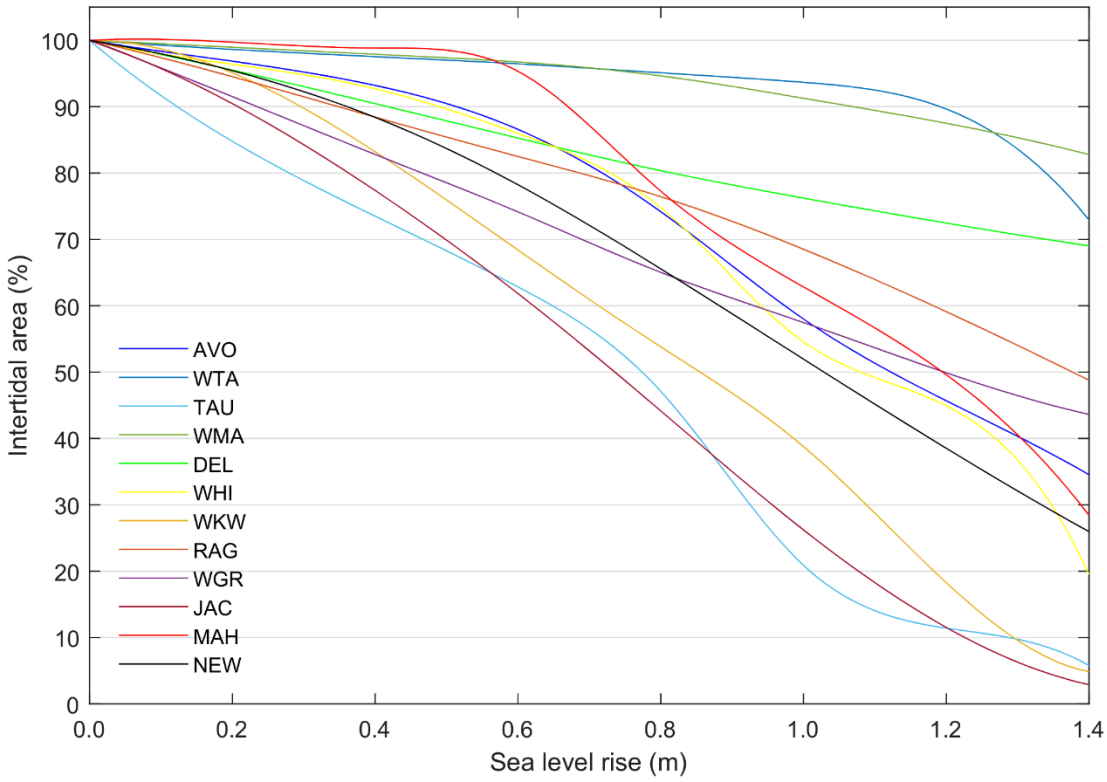

Figure 2.8: Calculated change in intertidal area (derived from hypsometric curves shown in Figure 2.7) as a function of sea level rise up to 1.4 m (predicted for 2100; Rahmstorf 2007, Turner et al. 2009, NRC 2012). Sites are ordered from highest to lowest median immersed photosynthetically active radiation over the 9 mo study period. Site abbreviations are defined in Table 2.1.

When these future predictions of intertidal area are coupled with light limitation estimates, the vulnerability of different estuaries to loss of MPB production can be considered. For example, both TAU sites exhibited a relatively low proportion of light limitation (~60 % during immersion), and therefore the large loss of the intertidal here is least likely to result in significant changes to benthic primary production and ecosystem functionality. Conversely, WHI has a predicted loss of 80 % intertidal area, in conjunction with having one of the poorest light climates during immersion at the upper estuarine site (WHI-2, 88 % light limitation). For WHI-2 and other sites where high turbidity and large reductions of intertidal area co-occur (e.g., RAG, WGR), vulnerability to the loss and degradation of ecosystem functioning will increase, as emersion periods, which were providing a level of resilience to estuarine ecosystems, become restricted. However, even estuaries with low turbidity may become vulnerable in the future if increases in the

frequency and intensity of extreme weather events deliver more land-derived sediment and nutrient inputs increasing water column turbidity (Seneviratne et al., 2012). Ultimately, the reduction in benthic MPB production will lead to a reduced capacity to moderate pollutant loads (NRC 2007), a loss of climate regulating services such as carbon sequestration (Yim et al., 2018) and changes in trophic structure, nutrient cycling and productivity (Dugan et al., 2018). These all feedback within the system, modifying trophic interactions and ecological networks, pushing ecosystems closer to tipping points (Scheffer and Carpenter, 2003, Thrush et al., 2014, Selkoe et al., 2015).

2.5 Conclusions

Using light measurements conducted across a large latitudinal gradient and a literature compilation of P–I curves, our findings demonstrate that light attenuation within estuaries can substantially limit MPB primary production. Considering that water column turbidity is a widespread and global stressor, that our study estuaries incorporate a range of estuarine topography, and the generality in overall patterns, we suggest these results are not only relevant to barrier-enclosed coastal lagoons such as those used in this study, but also to other coastal systems where MPB are the dominant primary producers. As a consequence of high light limitation observed at some sites, benthic productivity can become entirely reliant on periods of emersion, resulting in reductions of overall productivity and the associated ecosystem functions and services provided by MPB. This will influence the vulnerability of estuaries, through the potential reduction of intertidal areas via both SLR and land reclamation practices. The health and functioning of an estuary under future global change, is therefore likely to be closely coupled to light climate reaching the sediment surface but also to the proportion of intertidal area within an estuary. A deeper understanding of how MPB respond to future local and global stressors in a changing climate is critical to prevent the ecological collapse of these fundamental coastal ecosystems on which humanity relies.

Chapter Three: Water column turbidity not sediment nutrient enrichment moderates microphytobenthic primary production

3.1 Introduction

Soft sediment intertidal habitats are under intense anthropogenic pressure which is diminishing ecological functioning and the delivery of ecosystem services upon which humanity relies. Globally, the most pervasive pressures include significant increases in nutrient and sediment delivery (Levin et al., 2001) predominately through discharges of surface run-off and groundwater inputs (Nixon, 1995, Valiela and Bowen, 2002). These act to modify coastal nitrogen cycling as well as increase light attenuation to the benthos (Vitousek et al., 1997, Smith, 2003). Ultimately, this can diminish benthic primary productivity which cascades to alter global carbon budgets, food web dynamics and water quality parameters (Miller et al., 1996, Duarte et al., 2005, Christianen et al., 2017). Despite its importance, there is currently a limited understanding of how these pervasive pressures may interact and influence benthic productivity on intertidal flats over alternating periods of high and low tide within ecologically relevant contexts. Here for the first time, we couple in situ submerged and emerged primary production estimates across two seasons, in response to elevated sediment nutrient enrichment, over a natural gradient of water column turbidity.

Microphytobenthos (MPB) are often the dominant primary producer in shallow temperate ecosystems, accounting for up to 50 % of total estuarine autochthonous primary production and up to 80 % of total benthic carbon fixation (Underwood and Kromkamp, 1999). While MPB productivity can supply high-quality labile carbon, and thus underpin coastal food webs (Christianen et al., 2017), MPB also modify sediment stability and, through oxygenation of the sediment and nutrient uptake, alter biogeochemical pathways including nutrient

recycling (Miller et al., 1996, Tolhurst et al., 2008, Hope et al., 2020). MPB are therefore fundamental constituents of intertidal habitats, with reductions in productivity likely to have cascading implications for entire coastal ecosystems.

Rates of MPB production are moderated by a number of factors such as hydrodynamic conditions, carbon supply, the availability of nutrients and light climate (Kromkamp et al., 1995, Perkins et al., 2001). Of particular importance during submerged tidal periods is light availability (Mangan et al., 2020a). Increases in water column light attenuation are predominately a product of suspended sediment concentrations (Anthony et al., 2004) but can additionally be influenced by phytoplankton blooms in response to nutrient enrichment (Rabalais et al., 2005). High water column turbidity restricts the amount of light reaching the seafloor and thus can directly diminish MPB production. While MPB have been shown to adapt to light conditions as low as 2.8 µmol m^{-1} s^{-1} (Gattuso et al., 2006), maximal rates of productivity are often proportional to light saturation values (Mangan et al., 2020a) and therefore productivity and the ecosystem services provided by MPB are often reduced with decreasing light availability. For example, reduced productivity (when light attenuation is high) causes feedbacks within the system via a reduction in labile organic carbon available to consumers, increases in the efflux of dissolved inorganic nitrogen from the sediment (Pratt et al., 2014), reductions in macrofaunal diversity (Morris and Keough, 2003) and alterations to sediment stability (Tolhurst et al., 2008).

Within subtidal environments where turbidity can remain consistently high, a tipping point can occur where the system moves from benthic to pelagic dominated primary production (Cooper and Brush, 1993). However, for intertidal environments, water column turbidity is a temporally displaced stressor as the tide recedes and exposes the sediment surface to high light availability. Therefore, exposure associated with low tide periods can provide some resilience to reduced MPB production during submerged periods. This has been demonstrated in several estuaries throughout the world, where benthic primary productivity is often reported to be limited to low tide periods (Guarini et al., 2002, Migné et al.,

2004, Spilmont et al., 2006, Migné et al., 2018). The dependence on this exposure period and the relative contribution of low tide MPB production may therefore be closely coupled to site turbidity (Drylie et al., 2018). Despite this crucial link, there are few studies where direct comparisons of emerged and submerged primary production exist (Denis et al., 2012, Walpersdorf et al., 2016, Migné et al., 2018), especially through time and along a transitional gradient of water column turbidity. These knowledge gaps are limiting our ability to understand the effects of increased anthropogenic pressure.

Increased water column turbidity often occurs concomitantly with increased nutrient inputs. While it is well known that increased nutrient availability can lead to phytoplankton blooms, increases in filamentous benthic macroalgae and ultimately coastal eutrophication (Duarte, 1995, Cloern, 2001), the response of MPB production is less understood. This may be partially attributed to the majority of research focusing on the individual influences of elevated nutrients during one phase of a tidal cycle. However, nutrient responses by MPB are likely to be tightly coupled to light availability (Stutes et al., 2006) and differ depending on tidal state. For example, an increase in nutrient availability has been shown to stimulate MPB productivity in a nutrient-limited system with high light availability during tidal submergence (Hillebrand et al., 2000). However, in a highly turbid but nutrient-rich estuary, light limitation was sufficient to prohibit MPB production and thus nitrogen uptake (Meyercordt and Meyer-Reil, 1999). Conversely, during tidal emergence in a high nutrient system, MPB were not observed to be nutrient-limited (de Jonge et al., 2012, Kwon et al., 2018), while in a low-nutrient system, the response of MPB is still largely unknown. Considering the multifaceted response of MPB within intertidal habitats to nutrient enrichment, it is vital for investigations to include a comparison of responses across tidal cycles, in combination with other pressures (such as water column turbidity) and which encompass timeframes that allow the incorporation of longer-term responses (e.g., microbial and macrofaunal community responses).

The objective of this study was to investigate the interactive effects of sediment nutrient enrichment and water column turbidity on both submerged and emerged MPB primary production. This was carried out by experimentally enriching the sediment at three levels for up to 20 months along a gradient of water column turbidity. Within the main objective, we postulate two questions; (1) how does water column turbidity influence submerged and emerged MPB primary production, and is this modified by sediment nutrient enrichment? In addition, (2) are these responses temporally variable? We hypothesised that water column turbidity would reduce submerged primary production resulting in an increased proportion of emerged productivity, and that both submerged and emerged productivity would increase with nutrient enrichment through an increase in MPB biomass. This research aims to fill a critical gap in our understanding of how two pervasive stressors may interact within natural environments, with a focus on MPB production, an often forgotten but integral component of coastal ecosystems (MacIntyre et al., 1996).

3.2 Materials and Methods

3.2.1 Study sites

This study was carried out at 6 sites within 4 estuaries of the North Island of New Zealand (Figure 3.1; for site-specific GPS coordinates see Table A2.1). All estuaries were shallow, barrier enclosed coastal systems with an extensive intertidal area and had semi-diurnal tides. Sites were chosen based on a perceived gradient of water column turbidity while having a similar latitude to normalise for daylength and temperature. In addition, sites were located within the mid-intertidal region and inhabited by the functionally important bivalve species *Austrovenus stutchburyi* and *Macomona liliana,* which have been shown to significantly influence benthic-pelagic coupling (Woodin et al., 2016).

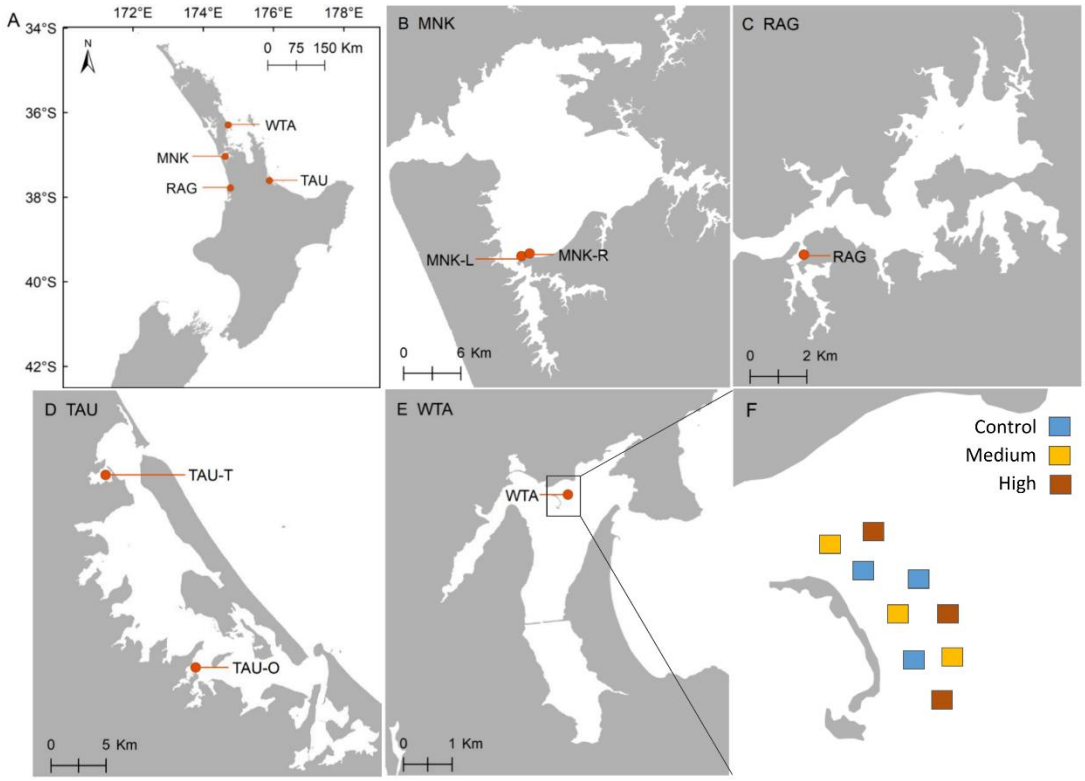

Figure 3.1: Location of the four estuaries within the North Island of New Zealand (A), and sampling sites within (B) Manukau (MNK), (C) Raglan (RAG), (D) Tauranga (TAU) and (E) Whangateau (WTA) estuaries. Panel (F) depicts an example of the allocation of nutrient enrichment treatments (control = 0, medium = 150 and high = 600 g N m^{-2}) to experimental plots within the Whangateau estuary. For site-specific GPS locations see Table A2.1.

3.2.2 Experimental design

The experimental period spanned a total of 20 months with sampling in November 2017 (T1), June 2018 (T2; 3 sites only: TAU-T, TAU-O, RAG) and November 2018 (T3), corresponding to 8, 15 and 20 months of sediment nutrient enrichment, respectively (Table 3.1). Two November sampling periods were chosen to correspond with warmer late spring temperatures and higher light availability, and allowed the incorporation of potentially longer-term responses to nutrient enrichment (e.g., alterations of macrofaunal communities). An additional winter sampling (June 2018) at three sites was conducted to examine the potential influence of reduced temperatures and light conditions on primary production measures.

Table 3.1: Experiment timeline and parameters measured. T1 and T3 sampling includes all 6 sites, T2 sampling includes only 3 (TAU-O, TAU-T and RAG). The alignment of tick marks denotes the order of procedure.

	March 2017	November 2017 (T1)	June 2018 (T2)	November 2018 (T3)
Sediment nutrient enrichment	√	√	√	
Characterisation of site PAR	→			
Primary production measures				
Submerged (O_2 flux)		√	√	√
Emerged (CO_2 flux)			√	√
Sediment characteristics		√	√	√
Macrofaunal composition		√		√

PAR = photosynthetically active radiation

At each site, nine 9 m^2 experimental plots were divided into three nutrient enrichment groups, either control 0 g N m^{-2}, medium 150 g N m^{-2} or high nutrient treatment 600 g N m^{-2} (Figure 3.1F). These levels were chosen to represent concentrations found in eutrophic estuaries globally and correspond to those previously used by Douglas et al. (2016). To achieve enrichment, a slow-release urea fertiliser (Nutricote 40:0:0 N:P:K) was added at two known quantities to a series of 180 evenly spaced holes at a depth of 15 cm by extracting a sediment plug (3 cm diameter) with a handheld corer, adding a known volume of fertiliser and then replacing the sediment plug. Nitrogen-only fertiliser was used since New Zealand estuaries are typically N limited and because the urea in Nutricote quickly hydrolyses to ammonium (NH_4^+), a form of nitrogen associated with eutrophication and the remineralisation of organic matter (Tay et al., 2013). This method results in an even elevation of porewater NH_4^+ throughout the experimental plots (Douglas et al., 2016). To maintain enrichment throughout the experimental period, fertiliser was first applied in March 2017 and reapplied following sampling in November 2017 and June 2018 (Table 3.1). Sampling, therefore, took place between 5 and 8 months after each application of fertiliser.

3.2.3 Primary production measurements

Primary production was measured during submergence at all sites in November 2017 and 2018, and at TAU-O, TAU-T and RAG in June 2018. On each sampling date, an Odyssey PAR (photosynthetically active radiation) logger (Dataflow Systems) was deployed in the middle of each site and on the shore to capture light availability at the sediment and water surface, respectively. Two benthic flux chambers were deployed in each plot for approximately 4 h during a midday high tide. Each chamber base (50 cm × 50 cm × 15 cm) was inserted 5 cm into the sediment at low tide and equipped with a light and temperature logger (HOBO Pendant®). On the incoming tide, chambers were sealed with a Perspex dome lid and any air bubbles removed, encapsulating 41 L of seawater over the sediment surface. An opaque shade cloth covered one of the two chamber lids per plot to block out all sunlight, while the other lid was left uncovered to receive ambient sunlight. Immediately after the chambers were sealed and at the end of the incubation, one 60 mL seawater sample was collected from each chamber to provide initial and final dissolved oxygen concentrations. Seawater dissolved oxygen concentration was measured on-site immediately after sampling using a handheld optical probe (PreSens FIBOX 3 LCD trace v7). In June and November 2018, this was supplemented with a dissolved oxygen logger (PME miniDOT) deployed within each chamber recording at a 1-min sampling frequency. Preliminary analysis of the probe and logger O_2 values showed sufficient compatibility between instruments and therefore logger values were used for all T2 and T3 analyses.

Emerged primary production was assessed within 10 d of the submerged measurements in June 2018 at TAU-O, TAU-T and RAG, and at all sites in November 2018 over a midday low tide. For the full emerged period, an Odyssey PAR light logger was deployed in the middle of the site to capture ambient light availability. Once the site was drained of water, one chamber base in each plot was inserted 5 cm into the sediment. During each measurement, the chamber contained an Odyssey PAR light logger, a pressure vent, a thermocouple measuring chamber air

temperature and a battery-powered fan. The fan maintained airflow and gentle mixing to ensure no dead spaces were created inside the chamber which could alter the diffusion of gases from the sediment (Eklund, 1992). A Perspex lid was then fitted over the chamber and connected to an infrared gas analyser (LI-COR 8100A Automated Soil CO_2 Flux System) where air was continuously circulated between the analyser and the chamber. Measurements of CO_2 concentration (ppm) were recorded at a frequency of 1 Hz for a total incubation period of 5 min. This method has been shown to provide a reliable quantification of CO_2 exchange in intertidal habitats, with a 5 min period resulting in a stable diffusion of CO_2 without increasing the humidity within the chamber (Migné et al., 2002, Drylie et al., 2018). Light incubations were conducted before an opaque shade cloth was placed over the chamber base and allowed to acclimate for 20 min prior to an additional CO_2 incubation performed in dark conditions.

3.2.4 Site characteristics

Water column turbidity was assessed by measuring light availability reaching the sediment surface every 10 min over a 9-month period (between March and November 2017; see Chapter 2), with PAR_{Site} an average of the maximum daily submerged PAR values during this period. To characterise sediment properties, on each submerged sample date, five pooled surface sediment cores (2.6 cm dia, 2 cm deep) were taken from each experimental plot and frozen at −20 °C (Arar and Collins, 1997) until analysis for sediment chlorophyll *a*, phaeopigments, grain size and organic matter content. Two separate replicates of 4 additional sediment core samples at depths of 0–2 cm and 5–7 cm were taken within each plot and kept on ice for analysis of sediment porosity and porewater ammonium concentrations. To assess any potential desiccation during emerged primary production measurements, four pooled 0–2 cm and 5–7 cm sediment cores (2.6 cm dia) were also taken and kept on ice until analysis of sediment porosity. Two macrofauna cores (13 cm dia, 15 cm depth) were taken from each plot in November 2017 and 2018 and sieved on a 500 µm mesh before being preserved in 70 % Isopropyl alcohol.

3.2.5 Laboratory analysis

Sediment samples were thawed and homogenised before analysis. To determine concentrations of chlorophyll *a* and phaeopigments, a sub-sample of sediment was freeze-dried, extracted with 90 % buffered acetone and measured before and after acidification using a fluorometer (Turner Designs 10-AU). Grain size was measured using laser diffraction (Malvern Mastersizer-3000) after the digestion of organic matter with 10 % hydrogen peroxide. Organic content was determined by weight loss on ignition following 3 d at 60 °C to ensure a constant weight and then combustion at 550 °C for 4 h. Sediment samples collected for porewater ammonium determination underwent water extraction within 24 h of collection. Four ml of de-ionised water was added to each sample before being vortexed and centrifuged. The supernatant was then filtered through a 0.45 µm Whatman GF/C glass fibre filter and stored at −20 °C. Analysis for porewater ammonium concentration was conducted on a Lachat QuickChem 8000 Series FIA+ (Zellweger Analytics Inc. Milwaukee, Wisconsin 53218, USA) using standard operating procedures for flow injection analysis. Sediment porosity samples (both for porewater calculations and those taken during each emerged incubation) were analysed by calculating the difference in wet and dry weight after 7 days at 60 °C (or until constant weight). Macrofauna samples (6 per treatment in T1 was reduced to 3 per treatment in T3 as no statistical difference in univariate measures were detected) were stained with Rose Bengal and fauna separated from any sediment and shell hash before being identified to the lowest possible taxonomic level (usually species) and counted.

3.2.6 Data analysis

Submerged dissolved O_2 and emerged CO_2 fluxes were estimated from the change in concentration during the incubation period and corrected for the chamber area and volume. Submerged O_2 fluxes were not corrected for water column processes owing to the small contribution relative to benthic production/respiration (<5 % of the measured chamber flux, data not presented). A respiratory quotient of 1 was used to convert CO_2 consumption and production measurements to O_2

production and consumption, respectively. This value is likely to be realistic for well-oxygenated sediments with low mud and organic content (Boucher et al., 1994), such as those within this study. Light chamber fluxes were equivalent to net primary production (NPP; µmol O_2 m^{-2} h^{-1}) and dark chamber fluxes to sediment oxygen consumption (SOC). The sum of these two fluxes from paired chambers within a plot provided an estimate of gross primary production (GPP). A productivity/respiration (p/r) ratio was calculated for each chamber, as defined by Eyre and Ferguson (2002): (hourly productivity (GPP) × daylight period)/(hourly respiration × 24 h), to estimate if the sediments were net autotrophic (p/r > 1; more carbon is produced than respired), or net heterotrophic (p/r < 1; more carbon is respired than produced).

Odyssey PAR logger data were converted from count measurements to PAR (µmol m^{-2} s^{-1}) by a calibrated regression with a LI-COR PAR sensor prior to deployment. Three values of PAR are used throughout this study: site PAR (PAR_{Site}), incident PAR (PAR_i) and sediment surface PAR (PAR_{Sed}). PAR_{Site} is used as a proxy for site turbidity as described above, where a higher PAR_{Site} value indicates lower site turbidity. The other two PAR measurements correspond to those taken during sampling and are used for normalising rates of primary production. PAR_i describes light received at the sediment surface during emerged incubations and at the water surface during submerged incubations. Whereas PAR_{Sed} refers to light received at the sediment surface during the submerged incubations and therefore accounts for water column attenuation. GPP was first normalised by PAR_i (GPP_i) to account for variability in light intensities between sampling dates while retaining attenuation effects of the water column (e.g., from turbidity). GPP was additionally normalised by PAR_{Sed} and photosynthetic biomass (sediment chl *a* i.e., productivity per unit of photosynthesising biomass (Pratt et al., 2014)) to determine photosynthetic efficiency ($GPP_{Sed + chla}$).

To determine if nutrient enrichment influenced primary production estimates and if this differed between sites and sampling events, a preliminary analysis using repeated measures PERMANOVA was conducted. For submerged fluxes, nutrient

enrichment (3 levels), site (6 levels) and time (2 levels; T1 and T3) were set as fixed factors and replicate plot nested within treatment. T2 was omitted because measurements were only made at 3 of the 6 sites. For emerged fluxes, site was reduced to 3 levels (RAG, TAU-O, TAU-T) and time included T2 and T3 (Figure A2.1, Table A2.5). These analyses revealed high spatial and temporal variability. This was expected due to the extent of the experiment (6 different sites within 4 estuaries, over 20 months) which spanned a range of environmental conditions expected to influence primary production. To differentiate between this natural heterogeneity (in both time and space) and reveal any potential treatment effects, submerged and emerged primary production estimates (NPP and GPP) were normalised by an average of the control plot values. This resulted in treatment effect size being relative to the site-specific background level and sampling date. Control normalised (CN) submerged and emerged primary production estimates were tested for differences from control values (i.e., NPP_{CN}, $GPP_{CN} \neq 1$) using one-sample *t*-tests. Differences between nutrient enrichment treatments (medium vs. high) were tested using two-sample *t*-tests and between sampling periods (for submerged data only) (T1 vs. T3) using paired two-sample *t*-tests. Statistical analyses for the control normalised data were performed using the R stats package (v3.6.2) in R Studio.

No significant treatment effects on primary production were detected in the PERMANOVA (Figure A2.1, Table A2.5) or control normalised analyses (see Results) and therefore raw (i.e., not control normalised) data were pooled for subsequent analysis. To investigate if site turbidity modified the relative importance of submerged and emerged primary production and to see if this was consistent through time, two repeated measures PERMANOVA's were conducted. The first using T3 (November 2018) data with site and tidal state as fixed factors (6 and 2 levels, respectively) and replicate plot nested within site. The second considered a temporal element by including site (fixed factor, 3 levels: TAU-O, TAU-T and RAG), time (fixed factor, 2 levels: T2 and T3) and tidal state (fixed factor, 2 levels: submerged and emerged) with replicate plots nested within the site. All similarity matrices were based on Euclidian distances, and primary production measures

tested were NPP, GPP, GPP_i, $GPP_{Sed + chla}$. Main effects were not considered if interaction terms were significant, and instead, posthoc tests identified differences between sites, tidal state and sampling date.

Distance-based Linear Models (DistLM) were then used to identify if any environmental (sediment characteristics, light etc.) or univariate macrofaunal variables were significant drivers of primary production measures across all nutrient enrichment treatments, sites and sampling dates. First, predictor variables were normalised to allow for comparisons despite differing units and scales. Significant individual predictors (marginal tests) could then be identified and the best combination of predictor variables (stepwise procedure) of NPP and GPP during submerged and emerged tidal periods calculated. The corrected Akaike information criterion (AICc) was used for all models as AICc is suggested to be most appropriate when there are a large number of predictor variables relative to the sample size (sample number/n. explanatory variable < 40) (Burnham and Anderson, 2002). Where co-linearity occurred among predictor variables ($r > 0.7$), the variable explaining the least amount of variability was omitted from the full model. For June 2018 (T2), macrofauna data between the two November samples were averaged so this sample date could be included. Variance partitioning was used to determine how much of the observed variability was attributed to significant environment variables (organic content, mud content, median grain size, sediment chl *a* content, phaeophytin content, PAR_i, PAR_{sed} (submerged data only), PAR_{site} and temperature (sediment surface)), community variables (total abundance, taxa richness, *A. stutchburyi* abundance and *M. liliana* abundance) and porewater variables (NH_4^+ concentration at 0–2 cm and 5–7 cm sediment depth and porosity at 0–2 cm (emerged data only)). The two bivalve species were included based on their known influence on benthic processes within these systems (Woodin et al., 2016). All PERMANOVA and DistLM analysis were performed using PRIMER 7 with the PERMANOVA+ package.

3.3 Results

3.3.1 Site characteristics

During the deployment of the PAR light loggers, no fouling or sediment deposition was observed and therefore the difference in measured light availability between sites during submergence confirms a gradient in water column turbidity was captured across the six sites (PAR_{Site}; Figure 3.2A). Light availability was lowest at MNK-L and MNK-R with a median maximum daily PAR of 218 and 290 µmol m^{-2} s^{-1}, respectively. In addition, the interquartile range (IQR) was relatively low for both sites (297 and 365 µmol m^{-2} s^{-1}, respectively), which is suggestive of a consistently low light climate and thus high turbidity. RAG while having a similar IQR to both the MNK sites (283 µmol m^{-2} s^{-1}), had a higher median maximum daily PAR of 500 µmol m^{-2} s^{-1}. In contrast, TAU-O, TAU-T and WTA had a considerably higher median maximum daily PAR (784–1140 m^{-2} s^{-1}), suggestive of overall less turbid water, and a high IQR (512–762 m^{-2} s^{-1}), indicative of intermittent increases in turbidity (rather than persistently high). Sediment surface PAR (PAR_{Sed}) measurements during submerged sampling periods suggest this gradient of water column turbidity was captured during each sampling event (Figure 3.2B–D). Where high incident light (PAR_i) occurred, greatest differences between PAR_{Sed} were observed at MNK-L, MNK-R and RAG. However, these differences are less pronounced with lower PAR_i values (e.g., during T2 sampling in winter).

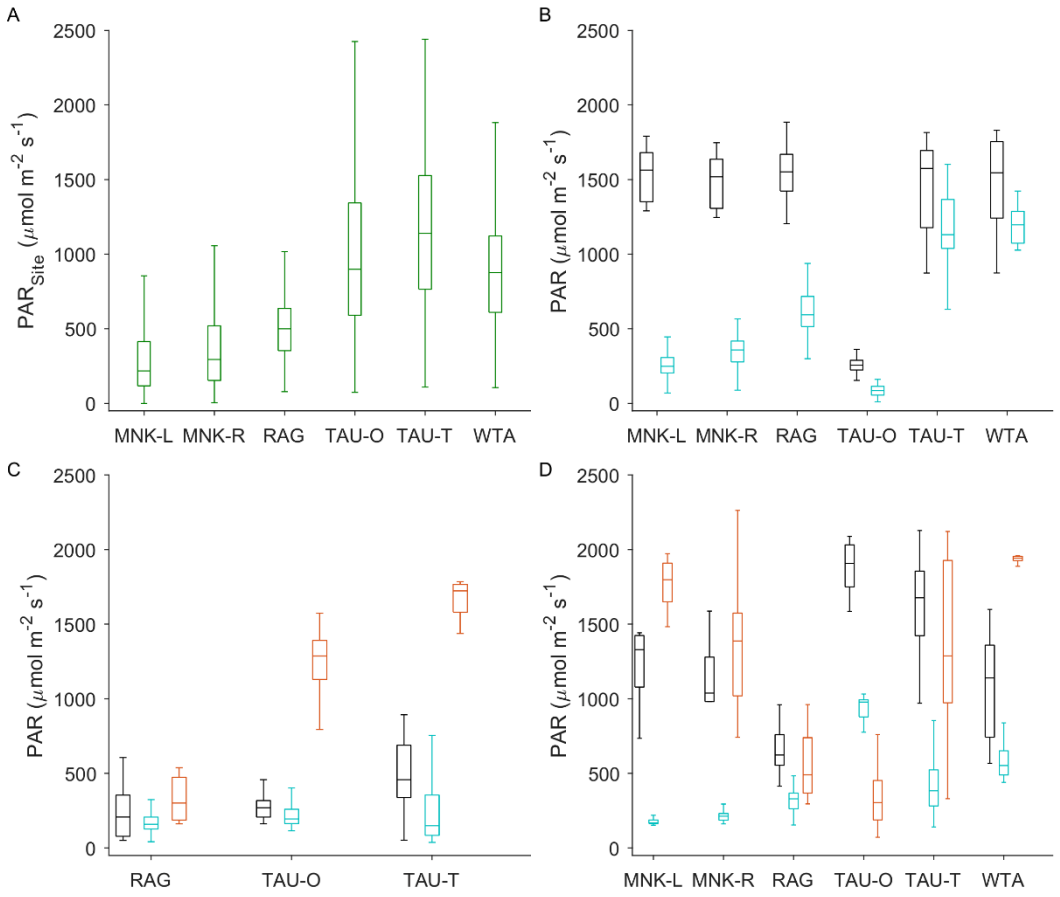

Figure 3.2: Measured photosynthetically active radiation (PAR) at each site; (A) PAR_{Site}, daily maximum value over a 9-month period (March–November 2017), and during primary production measurements in (B) November 2017 (T1), (C) June 2018 (T2) and (D) November 2018 (T3). Black and blue bars indicate PAR_i (incident, water surface) and PAR_{Sed} (sediment surface), respectively, during submerged sampling periods. Red indicates PAR_i during emerged sampling. Boxes represent the 25th and 75th percentiles, whiskers the 5th and 95th percentiles and a solid line within each box denotes the median.

No consistent relationship was found between water column turbidity and sediment characteristics (Table 3.2). On average, mud content was relatively low (<4 %) at MNK-R, TAU-T and WTA on all sampling dates. The highest mud content was recorded at RAG (maximum of 28 %) with both MNK-L and TAU-O predominately >10 %. Organic content was also relatively low at all sites (<5 %) while median grain size (MGS) varied between sites (an average of 123 µm in RAG to 248 µm in WTA). Microalgal biomass (sediment chl *a* content) was highly variable with no clear relationship between sites or sampling dates. Univariate measures of macrofaunal community differed between sites (Table 3.2; see Tables A2.3 and A2.4 for community composition data). Most notable was the high

abundance of *A. stutchburyi* (>50 core^{-1}) at MNK-L, RAG and WTA which contributed to higher total macrofaunal abundance.

3.3.2 Treatment effects on sediment properties

Sediment nutrient enrichment successfully increased porewater ammonium concentration at all sites throughout the experimental period (Table A2.2). On average, porewater ammonium (NH_4^+) increased 40-fold in medium treatments and 800-fold in high treatments relative to control concentrations at a depth of 0–2 cm. Porewater NH_4^+ concentration was typically higher at a depth of 5–7 cm relative to 0–2 cm, with 70 and 990-fold average increases in the medium and high treatments, respectively (relative to control concentrations). Successful nutrient enrichment consequently altered sediment porewater N:P ratios (Figure A2.2). Within control plots, N-limitation was predicted to occur at all sites through time (N:P < 16), while a switch to P-limitation likely occurred in all enriched plots through time (assuming a switch from N- to P-limitation is likely to occur at an N:P ratio between 10 and 16 (Redfield, 1963, Montani et al., 2003)). Overall, sediment enrichment did not translate into substantial changes in sediment properties (grain size, mud content and organic content) (Table A2.2). A medium level of nutrient enrichment typically did not alter macrofaunal communities (Tables A2.2–A2.4). However, negative responses were observed within high treatment plots, such as reduced abundance or loss of *A. stutchburyi* and *M. liliana* (Table A2.2).

Table 3.2: Site characteristics during November 2017 (T1), June 2018 (T2) and November 2018 (T3). Data presented are an average across the three nutrient enrichment treatments (n = 9), with the range in parentheses.

Site	Time	Sediment Properties			Porewater	Microphytobenthic Biomass		Macrofaunal Community			
		OC	Mud	MGS	NH_4^+ (0–2 cm)	Chl *a*	Phaeo	N	S	*A. Stutchburyi*	*M. Liliana*
		%	%	µm	µmol N L^{-1}	µg DW g^{-1}	µg DW g^{-1}	n $core^{-1}$	n $core^{-1}$	n $core^{-1}$	n $core^{-1}$
MNK-L	T1	2.2 (2.0–2.3)	9.6 (7.0–12)	202 (196–211)	1448 (178–5479)	15 (2.1–24)	10 (0.6–26)	66 (44–82)	14 (11–19)	1 (0–4)	3 (0–8)
	T2	-	-	-	-	-	-	-	-	-	-
	T3	3.0 (2.4–3.4)	11 (9.0–14)	197 (188–214)	2097 (27–9277)	14 (3.9–19)	13 (8.8–25)	207 (102–343)	18 (11–24)	76 (52–100)	6 (0–14)
MNK-R	T1	1.2 (1.0–1.4)	1.3 (0.6–2.3)	198 (194–201)	1815 (171–6721)	9.3 (4.5–13)	5.0 (0.5–17)	89 (12–117)	15 (7–19)	6 (1–12)	3 (0–7)
	T2	-	-	-	-	-	-	-	-	-	-
	T3	1.3 (1.0–1.7)	3.8 (0.9–9.7)	196 (183–204)	6478 (3.7–28861)	8.3 (4.8–11)	5.7 (3.9–8.3)	72 (30–136)	16 (9–25)	9 (4–13)	12 (1–25)
RAG	T1	3.8 (3.6–4.3)	17 (15–23)	130 (118–140)	3577 (21–21214)	15 (5.0–28)	10 (0.9–22)	167 (116–222)	20 (15–22)	53 (25–83)	2 (0–6)
	T2	3.2 (3.1–3.3)	25 (24–26)	119 (118–122)	1132 (63–4425)	16 (14–18)	10 (8.5–12)	-	-	-	-
	T3	4.2 (3.5–4.7)	24 (19– 28)	121 (112–132)	28484 (13–96923)	16 (14–20)	9.4 (7.4–13)	131 (65–225)	14 (9–22)	66 (35–87)	2 (0–8)
TAU-O	T1	2.6 (2.5–3.0)	13 (9.4–18)	166 (150–187)	1029 (7.6–3584)	19 (15–31)	4.9 (2.4–8.6)	197 (132–323)	19 (15–24)	22 (10–50)	11 (2–20)
	T2	1.3 (1.3–1.4)	4.1 (3.5–4.9)	200 (199–202)	4125 (0.1–13512)	11 (8.7–14)	3.9 (3.4–4.8)	-	-	-	-
	T3	2.8 (2.6–3.0)	12 (10–14)	157 (148–167)	2763 (3.8–11798)	15 (9.4–22)	5.2 (3.1–8.1)	26 (2–46)	8 (2–13)	1 (0–1)	2 (0–7)
TAU-T	T1	1.3 (1.1–1.6)	4.0 (2.6–4.8)	203 (193–212)	1264 (7.0–6741)	8.8 (4.2–12)	2.4 (1.1–3.1)	55 (24–88)	15 (9–22)	3 (0–7)	11 (2–21)
	T2	2.4 (2.2–2.6)	13 (12–13)	156 (153–159)	691 (0.3–3215)	14 (11–20)	6.9 (3.4–9.1)	-	-	-	-
	T3	1.5 (1.4–1.7)	3.0 (2.5–3.8)	198 (189–208)	3571 (4.9–26193)	8.6 (5.9–12)	3.2 (2.2–4.3)	54 (28–82)	12 (6–16)	4 (0–10)	3 (0–6)
WTA	T1	1.4 (1.2–1.6)	3.4 (2.5–4.9)	252 (244–260)	1381 (128–1050)	11 (6.8–18)	3.4 (0.9–5.8)	232 (112–317)	24 (20–28)	37 (5–58)	3 (0–7)
	T2	-	-	-	-	-	-	-	-	-	-
	T3	1.7 (1.3–2.8)	3.2 (1.4–7.0)	244 (233–256)	367 (3.7–1978)	12 (5.5–16)	6.8 (2.8–19)	205 (93–296)	22 (13–27)	29 (12–46)	3 (0–7)

OC = organic content, Mud = mud content, MGS = median grain size, Chl a = chlorophyll a, Phaeo = phaeopigment, DW = dry weight; N = total abundance, S = taxa richness.

3.3.3 Treatment effects on MPB biomass and primary production

MPB biomass varied with site, sample date and sediment enrichment level, but not in a consistent manner (e.g., high treatments having greater biomass than other treatments, or consistent relationships within a site through time) (Table A2.2). Any deviations in MPB biomass from control plots primarily occurred at sites with the lowest water column turbidity (TAU-O, TAU-T and WTA) while no difference in chl *a* was observed at the most turbid sites (MNK-L and MNK-R during T1 and RAG throughout the experimental period) (Table A2.2).

Preliminary analysis of nutrient enrichment effects on primary production measures revealed high variability between sites and sample dates (Figure A2.1, Table A2.5), and so site-specific data were control normalised to see whether this would reduce variability and reveal effects of nutrient enrichment on primary production (Figure 3.3). Nutrient enrichment did not have a significant effect on submerged NPP_{CN} or GPP_{CN} after 8 (T1) and 20 (T3) months of enrichment regardless of treatment level (medium or high) (Table 3.3). While it was not possible to distinguish long-term treatment effects (between T1 and T3) for emerged production measures, nutrient enrichment effects on NPP_{CN} and GPP_{CN} were not observed after 20 months of enrichment (T3). Therefore, nutrient enrichment treatment data were pooled for all subsequent analysis.

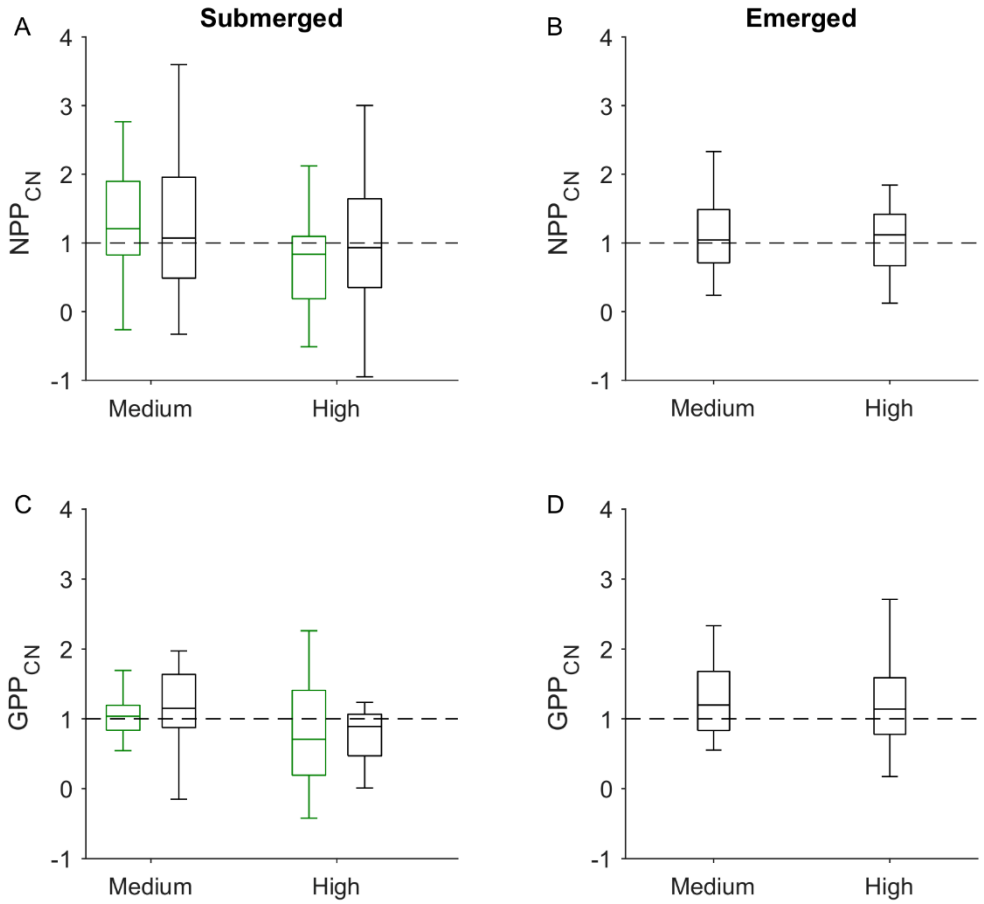

Figure 3.3: Effect of nutrient enrichment on control normalised net primary production (NPP) (A,B) and gross primary production (GPP) (C,D) during submerged and emerged tidal periods, respectively. Data are pooled across sites and green boxes represent data from T1 (November 2017 where no emerged data were collected) and black boxes from T3 (November 2018). Boxes are the 25th and 75th percentiles, and whiskers the 5th and 95th percentiles. The dotted line is provided as a reference to control values.

Table 3.3: *t*-test results examining nutrient treatment effects on control normalised (CN) primary production measures.

		Difference from Control		Difference between Treatment Means		Difference between T1 and T3 Means	
	Mean	t	*p*	t	*p*	t	*p*
Submerged							
NPP_{CN}							
T1 Medium	1.41	1.72	0.104	−1.47	0.150		
T1 High	0.91	−0.37	0.715				
T3 Medium	1.38	1.38	0.187	−1.08	0.289		
T3 High	1.00	−0.00	0.999				
Medium						0.08	0.935
High						−0.31	0.757
GPP_{CN}							
T1 Medium	0.97	−0.22	0.830	−1.01	0.322		
T1 High	0.74	−1.43	0.171				
T3 Medium	1.10	0.77	0.451	−1.03	0.313		
T3 High	0.90	−0.69	0.502				
Medium						−0.74	0.470
High						−0.65	0.528
Emerged							
NPP_{CN}							
T3 Medium	1.01	0.13	0.901	−1.23	0.228		
T3 High	1.56	1.30	0.207				
GPP_{CN}							
T3 Medium	1.20	1.51	0.144	−1.01	0.321		
T3 High	1.68	1.47	0.154				

3.3.4 Submerged vs. emerged primary production and its predictors

To investigate the relative importance of submerged and emerged primary production and if this differed over a gradient of water column turbidity, primary production measures as a function of site and tidal period during T3 were compared (Figure 3.4). At the three sites with the highest water column turbidity (MNK-L, MNK-R and RAG), submerged NPP was significantly lower than emerged NPP and negative at the two most turbid sites (MNK; Table 3.4). In contrast, at the three sites receiving the greatest light availability, submerged NPP was equal to or greater than emerged NPP. The relationship between GPP and water column turbidity was weaker, with emerged GPP at the three most turbid sites being only slightly greater than or equal to emerged GPP from the least turbid sites (Figure 3.4B). After standardising GPP by incident PAR, submerged GPP_i did not strongly relate to water column turbidity. This may be partially attributed to the low incident light recorded at RAG (Figure 3.2D). Emerged GPP_i was highly variable

among sites and did not significantly exceed submerged GPP_i (Table 3.4). Emerged GPP_i was considerably higher at TAU-O when compared to the other sites, however, this is likely to be an artefact of both low light availability during the emerged sampling, and high incident light during the submerged sampling event (Figure 3.2D). Photosynthetic efficiency ($GPP_{Sed + chla}$: correcting GPP by PAR_{Sed} and photosynthesising biomass (chl *a*)) appeared to be independent of water column turbidity during submerged tidal periods, with little difference observed among sites (Figure 3.4D). The only exception occurred at MNK-R where photosynthetic efficiency was notably higher. Submerged $GPP_{Sed + chla}$ was greater than emerged $GPP_{Sed + chla}$ at all but one site (TAU-O) where photosynthetic efficiency was equal between tidal periods.

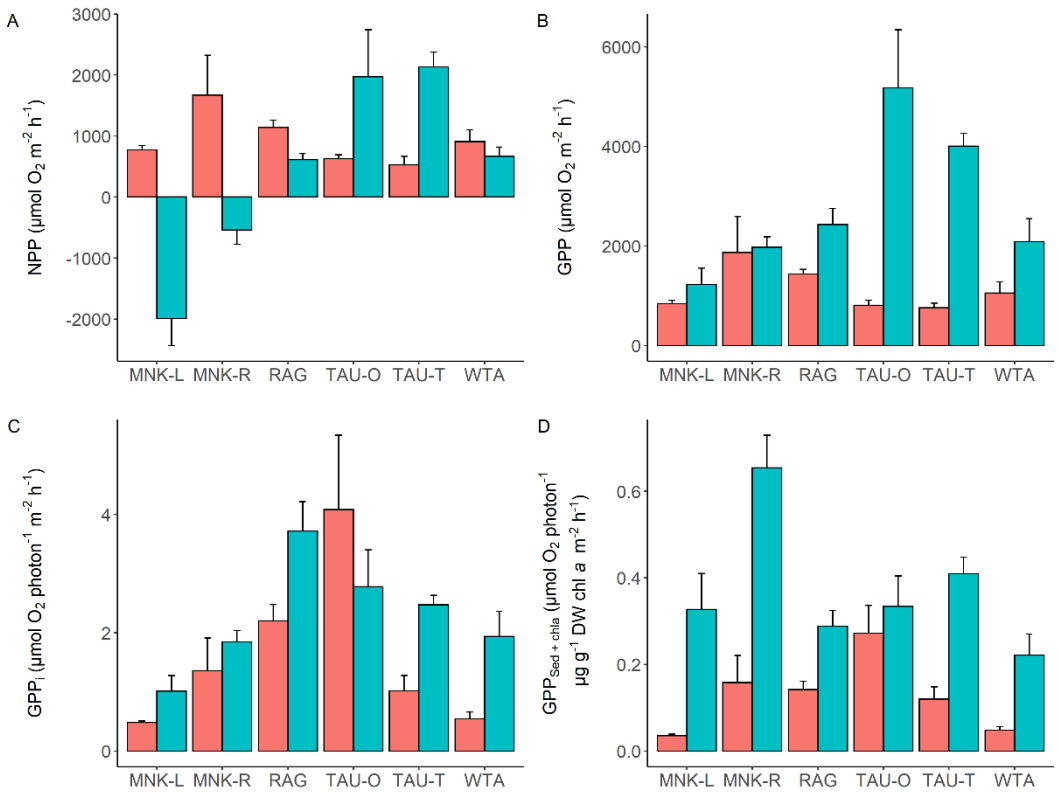

Figure 3.4: Net primary production (NPP) (A), gross primary production (GPP) (B), gross primary production corrected by PAR_i (GPP_i) (C), and gross primary production corrected by PAR_{Sed} and photosynthetic biomass (sediment chl *a* content) ($GPP_{Sed + chla}$) (D), during emerged (red) and submerged (blue) tidal conditions in November 2018 (T3). Bars represent means (n = 9) with standard error bars displayed.

Table 3.4: Results of repeated measures PERMANOVAs testing the effect of site and tidal state on measures of primary production made in November 2018 (T3). Site (6 levels) and tide (2 levels) were treated as fixed factors, and replicate plot nested within site. Site names have been further abbreviated to: M = MNK-L, N = MNK-R, R = RAG, O = TAU-O, T = TAU-T, W = WTA, and submerged and emerged tidal periods to sub and em, respectively. Significant effects ($p<0.05$) are given in bold.

	Term	df	Pseudo-F	p (perm)	Post-Hoc Pairwise Tests	
					Site	Tide
NPP	Site	5	7.77	**0.001**		
	Tide	1	5.83	**0.017**		
	Replicate (Site)	48	1.17	0.286		
	Site × Tide	5	14.34	**0.001**	**Sub,** O = T,O = R,O > M,O > N,O = W,T > R,T > M, T > N,T > W,R > M,R > N,R = W,M < N,M < W,N < W **Em,** O = T,O < R,O = M,O = N,O = W,T < R,T = M, T = N,T = W,R > M,R = N,R = W,M = N,M = W,N = W	**O, W,** sub = em; **T,** sub > em **R, M, N,** sub < em
GPP	Site	5	4.00	**0.004**		
	Tide	1	45.07	**0.001**		
	Replicate (Site)	48	1.19	0.265		
	Site × Tide	5	7.76	**0.001**	**Sub,** O = T,O > R,O > M,O > N,O > W,T > R,T > M, T > N,T > W,R > M,R = N,R = W,M = N,M = W,N = W **Em,** O = T,O < R,O = M,O = N,O = W,T < R,T = M, T = N,T = W,R > M,R = N,R = W,M = N,M = W,N = W	**M, N, W,** sub = em; **O, T, R,** sub > em
GPP_i	Site	5	6.80	**0.001**		
	Tide	1	7.41	**0.011**		
	Replicate (Site)	48	1.48	0.089		
	Site × Tide	5	3.11	**0.011**	**Sub,** O = T,O = R,O > M,O = N,O = W,T < R,T > M, T > N,T = W,R > M,R > N,R > W,M < N,M = W,N = W **Em,** O > T,O = R,O > M,O > N,O > W,T < R,T > M, T = N,T = W,R > M,R = N,R > W,M = N,M = W,N = W	**O, M, N,** sub = em; **T, R, W,** sub > em
$GPP_{Sed + chla}$	Site	5	6.10	**0.002**		
	Tide	1	78.36	**0.001**		
	Replicate (Site)	48	1.36	0.184		
	Site × Tide	5	5.12	**0.001**	**Sub,** O = T,O = R,O = M,O < N,O = W,T > R,T = M, T < N,T > W,R = M,R < N,R = W,M < N,M = W,N > W **Em,** O = T,O = R,O > M,O = N,O > W,T = R,T > M, T = N,T > W,R > M,R = N,R > W,M = N,M = W,N = W	**O,** sub = em; **T, R, M, N, W,** sub > em

These relationships appear to be relatively robust through time at the three sites where a June comparison is available (Figure 3.5). Submerged NPP was lowest at the most turbid site (RAG) during T2 and T3, and significantly lower than emerged NPP compared to sites with higher light availability (TAU-O and TAU-T). Emerged NPP at RAG was significantly higher than both TAU sites during both sampling dates (Table 3.5). All GPP estimates showed no clear relationship with time, however, RAG was observed to have the lowest submerged GPP and highest emerged GPP across both sampling dates. Once corrected for incident light, submerged GPP_i was three times higher at TAU-O, compared to all other sites and across the two sampling dates, while all other submerged GPP_i fluxes were relatively consistent. Photosynthetic efficiency remained significantly higher during submergence at all sites and sampling dates except for RAG during T2 and TAU-O during T3 where similar estimates between tidal periods were observed.

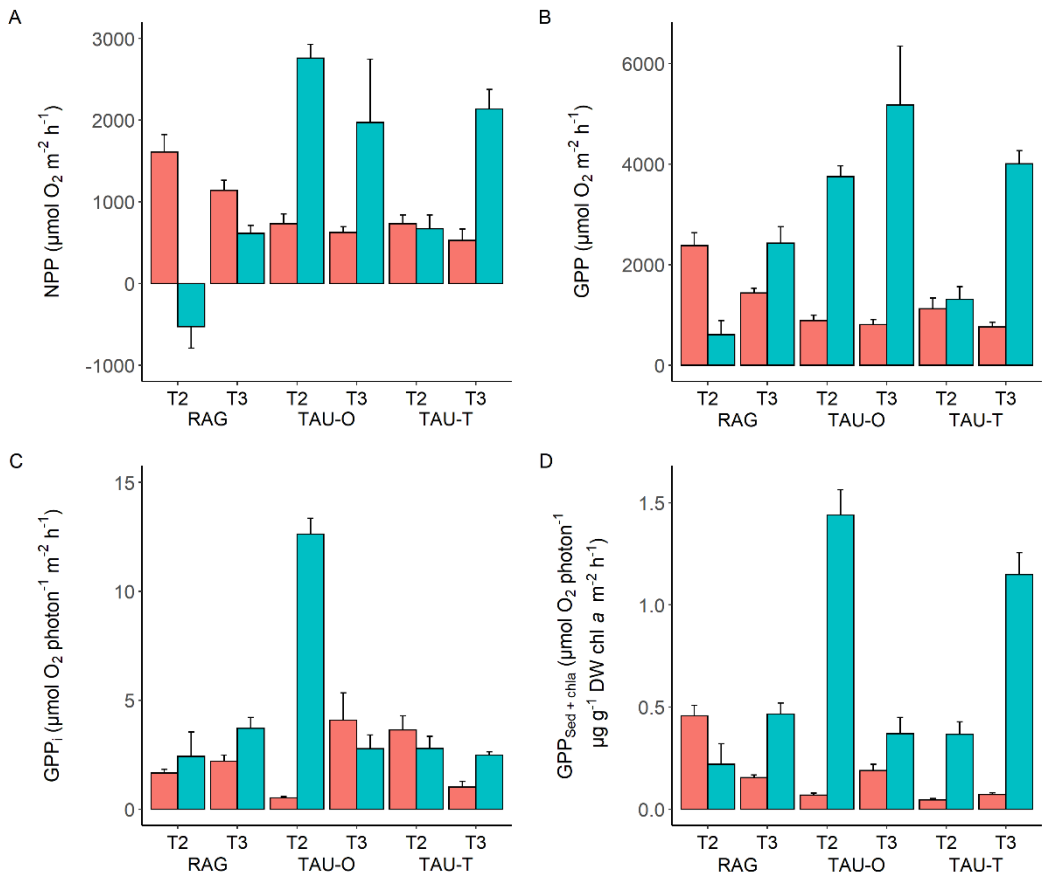

Figure 3.5 Net primary production (NPP) (A), gross primary production (GPP) (B), gross primary production corrected by PAR_i (GPP_i) (C), and gross primary production corrected by PAR_{Sed} and photosynthetic biomass (sediment chl *a* content) ($GPP_{Sed + chla}$) (D), during emerged (red) and submerged (blue) tidal state in June (T2) and November 2018 (T3). Bars represent means (n = 9) with standard error bars displayed.

Table 3.5: Results of repeated measures PERMANOVAs testing the effect of site and tidal state at two different sampling dates on measures of primary production. Site (3 levels: RAG, TAU-O and TAU-T), time (2 levels: T2 and T3) and tide (2 levels; submerged and emerged) were treated as fixed factors and replicate plot nested within site. Site names have been further abbreviated as: R = RAG, O = TAU-O and T = TAU-T and submerged and emerged tidal periods to sub and em, respectively. Significant effects ($p<0.05$) are given in bold.

	Term	df	Pseudo-F	p (perm)	Post-Hoc Pairwise Tests		
					Site	Time	Tide
NPP	Site	2	8.05	**0.006**			
	Time	1	1.10	0.323			
	Tide	1	5.87	**0.025**			
	Site × Time	2	3.78	**0.026**			
	Site × Tide	2	33.43	**0.001**			
	Time × Tide	1	9.06	**0.007**			
	Site × Time × Tide	2	7.18	**0.006**	**Sub T2,** R < T< O; **T3,** O = (R < T) **Em T2, T3,** R > (O = T)	**R, T sub,** T2 < T3; **em,** T2 = T3 **O sub, em,** T2 = T3	**R T2, T3,** sub < em; **O T2,** sub > em **T3,** sub = em; **T T2,** sub = em; **T3,** sub > em
GPP	Site	2	5.73	**0.007**			
	Time	1	12.10	**0.002**			
	Tide	1	51.88	**0.001**			
	Site × Time	2	0.96	0.404			
	Site × Tide	2	25.59	**0.001**	**Sub,** R < T<O; **Em,** R > (O = T)		**R,** sub = em; **O, T,** sub > em
	Time × Tide	1	33.06	**0.001**		**Sub,** T2 < T3; **em,** T2 > T3	**T2, T3,** sub > em
	Site × Time × Tide	2	1.26	0.282			
GPP_i	Site	2	14.75	**0.001**			
	Time	1	11.72	**0.002**			
	Tide	1	36.67	**0.001**			
	Site × Time	2	10.81	**0.001**			
	Site × Tide	2	17.51	**0.001**			
	Time × Tide	1	33.09	**0.001**			

	Term	df	Pseudo-F	p (perm)	Post-Hoc Pairwise Tests		
					Site	Time	Tide
	Site × Time × Tide	2	69.39	**0.001**	**Sub T2,** O > (R = T); **T3,** T < R = O) **Em T2,** R > (O = T); **T3,** T < (R = O)	**R sub em,** T2 = T3; **O sub,** T2 > T3, **em,** T2 < T3; **T sub,** T2 = T3; **em,** T2 > T3	**R T2, T3,** sub = em; **O T2,** sub > em, **T3,** sub = em; **T T2,** sub = em, **T3,** sub > em
$GPP_{Sed + chl}$	Site	2	6.38	**0.004**			
	Time	1	0.97	0.341			
	Tide	1	162.88	**0.001**			
	Site × Time	2	56.30	**0.001**			
	Site × Tide	2	35.37	**0.001**			
	Time × Tide	1	0.29	0.568			
	Site × Time × Tide	2	74.27	**0.001**	**Sub T2,** O > (R = T); **T3,** O = (R < T) **Em T2,** R > O > T; **T3,** T < (R = O)	**R sub,** T2 < T3; **em,** T2 > T3; **O sub,** T2 > T3; **em,** T2 < T3; **T sub,** T2 < T3; **em,** T2 = T3	**R T2,** sub = em; **T3,** sub > em; **O T2,** sub > em; **T3,** sub = em; **T T2, T3,** sub > em

The influence of water column turbidity on overall productivity at each site through time is highlighted in Figure 3.6. Net autotrophy (more carbon produced than respired) dominated all sites during tidal emergence. However, during submerged tidal periods, sites with high water column turbidity consistently had a p/r ratio <1 suggesting net heterotrophy (more carbon respired than produced). In contrast, sites with low water column turbidity predominately remained net autotrophic during submergence at all three sampling dates.

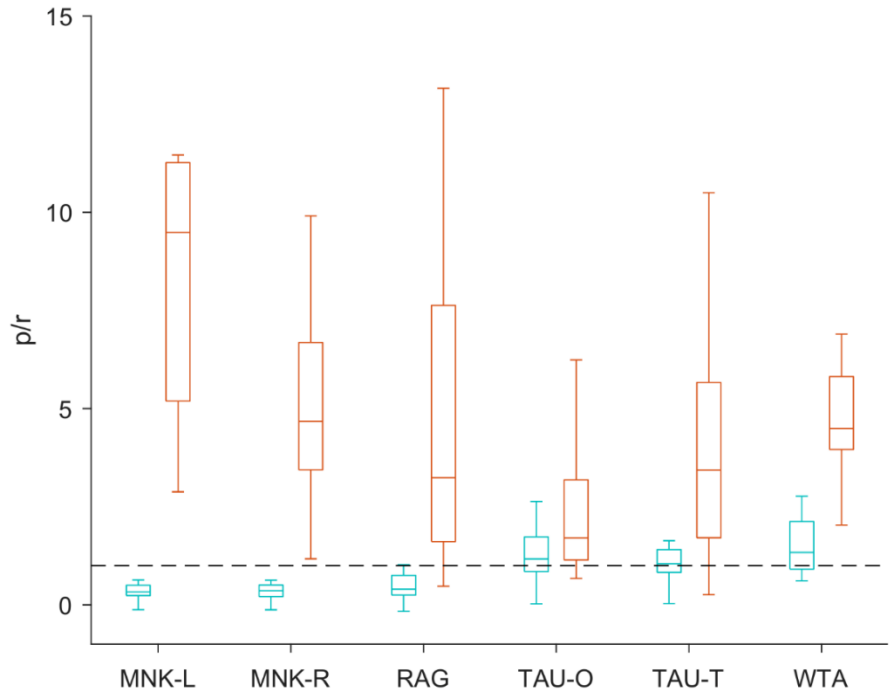

Figure 3.6: Photosynthesis/respiration ratio (p/r) during submerged (blue) and emerged (red) tidal periods with data pooled across all sampling dates and treatments. Boxes are the 25th and 75th percentiles, and whiskers the 5th and 95th percentiles. The dotted line is provided as a reference to p/r = 1.

The variability in primary production among sites and tidal stages was partitioned using DistLM analysis (Figure 3.7, Table 3.6). The analysis revealed environmental variables contributed 10–25 % of overall variability for submerged and emerged primary production estimates. When considering the shared effects of community variables for submerged estimates, and porewater variables for emerged estimates, the total amount of explained variability increased to 19–39 %. PAR_{Site} was significantly correlated with submerged primary production estimates,

explaining 8–40 % of the total variance when considered individually, supporting earlier evidence of the influence of water column turbidity on benthic primary production. Temperature explained the second largest proportion of variability and was included in the full model during both submerged GPP and emerged NPP estimates (11 % and 4 %, respectively). Other significant individual predictors for both submerged and emerged estimates included sediment properties (either mud content, organic content or grain size), phaeopigments and porewater NH_4^+ concentration while the addition of total abundance of *A. stutchburyi* and porosity were significant for emerged estimates. Porewater NH_4^+ concentration explained a maximum of 4 % variability, further highlighting the marginal influence of sediment enrichment on primary production estimates.

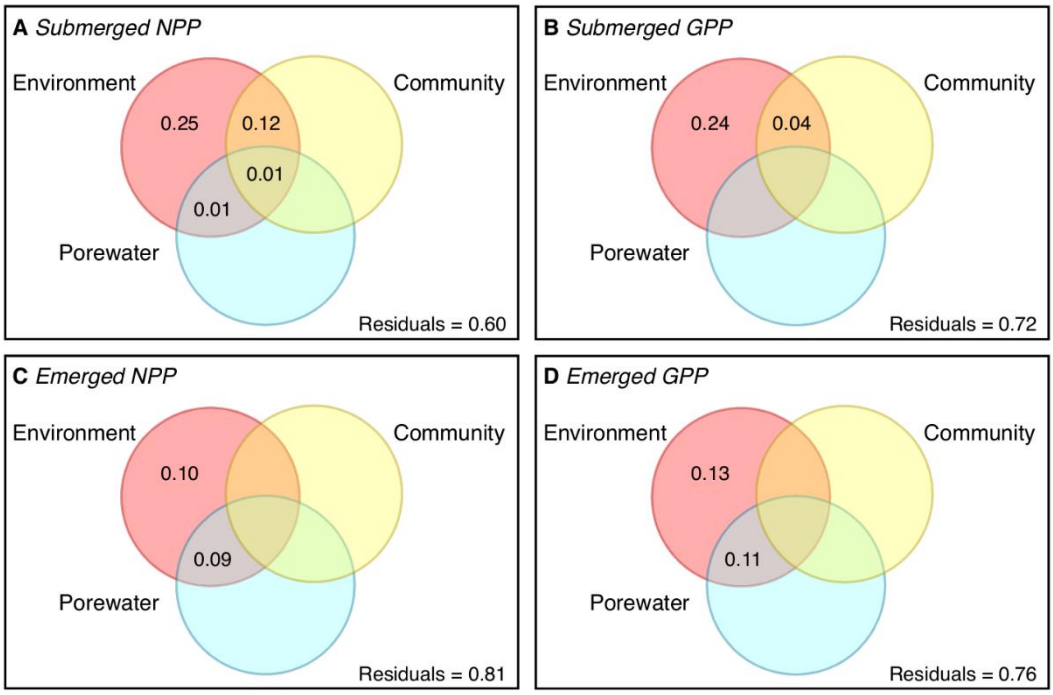

Figure 3.7: Results of variance partitioning analysis between environmental, community and porewater variables and the variance attributed to unique and shared effects. Results from the full DistLM are described in Table 3.6.

Table 3.6: DistLM results for submerged and emerged primary productions measures. Marginal tests provide the proportion of variation explained when considered individually. Full model shows the variables included in the stepwise DistLM and the variance attributed to each. Partitioning of variance shows the variance explained solely by environment, community and porewater predictors, and in parentheses, the variance shared by two or more predictor groups. Significance levels are * $p < 0.1$, ** $p < 0.05$, *** $p < 0.01$ and correlation directions are in parentheses.

	Predictor	Marginal tests		Full Model (%)	Variance Partitioning (%)
		Pseudo-F	Proportion		
Submerged					
NPP	Environment				25 (14)
	OC	14.05	0.10 *** (−)	2	
	Phaeo	22.37	0.14 *** (−)		
	PAR_{Sed}	13.42	0.09 *** (+)		
	PAR_{Site}	87.00	0.40 *** (+)	40	
	Community				(13)
	A. stutchburyi	22.08	0.14 *** (−)		
	Porewater				(2)
	NH_4^+ (5–7 cm)	4.14	0.03 ** (−)		
			Total	42	39
GPP	Environment				24 (4)
	MGS	3.62	0.03 * (+)		
	Phaeo	9.98	0.07 *** (−)		
	PAR_{Sed}	13.68	0.09 *** (+)		
	PAR_{Site}	27.58	0.17 *** (+)	17	
	Temperature	11.91	0.08 *** (+)	11	
	Community				(4)
	A. stutchburyi	6.25	0.05 ** (−)		
			Total	28	28
Emerged					
NPP	Environment				10 (9)
	Mud	5.69	0.07 ** (+)		
	Phaeo	6.44	0.08 ** (+)		
	PAR_{Site}	9.46	0.11 *** (−)	11	
	Temperature	3.98	0.05 ** (−)	4	
	Porewater				(9)
	NH_4^+ (0–2 cm)	3.15	0.04 ** (+)		
	NH_4^+ (5–7 cm)	2.40	0.03 * (+)		
	Porosity (0–2 cm)	3.91	0.05 ** (+)		
			Total	15	19
GPP	Environment				13 (11)
	Mud	12.82	0.14 *** (+)	14	
	Chl *a*	2.93	0.04* (+)		
	Phaeo	7.61	0.09 ** (+)		
	PAR_i	4.09	0.05 ** (−)		
	PAR_{Site}	7.13	0.08 ** (−)	3	
	Temperature	7.79	0.09 *** (−)		
	Porewater				(11)
	NH_4^+ (0–2 cm)	1.80	0.02 * (+)		
	Porosity (0–2 cm)	8.58	0.10 *** (+)		
			Total	17	24

3.4 Discussion

Comparisons of MPB productivity on intertidal flats during periods of tidal inundation and exposure are rare, despite the potential of several anthropogenic stressors to restrict productivity to emerged periods. This study considered both submerged and emerged productivity and integrated these estimates over a 20-month period within six different estuaries, to investigate the combined effects of two pervasive coastal pressures—increased nutrient availability and water column turbidity. To achieve this, MPB productivity was measured at both high and low tide (i.e., photosynthetic O_2 production and CO_2 uptake on submerged and exposed tidal flats, respectively) and analysed according to nutrient enrichment treatment across a natural turbidity gradient (Figure 3.2A). Experimental nutrient enrichment resulted in sediment porewater ammonium concentrations increasing by 40- and 800-fold in medium and high treatments, respectively. These concentrations were comparable to those found in eutrophic estuaries globally such as in Great Bay estuary, USA (maximum of 1400 µM; Percuoco et al. (2015)), Mahurangi estuary, New Zealand (maximum of 1542 µM; Lohrer et al. (2010)) and the Santos-Cubatao Estuarine System, Brazil (maximum of 4989 µM; Gonçalves et al. (2012)). The large gradient of environmental conditions encompassed within this field study ensured our estimates of MPB productivity fell within ranges reported within intertidal habitats both in New Zealand and worldwide. For example, NPP estimates have previously been described between 500 and 3000 µmol O_2 m^{-2} h^{-1} within emerged habitats (Migné et al., 2005, Drylie et al., 2018) and between −3000 and 4000 µmol O_2 m^{-2} h^{-1} when measured continuously over several tidal cycles (Denis and Desreumaux, 2009).

MPB productivity measurements were spatially and temporally variable and, even after normalising for background site values (i.e., NPP_{CN} and GPP_{CN}), both emerged and submerged MPB production were independent of nutrient enrichment (Table A2.5; Figure 3.3). This was unexpected considering each site was considered to be nitrogen-limited (within control plots) according to the calculated N:P porewater ratios (Figure A2.2) (Redfield, 1963, Montani et al., 2003). The negligible role of

sediment nutrient enrichment may be explained by the dilution of plot effects from the suspension and removal of MPB with bedload transport (Underwood, 2001), and/or the potential oversupply of nitrogen relative to phosphorus, switching the system from being predominately nitrogen to phosphorus limited. However, the absence of a response from MPB to stoichiometrically balanced nutrient additions have previously been observed (Stutes et al., 2006). This may occur if nutrients were not limiting, for example, as a product of both water-column assimilation and sediment porewater nutrients, the replenishment of depleted nutrients through advective flushing (by macrofauna and physical processes (Huettel et al., 1998, Volkenborn et al., 2007)), and/or through intense grazing pressure reducing MPB biomass and therefore reducing N demand (Hillebrand et al., 2000). Additionally, light limitation can prevent MPB growth (Barranguet et al., 1998, Meyercordt and Meyer-Reil, 1999), which while plausible for sites in this study with high water column turbidity (MNK, RAG), is unlikely to prevent a response by MPB at the least turbid sites. We therefore postulate that a combination of factors may have prevented an observed increase in MPB growth in this study, such as high bedload transport, carbon supply, light availability, phosphorus limitation, or grazing activity and therefore the enrichment of sediment nitrogen had no observable effect on MPB production.

In contrast to nutrient enrichment effects, site turbidity had a substantial influence on primary production estimates. For example, NPP was negative at the most turbid sites and increased with decreasing site turbidity. Although comparisons of GPP across sites did not show as strong a relationship with water column turbidity, submerged GPP was greatest at two of the least turbid sites (TAU-O, TAU-T). These results are further supported by the DistLM analysis where 40 and 17 % of submerged NPP and GPP variability, respectively, could be explained by site turbidity (Table 3.6). While there was still a large proportion of unexplained variation, this is most likely an artefact of dynamic variations in sediment biogeochemistry caused by microbial and macrofaunal activities and detrital inputs (Thrush et al., 1994, Eyre and Ferguson, 2002, Huettel et al., 2014) which will all contribute to small scale variations between plots. Nevertheless, the

strong relationship with site turbidity appears to dominate benthic primary production estimates over time by occluding the light required by MPB for photosynthesis. These results highlight the effectiveness of incorporating a natural gradient of water column turbidity as a way of understanding the complexities of multiple stressors on ecosystem functioning in real-world settings.

As the tide recedes and exposes the sediment surface, MPB production becomes unconstrained by light limitation, confirmed by our results showing decreased effects of light on MPB production during emerged tidal periods. For example, PAR_{Site} explained just 11 and 3 % of emerged NPP and GPP variability, respectively. As the effects of light decreased, the influence of sediment characteristics and, to a lesser extent, temperature, increased (GPP, mud 14 %; NPP, temperature 4 %; Table 3.6). However, considering the large influence temperature can have on MPB metabolism and previously reported production estimates (Blanchard et al., 1997, Barranguet et al., 1998, Migné et al., 2018), we postulate the amount of variability explained by temperature may increase if sampled over a larger temperature gradient (13.6–18.7 ˚C during emerged periods in this study). Sediment characteristics, in contrast, can modify primary production estimates through several direct and indirect pathways. These include alterations in the penetration depth of light into the sediment, changes in solute transport in less permeable sediments, and a reduction in the metabolic status of MPB (Billerbeck et al., 2007). Moreover, sediment properties can also alter MPB community composition, resulting in different assemblages between sites (Thornton et al., 2002, Clark et al., 2020). While this study incorporated the effects of these environmental differences (including turbidity responses) and the effect of long-term nutrient enrichment on MPB production, characterisation of MPB assemblage responses presents an interesting avenue for future research.

The disparity in environmental conditions experienced during emerged vs. submerged periods is likely to be a contributing factor to the observed difference in photosynthetic efficiency between tidal states. During periods of submergence, few differences in photosynthetic efficiency were observed between sites,

suggesting potential photoadaptation to lower light availability. Once released from light limitation during emerged periods, photosynthetic efficiency was significantly lower when compared to submerged tidal periods, and this was consistent through time (Figure 3.5). During periods of emergence, MPB efficiency can be reduced through high light and UV-B exposure, temperature extremes and desiccation stress (and the subsequent changes to salinity) (Blanchard et al., 1997, Rijstenbil, 2003, Coelho et al., 2009). However, a consistent difference in photosynthetic efficiency was not observed between the summer and winter sampling periods and no change in sediment porosity (and therefore desiccation) was detected over each emerged period (Table A2.2), suggesting these factors were unlikely to significantly reduce photosynthetic efficiency in this study. Alternatively, protective mechanisms such as diel migration are likely to have altered photosynthetic efficiency during emergence (Saburova and Polikarpov, 2003).

At the three most turbid sites, the contribution of emerged productivity was significantly greater than submerged (Tables 3.4 and 3.5), supporting a previous study suggesting the importance of emerged MPB production increases with site turbidity (Drylie et al., 2018). In addition, the significant contribution of emerged primary production to total productivity is highlighted by the dominance of net heterotrophy at highly turbid sites during submergence, compared to predominately net autotrophy at the least turbid sites (Figure 3.6). This suggests highly turbid sites may rely on emerged periods (which were net autotrophic across all sites) to sustain and support benthic primary production. This is in agreement with studies from around the world reporting the restriction of benthic primary production to emerged periods only, owing to light limitation through high turbidity (Guarini et al., 2002, Migné et al., 2004, Yamochi et al., 2017). Despite the maintenance of MPB productivity over emerged periods, the higher production during emergence does not always fully compensate for the lower production during submergence, as evidenced by the consistently higher MPB production estimates during submerged compared to emerged tidal periods at the least turbid sites (Figures 3.4 and 3.5). Increased heterotrophy has further

consequences for coastal ecosystem functioning via the associated release of inorganic nutrients through increased respiration (rather than assimilation to support productivity during periods of net autotrophy). This ultimately can have substantial implications for coastal ecosystems through indirectly facilitating the removal of nutrients in oligotrophic systems or contributing to accelerating water column primary production in eutrophic systems. Consequently, reduced MPB productivity during submergence not only has direct implications on the supply of labile carbon and therefore coastal food webs (Christianen et al., 2017) but can cascade onto reductions in the capacity to moderate pollutants, changes in trophic structure and alterations in nutrient cycling and transformation pathways (2007, Dugan et al., 2018, Hope et al., 2020). In combination, these changes feedback within the system to modify ecological interaction networks and push ecosystems closer towards tipping points (Scheffer and Carpenter, 2003, Thrush et al., 2014, Selkoe et al., 2015).

Through coupling measurements of submerged and emerged primary production, this study highlights the multifaceted nature of intertidal habitats where productivity is moderated by a complex network of ecosystem interactions. However, it is clear that reductions in seafloor light climate leading to any decline in primary productivity by MPB will have a cascading influence on the health and functioning of coastal habitats. Our study highlights the importance of low tide MPB production in turbid estuaries and therefore as a contributor to the system's resilience to elevated turbidity. Intertidal areas are already vulnerable and it is estimated that there has been a 16 % loss of intertidal habitats globally (Murray et al., 2019), with this expected to increase in the future (Passeri et al., 2015). As emerged tidal habitat becomes restricted and lost, the ecological resilience that these areas were providing is also lost, having significant implications for the effective management of these valuable ecosystems.

Chapter Four: The effects of sediment nutrient enrichment on biogeochemical cycling within multiple estuaries

4.1 Introduction

Soft sediment coastal ecosystems play a fundamental role in biogeochemical cycling, altering the uptake, transformation and removal of bioavailable nitrogen (N) as well as regulating the production and metabolism of carbon (C) (Seitzinger et al., 2006, Anderson et al., 2014). The processes and pathways involved in both N and C cycling are increasingly affected by the multitude of pressures facing coastal ecosystems. In particular, the anthropic acceleration of the global N cycle has resulted in N sources exceeding sinks by more than 40 % (Fowler et al., 2013), due to an exponential increase in agricultural productivity which has led to the export of N to coastal ecosystems (Nixon, 1995, Vitousek et al., 1997). If this N enrichment exceeds the capacity for assimilated-enhanced benthic production and/or removal then a system can be pushed beyond a tipping point whereby pelagic primary production dominates and coastal eutrophication persists (Cooper and Brush, 1993, Scheffer and Carpenter, 2003). Despite the importance of biogeochemical cycling in all estuarine ecosystems, the majority of research has focused on heavily eutrophic and degraded estuaries which have already undergone significant transitions (Vieillard et al., 2020). This bias has broad implications for all ecosystem services that interact with or depend on N processing, and thus restricts our ability to manage effectively and prevent ecological shifts in low-nutrient systems, as well as compromising the recovery and restoration of eutrophic systems through the inability to set baseline targets. Here we aim to increase our knowledge of how N enrichment in low-nutrient estuaries affects both N and C processing and to couple these measurements to changes in macrofaunal communities.

Estuarine sediments are able to efficiently and permanently remove bioavailable N via the production of dinitrogen (N_2). This can occur during denitrification (DNF), where nitrate is used as an electron acceptor to oxidise organic matter (OM), and during anaerobic ammonium oxidation (anammox), a chemotrophic process whereby ammonium (NH_4^+) is oxidised using nitrite (Dalsgaard et al., 2005). While these processes can co-occur, DNF is estimated to be the dominant pathway in coastal ecosystems (Risgaard-Petersen et al., 2004a, Dalsgaard et al., 2005) owing to the higher availability of OM and thus the stimulation of fast-growing heterotrophic denitrifying bacteria (Risgaard-Petersen et al., 2004a). The production of biologically inert N_2 gas can aid the resilience of coastal ecosystems to excess N availability (Teixeira et al., 2010) and is therefore a central process in understanding the effects of increased N availability.

DNF is primarily controlled by the availability of oxygen (O_2), C and nitrate (NO_3^-) (Seitzinger et al., 2006), which in turn are largely regulated by ambient concentrations in the overlying water column and within the sediment, benthic primary producers, macrofaunal communities and sediment properties (Rysgaard et al., 1995, Middelburg et al., 1996, Aller and Aller, 1998, Devol, 2015). Within low-nutrient estuaries with little excess N, nitrate is predominately supplied by nitrification (NTR; NH_4^+ - NO_2^- (nitrite) - NO_3^-) resulting in tightly coupled NTR-DNF (Jenkins and Kemp, 1984), with the ammonium needed for NTR largely a product of ammonification during organic matter (OM) mineralisation (Devol, 2015). However, the limited availability of these solutes results in competition with benthic primary producers and nitrifying and denitrifying bacteria which can lead to the suppression of DNF (Risgaard-Petersen et al., 2004b). As the concentration of N increases within the sediment, changes in biogeochemical pathways occur, such as an uncoupling of NTR-DNF and an increase in uncoupled, direct DNF (Dong et al., 2000, Magalhães et al., 2005). However, the capacity for the benthos to assimilate or denitrify excess N can be compromised, resulting in an increased efflux of N from the sediment (usually as NH_4^+) (Kemp et al., 1990). This can fuel pelagic production which in addition to other changes will lead to the significant alteration of ecosystem interaction networks, increasing the likelihood of a shift

towards a more eutrophied state dominated by pelagic primary production (Scheffer and Carpenter, 2003, Smith, 2003).

Coupled NTR-DNF is partly regulated by the boundary between oxic and sub-oxic sediment layers because of the opposing oxygen requirements necessary for nitrification (oxic) and denitrification (sub-oxic, <0.2 mg O_2 L^{-1} (Seitzinger et al., 2006)). A sufficient oxic layer can increase the supply of NO_3^- through the stimulation of NTR unless the diffusion distance increases to a point where it can become prohibitive and therefore lead to a suppression of DNF (Risgaard-Petersen, 2003). However, the interface between oxic-anoxic sediments can be augmented by macrofaunal activities, such that burrowing activity can increase the oxygen penetration depth via the oxygenation of burrow linings, resulting in higher bacterial density and metabolic activity (Laverock et al., 2011, Stief, 2013). In addition, bioturbation activity has been shown to increase the movement and vertical distribution of solutes, oxygen and C, enhancing N transformation by increasing the spatial and temporal heterogeneity of sedimentary redox zones (Volkenborn et al., 2012, Stief, 2013). The positive influence of macrofaunal activities on denitrification and nutrient processing is however, likely to be diminished if communities are negatively affected by increasing nutrient enrichment (Douglas et al., 2017). This can occur through ammonium toxicity, the formation of hydrogen sulphide and/or increased anoxia within the sediment (Fenchel and Riedl, 1970, Gray et al., 2002, Posey et al., 2006). While the response of macrofaunal communities to sediment N enrichment is largely species and location dependent (Morris and Keough, 2003, Posey et al., 2006), understanding the response of key macrofaunal species is likely to be a crucial component in understanding any alterations in coastal biogeochemical cycling.

The energy required to drive N cycling redox reactions, either directly or indirectly, is derived from the degradation of OM. In particular, DNF requires a source of OM to proceed and therefore the supply of OM can exert a significant control over rates of DNF, especially in the absence of photosynthesis (Maher and Eyre, 2012, Eyre et al., 2013). Several studies have additionally identified strong relationships

to benthic metabolism, which is used as a proxy for the quantity of organic matter oxidation (Glud, 2008, Eyre et al., 2013). However, competition for N by heterotrophs processing OM can supress DNF and thus increased OM does not necessarily correspond to increasing DNF. While most research has focused on C quantity, the quality of OM can also influence C degradation, which in turn can significantly influence DNF (Eyre et al., 2013). Furthermore, C degradation has been shown to influence the efficiency at which DNF removes N as N_2 (rather than the release of NH_4^+) (Fulweiler et al., 2008, Eyre and Ferguson, 2009, Piehler and Smyth, 2011). Incorporating measures of C processing (e.g. benthic metabolism, C degradation rate and C quality) with DNF measurements is therefore valuable to further our understanding of biogeochemical cycling in low nutrient systems, especially considering these relationships may be modified under increasing N enrichment.

It is evident that the strong coupling between N and C cycling as well as biodiversity-ecosystem relationships govern nutrient processing in coastal habitats (Eyre and Ferguson, 2002, Stief, 2013, Douglas et al., 2017). However, the increased delivery of N is intensifying, invoking changes to ecosystem interactions and increasing the likelihood of nonlinear responses, which can collectively degrade ecosystem functionality and reduce the ability of an ecosystem to adapt to further stress (Kemp et al., 2005, Howarth and Marino, 2006). Few studies have examined these relationships *in situ*, especially in combination and across multiple estuaries. Therefore, the overall aim of this study was to investigate the effects of sediment nutrient enrichment on N and C cycling within multiple low-nutrient estuaries. This was achieved by experimentally enriching sediment N over a 20-month period at 6 sites located within 4 different estuaries followed by coupled *in situ* measurements of both N and C cycling across two seasons. It was hypothesised that increasing sediment N availability in estuaries characterised by N limitation (Mangan et al., 2020b) would increase autochthonous OM production, and stimulate higher DNF through reduced competition for N and increased C supply. However, at high N enrichment it is hypothesised reductions in the abundance of key bioturbating species (Gray et al., 2002, Douglas et al., 2017) will

lead to the suppression of DNF despite increases in porewater concentrations, owing to increased sediment anoxia.

4.2 Materials and methods

4.2.1 Study sites

This study was carried out within the North Island of New Zealand at 6 sites within 4 shallow, barrier enclosed estuaries (Figure 4.1). Each estuary had an extensive intertidal area (62 – 85 % of the total area (Hume et al., 2007)) and semi-diurnal tides. Sites were chosen to increase spatial heterogeneity while maintaining a similar latitude in order to minimise differences in day length and temperature. Additionally, site characteristics included the presence of two functionally important bivalve species (*Austrovenus stutchburyi* and *Macomona liliana*) and variation in sediment properties (organic content and mud content), both of which can substantially alter biogeochemical processes (Woodin et al., 2016, Douglas et al., 2018). All of the sites were positioned within the mid-intertidal region and located along a gradient in water column turbidity (Mangan et al., 2020a), such that light availability (measured as photosynthetically active radiation) reaching the sediment surface ranged from a median of 38 – 283 µmol m^{-2} s^{-1} during tidal submergence during 9 months of the N enrichment period (March – November 2017).

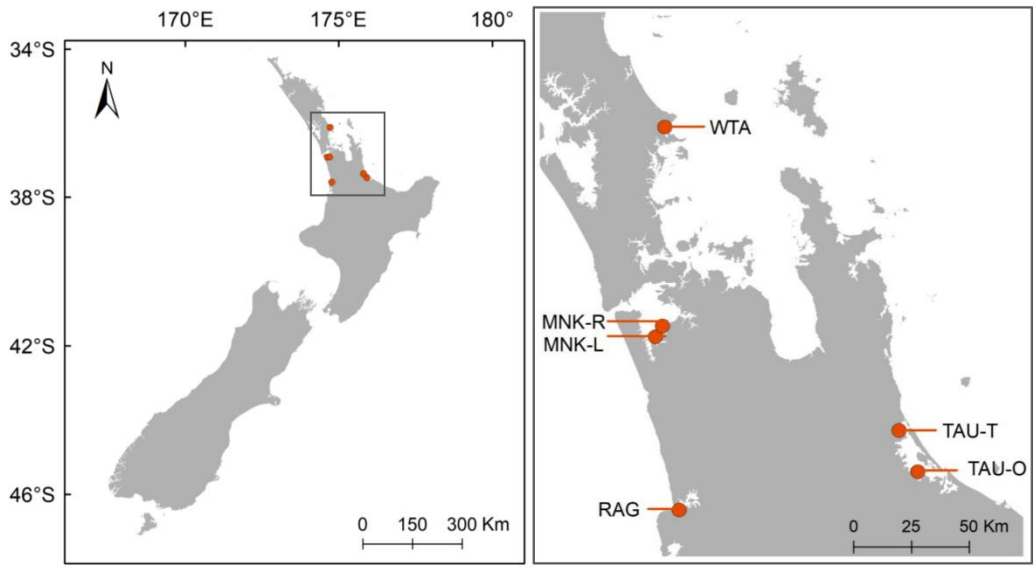

Figure 4.1: Locations of the 6 sites, within 4 estuaries situated within the North Island of New Zealand.

4.2.2 Experimental design

Within each site, sediment nutrient concentrations were elevated at three levels (control: 0 g N m^{-2}; medium: 150 g N m^{-2}; high: 600 g N m^{-2}) across nine 9 m^2 experimental plots. The uniform elevation of porewater N was achieved following Douglas et al. (2016). In brief, a sediment plug (3 cm diameter, 15 cm deep) was extracted from 180 evenly spaced holes using a handheld corer, a known volume of slow-release urea fertiliser (Nutricote; 40:0:0 N:P:K) was added and then the sediment plug replaced. Urea fertiliser was chosen as it quickly hydrolyses to ammonium (NH_4^+), a product released during the remineralisation of OM and a typically limiting nutrient within New Zealand estuaries (Tay et al., 2013). To maintain nutrient enrichment over the full experimental period, fertiliser was applied in March and November 2017 and following the sampling in June 2018. This resulted in a minimum of 5 months between the application of fertiliser and sampling.

Sampling first took place after 15 months of sediment nutrient enrichment in June 2018 (winter; 3 sites TAU-T, TAU-O, RAG) and after 20 months in November 2018

(early summer; all 6 sites). The gap between sediment enrichment and sampling provided the opportunity to incorporate longer-term processes such as any alterations of microbial and macrofaunal communities, while the seasonal component incorporated temperature variations.

4.2.3 Field sampling

At three sites during winter (TAU-O, TAU-T and RAG) and all sites during summer, benthic incubation chambers were deployed over a full submerged tidal period of approximately 4 h to assess solute and gas fluxes. During the preceding low tide, one chamber base (50 cm x 50 cm x 15 cm) per plot was inserted 5 cm into the sediment and equipped with a light and temperature logger (HOBO Pendant®) and a dissolved oxygen logger (PME miniDOT). On the incoming tide, a Perspex dome lid (enclosing ~40 L) was placed onto each chamber and all air bubbles were removed before each chamber was sealed and then covered with an opaque shade cloth to prevent exposure to sunlight. Dark only measurements were chosen to exclude the influence of photosynthetic O_2 production by microphytobenthos (MPB), the dominant primary producer at each site (Mangan et al., 2020a), as increases in oxygen saturation can disrupt N_2 quantification for assessment of denitrification rate (Eyre et al., 2002). Once sealed and at the end of the incubation, seawater samples (1 x 60 mL syringe for solute, 2 x 60 mL airtight syringes for gas concentrations) were extracted from each chamber. Solute samples were filtered on-site through a 0.45 µm Whatman GF/C glass fibre filter and frozen at −20 °C until analysis, and gas samples were transferred to airtight exetainers (Labco, UK) and preserved with zinc chloride at 4 °C until analysis.

To assess the vertical variation in sediment OM degradation within each plot, rapid organic matter assay (ROMA) plates were deployed between 7 and 10 d prior to the benthic chamber measurements during the summer sampling, following the methods described by O'Meara et al. (2018). In brief, each plate consisted of 3 x 0.9 mL wells at depths of 1, 3, 5, 7, 10 and 15 cm, and filled with an agar mixture consisting of 0.029 g C mL^{-1}. During deployment and removal, minimal disturbance was caused to both the sediment surface and subsurface stratification via the

creation of a gap leveraged with a spade and the plate slotted in, which can then be removed vertically. Once removed, each plate was gently washed to remove any sediment before measuring the change in agar volume per well within 6 h of collection.

For determination of sediment characteristics (sediment chlorophyll *a*, phaeopigments, grain size and organic content) during both sampling events, five pooled sediment cores (2.6 cm dia) were collected from each experimental plot at a depth of 0–2 cm and frozen at −20 °C until analysis. Three separate replicates of four pooled sediment cores were additionally taken at depths of 0–2 cm and 5–7 cm for analysis of sediment porosity, porewater dissolved inorganic nutrient concentrations and fluorescence characteristics of dissolved organic matter (DOM). One macrofauna core (13 cm dia, 15 cm depth) was taken from each plot (3 per treatment per site) and sieved on a 500 µm mesh before being preserved in 70 % Isopropyl alcohol.

4.2.4 Laboratory analysis

To determine sediment properties, samples were thawed and homogenised. Organic content was determined by weight loss on ignition, where samples were dried at 60 °C until a constant weight and then combusted at 550 °C for 4 h. For grain size determination samples were digested in 10 % hydrogen peroxide before being measured by laser diffraction (Malvern Mastersizer-3000). Chlorophyll *a* and phaeopigments were extracted from freeze-dried sediment using 90 % buffered acetone and then measured before and after acidification using a fluorometer (Turner Designs 10-AU).

Samples for sediment porosity and porewater extraction were processed within 24 h of collection. To calculate sediment porosity, the difference in wet and dry weight was determined after drying (60 °C) for 7 d or until a constant weight. To extract sediment porewater for determination of dissolved inorganic nutrient concentrations and fluorescence characteristics of DOM, 4 mL of de-ionised water was first added to each sample, before being vortexed, centrifuged and then

filtered through a 0.45 µm Whatman GF/C glass fibre filter and stored at −20 °C. Analysis of dissolved inorganic nutrient concentrations (from the chamber incubations and extracted porewater; NH_4^+- N, NO_x^--N, NO_2^--N and PO_4^{3-}-P) was conducted using standard operating procedures for flow injection analysis on a Lachat QuickChem 8000 Series FIA+ (Zellweger Analytics Inc.). Fluorescence characteristics of porewater DOM were analysed using a fluorescence spectrometer (Horiba Jobin Yvon Aqualog®) with a 2 s integration time, 3 nm step-size and a measurement range of 240 – 600 nm excitation and 245 – 800 nm emission.

Analysis of gas samples were performed using Membrane Inlet Mass Spectrometry (MIMS) as per O'Meara et al. (2020). Transformation of raw data into dissolved gas concentration (µmol L^{-1}) was based on gas solubility, which was calculated using *in situ* temperature, pressure and salinity measurements (taken at the same time of sampling) as per Hamme and Emerson (2004). Variations in N_2 concentrations were normalised with Argon (Ar), a biologically inert gas, and the resulting N_2/Ar ratios used to calculate N_2 gas concentration.

Macrofauna samples from the summer sampling (3 per treatment) were stained with Rose Bengal and fauna separated from any shell hash before being identified to the lowest possible taxonomic level (usually species) and counted. For the winter samples, only adult (>10 mm) *Austrovenus stutchburyi* and *Macomona liliana* were counted.

4.2.5 Parameter derivations

Fluxes of dissolved oxygen, inorganic nutrients and N_2 gas were calculated as the difference between final and initial concentrations, before being standardised by chamber volume, sediment surface area and incubation time. Oxygen fluxes are presented as sediment oxygen consumption (SOC; µmol O_2 m^{-2} h^{-1}) with a positive flux representing uptake by the sediment. Conversely, a positive and negative nutrient flux represents an efflux and influx from the sediment, respectively. Ammonium comprised 91 – 100 % of total dissolved inorganic nitrogen (DIN) flux

and therefore fluxes of NO_3^- and NO_2^- are not presented individually but are used to calculate total DIN. In addition, fluxes of PO_4^{3-} were close to detection limits and therefore were not analysed statistically. N_2 fluxes represent a balance between N fixation and denitrification and therefore a positive net flux was attributed to net denitrification (DNF), produced via denitrification and/or anammox pathways. Negative fluxes (n = 3) were omitted based on the likelihood of high O_2 saturation (>96 %) within the chambers from the formation of bubbles, which can be erroneously interpreted as N fixation (Eyre et al., 2002).

Data were partitioned into measures of nitrogen or carbon cycling. Nitrogen cycling parameters included the removal of bioavailable N (net denitrification rate; DNF), the efflux of NH_4^+ out of the sediment (NH_4^+ flux) and the efficiency of N removal (denitrification efficiency; DE) which was calculated as the percentage of DIN released as N_2 (Seitzinger, 1987, Eyre and Ferguson, 2002).

Carbon parameters included benthic metabolism (SOC) owing to the consumption of O_2 during OM degradation (in addition to macrofaunal respiration) (Glud, 2008), C degradation rate at the sediment surface (CD_S) and a photosynthesis respiration ratio (PR), a measure which indicates the trophic status of the system which has previously been suggested to be a major control of benthic nutrient fluxes (Eyre and Ferguson, 2002). Carbon degradation rates (g m^{-2} d^{-1}) were derived from the ROMA plates and calculated for each depth before being standardised by deployment time and surface area. CD_S represents the average of carbon degradation rate measured at depths of 1 and 3 cm beneath the sediment surface. To allow comparisons of C degradation rate at depth (CD_D), data at 5 and 7 cm were averaged and are included in the correlational analysis (see below). PR was previously calculated by Mangan et al. (2020b) using paired SOC and gross primary production measurements within each plot, where values < 1 indicate a state of net heterotrophy and those > 1 net autotrophy (Eyre and Ferguson, 2002).

To attain information on the biochemical characteristics of DOM using a rapid (>100 sample day^{-1}) and cost-effective (no analytical or chemical costs) method, three-dimensional excitation-emission matrix (3D EEM) fluorescence was used.

Data were first corrected for porewater dilution effects and instrument-specific biases (Stedmon and Bro, 2008) before each matrix was corrected for inner-filter effects, scatter lines were Rayleigh masked, and spectra were normalised to the mean Raman peak area of distilled de-ionised water. Fluorescence data were then processed using parallel factor analysis of components (PARAFAC), a multivariate modelling technique using the N-way toolbox in MATLAB (Andersson and Bro, 2000). PARAFAC enables fluorescence signals to be distinguished and separated into statistically independent components and therefore can estimate the relative contribution of each as well as quantify the common fluorophores present in each sample. Validation of the model was carried out using the drEEM toolbox (Murphy et al., 2013).

Four fluorescence peaks were identified in all EEMs plots (Figure A3.1), as reviewed by Coble (2007) (see Table A3.1 for a description of the excitation and emission wavelengths assigned to each peak and the potential sources attributed to each). These include three humic-like peaks (A, C and M) and one protein-like peak (T). Data are presented as total humic-like and total protein-like fluorescence at sediment depths of 0 – 2 and 5 – 7 cm. Humic-like fluorescence represents a proxy for total dissolved organic carbon and degraded OM (Burdige et al., 2004, Hansen et al., 2016), while total protein-like fluorescence has previously been used as an indicator of water quality (Baker and Inverarity, 2004), microbial activity and has strong correlations with dissolved organic N as well as sediment O_2 consumption (Clark et al., 2017).

4.2.6 Statistical analyses

Sites were chosen to increase spatial heterogeneity while including the presence of important bivalve species in order to gain a broad understanding of N and C cycling in low nutrient estuaries, accordingly, site data were pooled for all analyses. To determine if nutrient enrichment influenced sediment properties, univariate measures of macrofaunal communities and measures of nitrogen and carbon processing, one-way PERMANOVAs were conducted. Nutrient enrichment (treatment) was set as a fixed factor (3 levels; control, medium and high) on data

collected in the summer (n = 18). Where a winter comparison was available (n = 9), two-way repeated measures PERMANOVAs were used to investigate the effects of nutrient enrichment (fixed factor; 3 levels) and season (fixed factor; 2 levels; winter and summer), with replicate plot nested within treatment. Euclidean distance was used for all matrices. Where a significant interaction was present, the main effects were not considered and instead, post-hoc tests were used to identify differences between treatments and seasons. Response parameters investigated include a multivariate analysis of sediment characteristics (organic content, mud content, median grain size), MPB biomass (chlorophyll *a*), phaeopigments, humic-like and protein-like DOM fluorescence at 0 – 2 and 5 – 7 cm and porewater NH_4^+ and NO_3^- concentrations at 0 – 2 and 5 – 7 cm. All PERMANOVA analysis was performed using the PERMANOVA+ package in PRIMER 7.

Measures of N and C cycling were highly variable with and without the addition of nutrient enrichment. Considering the relatively large gradient of environmental variables and abundances of key bivalve species, correlations to N and C cycling were explored to investigate if any significant relationships could be distinguished. Pearson's correlation matrices were calculated for control, medium and high nutrient enrichment treatments separately (Figure A3.2). Variables that were depth resolved (i.e., humic-like and protein-like DOM and porewater NO_3^- and NH_4^+ concentration) were averaged prior to use in the correlation analyses. To visualise the main relationships, environmental and univariate macrofauna variables which significantly correlated to measures of N and C cycling were then interpolated into a network analysis based on the derived Pearson correlation coefficients (Pearson's r >0.5) for each nutrient enrichment treatment.

The network analysis revealed the relationships between biogeochemical cycling measures and macrofaunal and environmental parameters were modified under different nutrient enrichment treatments. Therefore, to increase our understanding of how increasing N enrichment modified important macrofauna and environmental indices and the potential origins of these changes, factor-

ceiling relationships were investigated. This approach allows the assessment of any changes in response (change in the slope or shape of the ceiling) to an increasing stressor (e.g. increased nutrient enrichment) and thus implies a constraining factor where the independent variable limits the possible magnitude of the response variable (Thomson et al., 1996). Log transformed surface (0 – 2 cm) porewater NH_4^+ was used as a proxy for nutrient enrichment treatment, and response variables included N and C cycling variables and univariate macrofaunal community indices. Maximum responses at the 90th quantile were modelled as proposed by Blackburn et al. (1992). For each model, data were divided into 4 – 6 bins or knots of approximately equal number and a constrained quantile curve fitted using a quadratic spline with up to two degree polynomials. The number of bins used was chosen to maximise the fit of the model, as assessed by comparing residual vs. predicted values. Data for the correlation matrices were analysed using the corrplot package, network analysis using the corrr package and factor-ceiling relationships using the cobs package in the R software package.

4.3 Results

4.3.1 Nutrient enrichment effects on sediment properties and macrofaunal communities

Sediment nutrient enrichment significantly increased porewater N concentrations with respect to NH_4^+ and NO_3^- (Table 4.1 and 4.2). Surface NH_4^+ (0 – 2 cm depth) was on average 40 and 800-fold higher in medium and high treatments, respectively ($p < 0.001$), which was consistent through time ($p = 0.85$; Table 4.2). Additionally, porewater NH_4^+ was typically higher at depth (5 – 7 cm), with increases of 70 and 990-fold in medium and high treatments, respectively. Nutrient enrichment did not significantly alter sediment characteristics (multivariate measure of organic content, mud content and median grain size) or phaeopigment concentration ($p > 0.24$). However, chlorophyll *a* (a proxy for MPB biomass) was on average 57 % higher in medium compared to control and high nutrient enrichment treatments (pseudo-F = 7.28; $p = 0.002$), with no significant

difference detected between winter and summer periods (p = 0.26). In addition, humic-like DOM fluorescence was significantly higher in high nutrient enrichment treatments at both sediment depths, while protein-like DOM was significantly higher under both medium and high nutrient enrichment at 0 – 2 cm but not 5 – 7 cm (Table 4.2).

Univariate measures of macrofaunal communities showed differing responses to nutrient enrichment (Table 4.2). Total abundance and the abundance of adult *A. stutchburyi* did not differ between treatments, whereas taxa richness, diversity (Shannon) and the abundance of adult *M. liliana* decreased with enrichment (p < 0.002; Table 4.2). No alterations in the abundance of the two bivalve species were observed between the winter and summer sampling events (Table 4.2).

Table 4.1: Sediment properties and univariate indices of macrofaunal communities as a function of sediment nutrient enrichment and season. Data are median with the range in parenthesis (n = 9 – 18).

	Control		Medium		High	
	Winter	**Summer**	**Winter**	**Summer**	**Winter**	**Summer**
Sediment properties						
OC (%)	2.15 (1.19–3.38)	2.00 (0.97–4.36)	2.40 (1.18–3.18)	2.82 (1.14–4.18)	2.40 (1.19–3.45)	2.07 (1.06–4.70)
Mud (%)	14 (3.20–27)	6.82 (0.94–24)	12 (2.58–25)	6.55 (2.40–28)	13 (3.91–25)	10 (2.51–27)
MGS (μm)	154 (115–205)	196 (117–256)	156 (115–205)	194 (112–245)	153 (117–204)	193 (113–243)
MPB						
Chlorophyll *a* (DW μg g^{-1})	11 (7.34–17)	8.36 (4.76–20)	18 (12–21)	15 (8.02–22)	13 (6.33–14)	12 (3.89–17)
Phaeopigments (DW μg g^{-1})	3.78 (2.94–9.99)	4.36 (2.18–13)	6.94 (4.75–15)	6.61 (3.51–13)	6.64 (2.48–14)	6.85 (3.28–25)
PR *	0.95 (−0.17–2.63)	0.75 (0.05–2.05)	0.80 (0.25–1.74)	0.71 (−0.04–1.44)	1.10 (−0.03–1.82)	0.89 (0.02–2.16)
Macrofauna (per core)						
Total abundance	-	125 (29–343)	-	90 (28–296)	-	60 (2–225)
Taxa richness	-	19 (10–25)	-	14 (7–27)	-	11 (2–22)
Shannon diversity	-	2.4 (1.7–2.9)	-	2.0 (1.1–2.7)	-	1.8 (0.4–2.5)
A. stutchburyi (>10 mm)	1 (0–24)	6 (0–57)	1 (0–25)	11 (0–49)	2 (0–29)	4 (0–56)
M. liliana (>10 mm)	3 (3–9)	3 (1–6)	1 (0–4)	1 (0–6)	0 (0–1)	0 (0–4)
DOM fluorescence						
Humic-like (0–2 cm)	-	211 (148–469)	-	285 (139–570)	-	451 (177–1233)
Humic-like (5–7 cm)	-	185 (92–703)	-	209 (98–589)	-	408 (124–1788)
Protein-like (0–2 cm)	-	73 (26–228)	-	111 (42–549)	-	195 (84–579)
Protein-like (5–7 cm)	-	80 (28–1351)	-	107 (48–258)	-	218 (37–1080)
Porewater (μmol N L^{-1})						
NO_3^- (0–2 cm)	1.23 (0.65–3.99)	1.40 (0.25–2.97)	5.68 (0.95–47)	7.21 (3.97–31)	41 (3.64–104)	28 (2.96–186)
NO_{3-} (5–7 cm)	1.31 (0.56–79)	1.30 (0.50–7.59)	6.09 (1.08–34)	27 (2.43–180)	81 (45–135)	151 (35–583)
NH_4^+ (0–2 cm)	2.19 (0.09–77)	12 (3.65–133)	602 (17–4425)	261 (12–4563)	1947 (202–13512)	4359 (371–18526)
NH_4^+ (5–7 cm)	45 (7.96–111)	37 (9.24–175)	6808 (125–12831)	2398 (26–18871)	65425 (1975–91593)	35472 (274–99917)

OC = organic content; Mud = mud content; MGS = median grain size; DW = dry weight; PR = photosynthesis respiration ratio

* Data from Mangan et al. (2020b)

Table 4.2: Results of one-way PERMANOVAs comparing summer multivariate sediment characteristics (median grain size, organic content and mud content) and univariate measures of MPB, macrofauna community, humic-like and protein-like DOM fluorescence and porewater nutrient concentrations. Repeated measures two-way PERMANOVAs are used to compare summer and winter values. Significant effects (p <0.05) are given in bold and post-hoc pairwise tests are shown for significant interactions. Nutrient enrichment treatments have been further abbreviated to C = control, M = medium, H = high, and winter and summer to W and S, respectively.

	Term	df	Pseudo-F	p (perm)	Post hoc pairwise tests	
					Treatment	Time
Summer						
Sediment characteristics	Treatment	2	0.13	0.947		
Chlorophyll *a*	Treatment	2	7.28	**0.002**	(C = H) < M	
Phaeopigments	Treatment	2	1.57	0.236		
Macrofauna						
Total abundance	Treatment	2	2.83	0.072		
Taxa richness	Treatment	2	7.45	**0.001**	(C = M) > H	
Shannon diversity	Treatment	2	6.94	**0.002**	C > (M = H)	
A. stutchburyi (>10 mm)	Treatment	2	0.14	0.868		
M. liliana (>10 mm)	Treatment	2	15.63	**0.001**	C > (M = H)	
DOM fluorescence						
Humic-like (0–2 cm)	Treatment	2	12.92	**0.001**	(C = M) < H	
Humic-like (5–7 cm)	Treatment	2	8.52	**0.001**	(C = M) < H	
Protein-like (0–2 cm)	Treatment	2	6.08	**0.004**	C < (M = H)	
Protein-like (5–7 cm)	Treatment	2	1.96	0.142		
Porewater						
NO_3^- (0–2 cm)	Treatment	2	10.81	**0.001**	C < M < H	
NO_{3-} (5–7 cm)	Treatment	2	17.69	**0.001**	C < M < H	
NH_4^+ (0–2 cm)	Treatment	2	22.02	**0.001**	C < M < H	
NH_4^+ (5–7 cm)	Treatment	2	16.16	**0.001**	C < M < H	
Seasonal						
Sediment characteristics	Treatment	2	0.17	0.988		
	Time	1	31.12	**0.001**		W ≠ S
	Treatment X Time	2	0.49	0.646		
Chlorophyll *a*	Treatment	2	5.97	**0.015**	(C = H) < M	
	Time	1	1.25	0.260		
	Treatment X Time	2	0.85	0.477		
Phaeopigments	Treatment	2	1.03	0.389		
	Time	1	4.96	**0.027**		W > S
	Treatment X Time	2	2.69	0.085		
Macrofauna						
A. stutchburyi (>10 mm)	Treatment	2	0.11	0.884		
	Time	1	1.65	0.194		
	Treatment X Time	2	0.19	0.839		
M. liliana (>10 mm)	Treatment	2	26.83	**0.001**	C > (M = H)	
	Time	1	0.62	0.439		
	Treatment X Time	2	1.35	0.292		
Porewater						
NO_3^- (0–2 cm)	Treatment	2	12.07	**0.001**	C < M < H	
	Time	1	1.19	0.282		
	Treatment X Time	2	1.87	0.161		
NO_{3-} (5–7 cm)	Treatment	2	22.20	**0.001**		

	Time	1	6.74	**0.007**		
	Treatment X Time	2	8.51	**0.001**	**S,** C < M < H; **W,** (C = M) < H	**C, M,** S = W **H,** S > W
NH_4^+ (0–2 cm)	Treatment	2	8.93	**0.001**	C < M < H	
	Time	1	0.04	0.848		
	Treatment X Time	2	0.10	0.921		
NH_4^+ (5–7 cm)	Treatment	2	14.88	**0.001**	C < M < H	
	Time	1	0.74	0.382		
	Treatment X Time	2	0.32	0.727		

4.3.2 Nutrient enrichment effects on nitrogen and carbon cycling

Nitrogen cycling variables were differentially influenced by sediment nutrient enrichment (Figure 4.2). DNF did not significantly differ between nutrient enrichment treatment or season, with DNF rates ranging from 3.6 – 207 µmol N m^{-2} h^{-1} (Figure 4.2A, Table 4.3). Effluxes of NH_4^+ from the sediment predictably increased with nutrient enrichment (pseudo-F = 18.07, p <0.001; Table 4.3), however, during the winter compared to summer were 59, 57 and 75 % lower in control, medium and high treatments, respectively. Considering DNF rates remained relatively constant with enrichment and through time, reductions to the relative percentage of total DIN returned as N_2 (DE) with increasing nutrient enrichment largely reflected changes in NH_4^+ efflux (Figure 4.2; pseudo-F = 12.47, p <0.001). For example, DE averaged 86, 7 and 2 % in control, medium and high nutrient enrichment treatments, respectively, with no difference between winter and summer periods (Table 4.3).

Carbon cycling parameters however were largely unaffected by increasing nutrient enrichment (Figure 4.2). No difference in SOC was detected in the summer after 20 months of nutrient enrichment (pseudo-F = 1.35, p = 0.258; Table 4.3). However, when comparing SOC over a reduced number of sites and across two sampling periods, a medium level of nutrient enrichment was significantly higher than both control and high treatments. In addition, significant reductions of 69, 62 and 76 % were observed in winter compared to summer periods in control, medium and high treatments, respectively (Table 4.3). Surface carbon degradation rate (CD_S) and the trophic state of the system (PR) additionally

showed no treatment effects during the summer sampling (pseudo-F = 1.19, p = 0.296), but both were highly variable across all treatments (e.g., CD_S ranged from 4 – 35 g C m^{-2} d^{-1}).

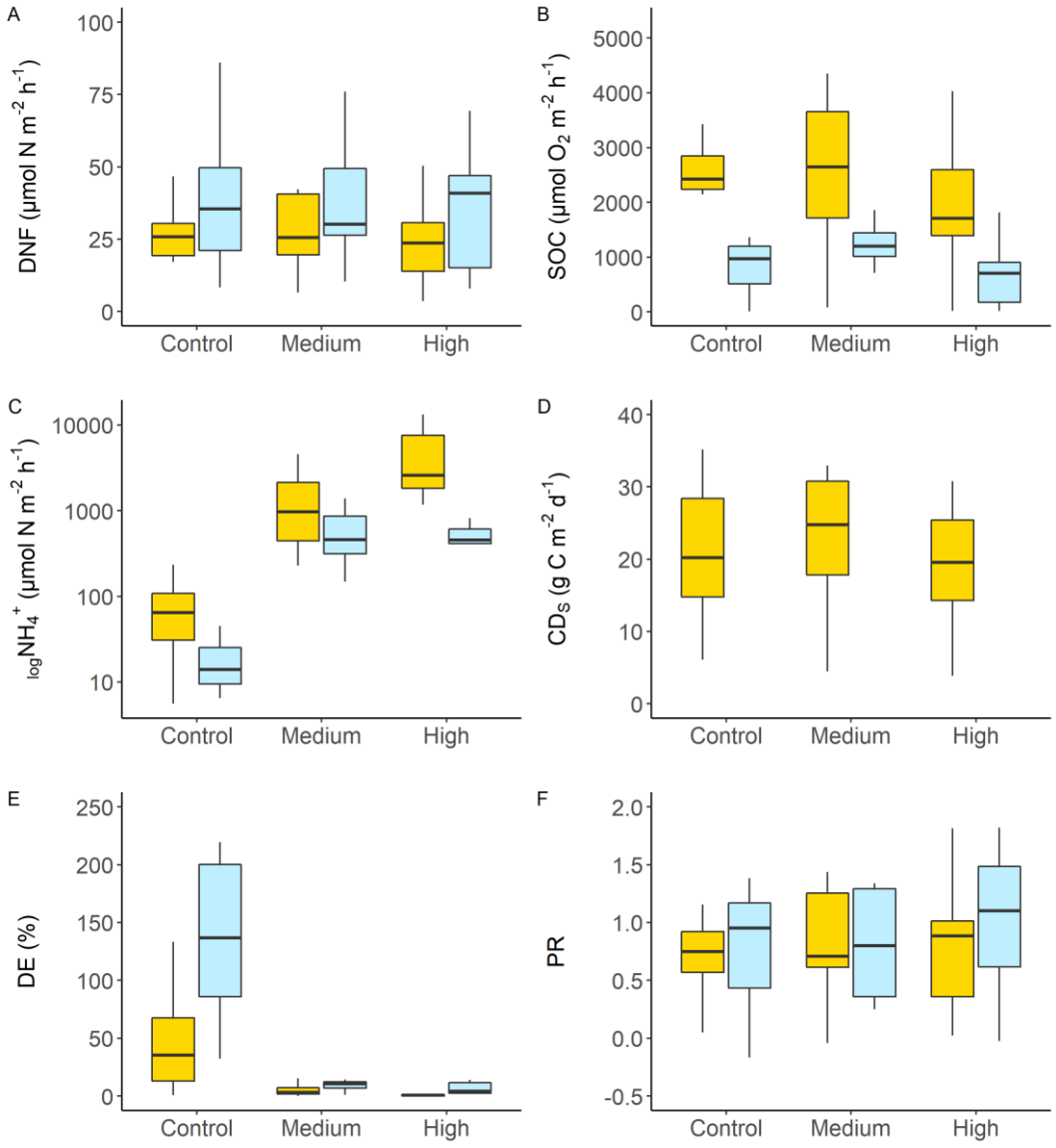

Figure 4.2: Measures of nitrogen (A, C, E) and carbon cycling (B, D, F) during summer (yellow) and winter (blue) as a function of nutrient enrichment treatment. Boxes represent the 25th and 75th percentiles, and whiskers are the 5th and 95th percentiles. A solid line within each box denotes the median. Note log_{10} scale of the y-axis in panel C.

Table 4.3: Results of one-way PERMANOVAs comparing summer univariate measures of nitrogen and carbon cycling as a function of nutrient enrichment treatment. Repeated measures two-way PERMANOVAs are used to compare summer and winter values. Significant effects (p <0.05) are given in bold and post-hoc pairwise tests are shown for significant interactions. Nutrient enrichment treatments have been further abbreviated to C = control, M = medium, H = high, and winter and summer to W and S, respectively.

	Term	df	Pseudo-F	p (perm)	Post hoc pairwise tests	
					Treatment	Time
Nitrogen processing						
Summer						
DNF	Treatment	2	0.79	0.499		
NH_4^+ efflux	Treatment	2	18.07	**0.001**	C < M < H	
DE	Treatment	2	0.89	0.646		
Seasonal						
DNF	Treatment	2	1.84	0.210		
	Time	1	2.65	0.145		
	Treatment X Time	2	0.71	0.501		
NH_4^+ efflux	Treatment	2	12.18	**0.001**		
	Time	1	12.38	**0.001**		
	Treatment X Time	2	7.06	**0.001**	**S,** C < M < H, **W,** C < (M = H)	**C, H,** S > W, **M,** S = W
DE	Treatment	2	12.47	**0.003**	C > M > H	
	Time	1	0.40	0.620		
	Treatment X Time	2	3.20	0.142		
Carbon processing						
Summer						
SOC	Treatment	2	1.35	0.258		
CD_S	Treatment	2	1.19	0.296		
PR	Treatment	2	0.19	0.813		
Seasonal						
SOC	Treatment	2	3.60	**0.036**	C = (M > H)	
	Time	1	30.46	**0.001**		S > W
	Treatment X Time	2	1.14	0.354		
PR	Treatment	2	0.17	0.798		
	Time	1	1.10	0.328		
	Treatment X Time	2	0.63	0.558		

4.3.3 Relationships between biogeochemical cycling and environmental variables

Measures of N and C cycling were highly variable with and without the addition of nutrients, therefore correlations with environmental and macrofaunal communities were investigated (Figure 4.3; for full Pearson's correlation matrices see Figure A3.2). While no strong relationships were revealed (Pearson's r > 0.70) without nutrient enrichment, DNF in control treatments was most strongly

correlated to C related parameters (CD_S Pearson's r = 0.50; humic-like DOM r = −0.49; OC r = 0.45), and to a lesser extent porewater NO_3^- concentration and taxa richness. Nutrient regeneration, measured as NH_4^+ efflux within control treatments, was most strongly correlated to PR (Pearson's r = −0.70, p <0.001) such that the more heterotrophic the system, the more NH_4^+ was released to the water column (which in turn is strongly correlated to water column turbidity (data not shown; Pearson's r = 0.64, p <0.001)). However, no relationship between NH_4^+ effluxes and sediment chlorophyll *a* was observed suggesting this was unlikely to be attributed to dark uptake by MPB. Instead, sites with lower NH_4^+ effluxes were likely to have higher rates of DNF (Pearson's r = −0.47, p < 0.001). This is also revealed by the positive relationship between DE and PR, suggesting the more autotrophic the system, the higher the percentage of N was removed as N_2 (Pearson's r = 0.66, p < 0.001). NH_4^+ regeneration in control plots was additionally correlated to all univariate macrofaunal indices, and in particular to total abundance and the abundance of adult *A. stutchburyi*. DE was most strongly correlated to CD_S (Pearson's r = 0.77, p < 0.001) in addition to macrofaunal activities (e.g., species richness: Pearson's r = −0.69, p < 0.001).

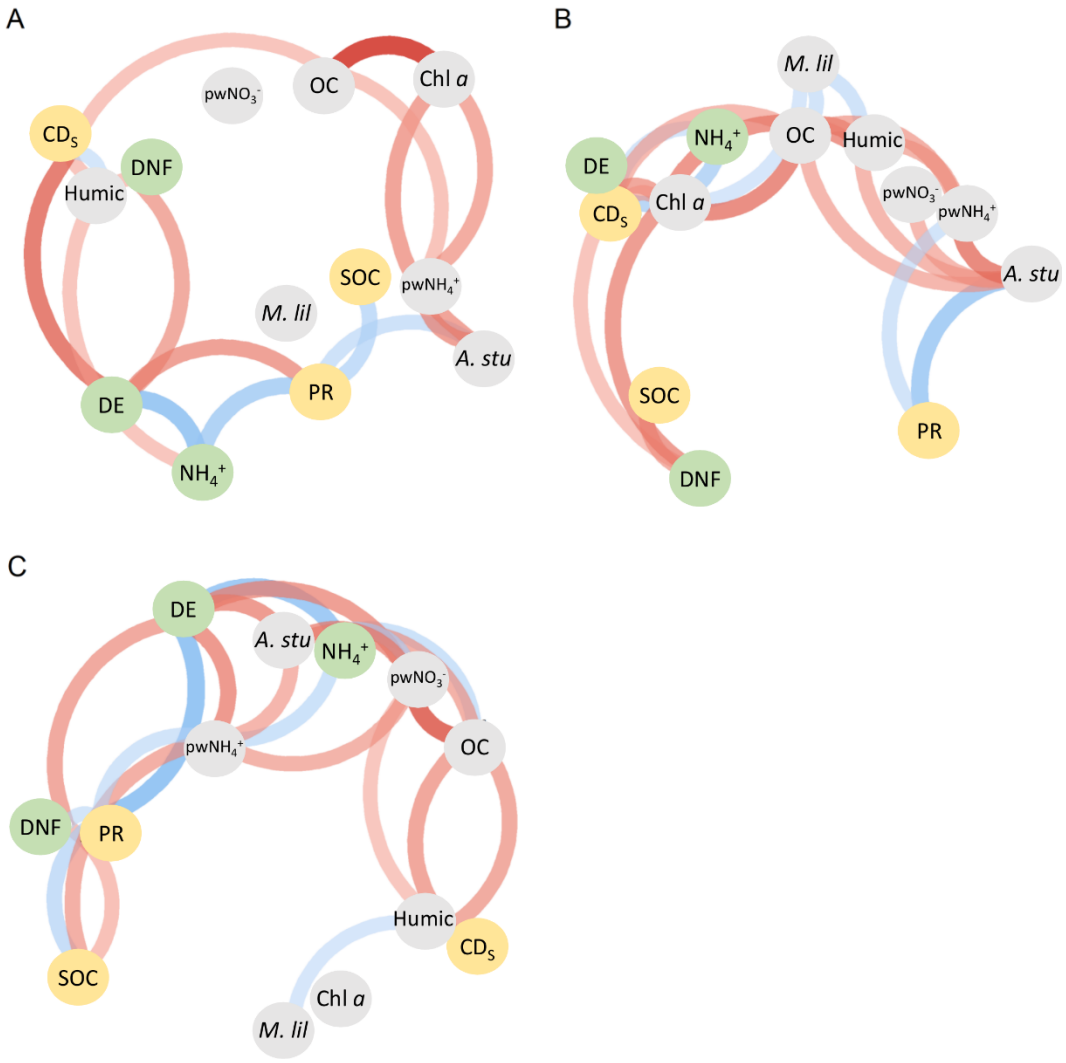

Figure 4.3: Network plots of Pearson's correlation matrices (Pearson's r >0.5) including N and C cycling parameters and key environmental variables and macrofauna species within A) control, B) medium and C) high nutrient enrichment treatments. For full correlation matrices see Figure A3.2. Positioning within the network is based on similarity clustering and correlations are coloured in shades of blue for negative and red for positive correlations. Green and yellow boxes refer to N and C cycling parameters, respectively. Data included are from the summer sampling (n = 18). DNF = net denitrification rate; NH_4^+ = NH_4^+ efflux; DE = denitrification efficiency; SOC = sediment oxygen consumption; CDS = carbon degradation rate at the sediment surface; PR = photosynthesis respiration ratio; *A. stu* = adult (<10 mm) *Austrovenus stutchburyi*; *M. lil* = adult (<10 mm) *Macomona liliana*; OC = sediment organic content; Humic = humic-like fluorescence; $pwNH_4^+$ = porewater ammonium concentration; $pwNO_3^-$ = porewater nitrate concentration.

In treatments without added nutrients, SOC showed no relationship to any of the other N or C cycling parameters. However, positive albeit weaker relationships were observed with the abundance of adult *A. stutchburyi* and to chlorophyll *a*

and OC (Pearson's r >0.27). In addition to significantly influencing DNF and DE, CD_s was predominately correlated to sediment OC (Pearson's r = 0.51). Trophic status (PR) was significantly correlated with NH_4^+ efflux (Pearson's r = −0.70) and thus DE (Pearson's r = 0.66), in addition to the abundance of adult *A. stutchburyi* (Pearson's r = −0.55), and protein like DOM fluorescence (Pearson's r = −0.70; Figure 4.3), a proxy for microbial activity and total dissolved organic N concentration.

These relationships and thus the contributions of particular variables were altered under increasing nutrient enrichment. Most notable was the increase in the number and strength of correlations between all N and C cycling parameters with porewater nutrient concentrations, particularly in the high nutrient enrichment treatments. In addition, while the links between C processing and DNF and DE were maintained with enrichment, the relative contribution of a particular variable changed. For example, under increasing nutrient enrichment the relationships between DNF and CD_s and humic-like DOM were lost but the correlation to SOC increased (Pearson's r > 0.53). Additionally, the relationship between DE and CD_S was weakened and then lost under high nutrient enrichment while the contribution of OC increased. Other notable relationships include the increase in correlation strength between DNF and sediment chlorophyll *a* content and total abundance in medium enrichment treatments, and the reversal of relationships with NH_4^+ effluxes in both medium and high treatments.

4.3.4 Response of environmental and macrofaunal community variables to increasing nutrient enrichment

Environmental characteristics and dominant macrofaunal species can have a substantial influence on sediment biogeochemical processes, therefore their relative importance in influencing N and C cycling and the response to increasing N enrichment was investigated (Figure 4.3). Under no N enrichment, a high correlation of total abundance to adult *A. stutchburyi*, a suspension-feeding bivalve (Pearson's r = 0.83, $p < 0.001$) was observed. The abundance of adult *A. stutchburyi* was also highly correlated to phaeopigment content (Pearson's r = 0.79, $p < 0.001$), a proxy for recent grazing activity and potentially bioturbation, in

addition to increasing sediment NH_4^+ availability (Pearson's r = 0.66, $p < 0.001$), a by-product of grazing and/or through increased excretory products.

Many of the relationships, however, did not consistently change with increasing nutrient enrichment and were therefore likely to be non-linear. For example, the correlation of adult *A. stutchburyi* to porewater NH_4^+ increased before decreasing under medium and high nutrient enrichment treatments, respectively. This has important ecological implications because ecosystem functioning can fundamentally shift without additional extreme environmental forcing once thresholds are reached. To investigate this further, surface (0 – 2 cm) porewater NH_4^+ concentration was used as a proxy for nutrient enrichment treatment to allow the examination of factor-ceiling relationships and thus identify any changes in response.

Models containing N and C cycling parameters and univariate measures of macrofaunal communities revealed a variety of different responses, indicating specific sensitivity to increasing NH_4^+ concentrations (Figure 4.4). Response types identified included decline, increase, unimodal and skewed unimodal. While NH_4^+ efflux and DE increased and decreased, respectively, within increasing N availability in agreement to the relationships previously described (Figure 4.2), DNF decreased with increasing porewater NH_4^+ concentration below plateauing under medium and high levels of nutrient enrichment.

The similarity of response between SOC and total abundance suggests changes in benthic metabolism were largely attributed to macrofaunal activity, and in particular adult *A. stutchburyi*. The skewed unimodal response of adult *A. stutchburyi* suggests partial tolerance to increasing NH_4^+ concentrations before reaching a threshold of change resulting in linear declines. Conversely, the abundance of adult *M. liliana* declined with increase porewater NH_4^+ such that abundances reached zero at high nutrient concentrations, highlighting the acute sensitivity to any increases in sediment pore water nutrient concentrations.

Factor-ceiling relationships of the trophic state (PR) of the system revealed a change in response at high levels of nutrient enrichment, where the system transitioned from being net autotrophic to increasingly more net heterotrophic, and therefore a switch from net C production to respiration. The initial increase in net autotrophy may partially be explained by the increasing MPB biomass (as measured by chlorophyll *a*) with increasing nutrient enrichment, before a change in response and a decline was observed at high levels of nutrient enrichment.

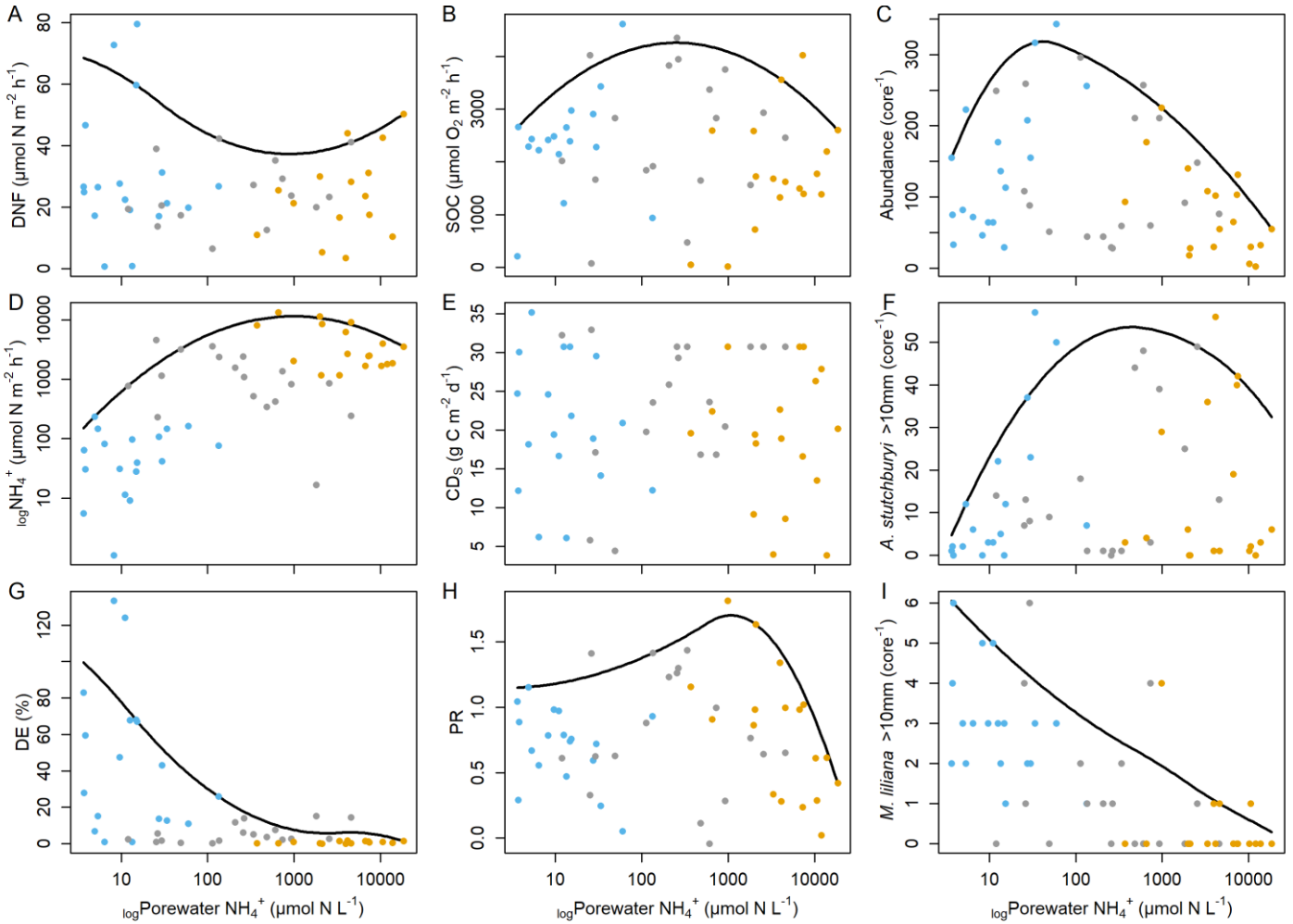

Figure 4.4: Bivariate scatter plots of nitrogen (A, D, F) and carbon (B, E, H) cycling parameters and univariate macrofaunal indices (C, F, I) showing factor-ceiling relationships (black line) at the 90th percentile. Where the line is missing, the relationship did not change with increasing enrichment. Blue, grey and orange dots are given as a reference to control, medium and high nutrient enrichment treatments, respectively. Data included are from summer only (n = 54).

4.4 Discussion

The ability of low-nutrient estuaries to process and remove excess N is fundamental in preventing reductions in ecosystem functionality and a shift towards a more eutrophic state under increasing nitrogen enrichment. In particular, DNF pathways have been suggested to increase the resilience of coastal habitats to increasing N loading owing to the removal of bioavailable N (Seitzinger et al., 2006). Net DNF rates within this study were comparable to those reported elsewhere in New Zealand and globally (e.g. Eyre and Ferguson, 2002, Braeckman et al., 2010, Eyre et al., 2013, Gongol and Savage, 2016, O'Meara et al., 2020), but were highly variable, ranging between 4 and 208 μmol N m^{-2} h^{-1}. In addition, no change in DNF rate was observed between season (Figure 4.2, Table 4.3). Current *in situ* measurements of DNF over multiple seasons are still relatively uncommon however, Piehler and Smyth (2011) observed similar rates of DNF in winter and spring (compared to winter and early summer in this study), while Eyre et al. (2013) reported both no seasonal response and lower winter rates at different intertidal locations.

The large variability in DNF enables the role of environmental and macrofaunal community variables in potentially regulating DNF to be investigated. When considering only variables measured under no nutrient enrichment, our results demonstrate strong correlations to C, as evidenced by the significant relationships with carbon degradation (CD_S), humic-like DOM (an indicator of total organic carbon concentration (Sierra et al., 2001, Burdige et al., 2004)) and sediment OC (Figure 4.3). Within low nutrient estuaries where there is limited or no excess N, NTR and DNF are often tightly coupled and therefore the degradation of OM crucially supplies NH_4^+ needed for NTR (Seitzinger et al., 2006). However, no relationship was found between DNF and SOC which has previously been suggested as a key indicator of DNF rate (Eyre and Ferguson, 2005, Piehler and Smyth, 2011). This may be a product of using multiple sites and thus the inclusion of significant spatial heterogeneity, in addition to the differences in the abundance of dominant macrofaunal species which are likely to differentially alter

bioturbation activity and rates of benthic metabolism (Glud, 2008) and thus may confound the relationship between SOC and DNF.

Higher rates of DNF in control plots were however, shown to correspond to lower rates of nutrient regeneration (NH_4^+ efflux) (Pearson's r = −0.47, $p < 0.001$; Figure 4.3), indicating competition between nitrifiers and benthic microalgae (Rysgaard et al., 1995). The likelihood of NH_4^+ being denitrified versus released into the water column may be associated with the trophic state of the system, such that the more heterotrophic the system (and thus the more turbid; Pearson's r = −0.64, $p < 0.001$; data not shown) the more likely NH_4^+ was effluxed rather than denitrified (Figure 4.3) (Eyre and Ferguson, 2002). In addition, while all measurements were taken in the absence of ambient sunlight and dark uptake of NH_4^+ by MPB was unlikely (no correlation to chlorophyll *a*), an overall reduction in C production in heterotrophic systems would both reduce C availability and O_2 production. The latter can suppress NTR and the production of NO_3^- and therefore NH_4^+ may be effluxed rather than assimilated or denitrified. This is supported by a previous study showing increasing NH_4^+ effluxes with increasing water column turbidity (and thus PR) (Pratt et al., 2014) in addition to Eyre and Ferguson (2002) similarly highlighting the increase of NH_4^+ effluxes under increasing net heterotrophy.

Increasing NH_4^+ effluxes are often linked to the beginning of a shift towards a more eutrophied state (Eyre and Ferguson, 2002), owing to potential increases in pelagic production and a reduction in N being assimilated by benthic producers, reducing the availability for secondary consumers and consequently resulting in a cascade of negative feedbacks. Therefore, assessing the potential for enhanced DNF with increasing N enrichment and the relative contribution of NH_4^+ effluxes can help quantify the potential vulnerability of a system to eutrophication. The enrichment of sediment porewaters over a 20-month period resulted in NH_4^+ concentrations comparable to those in eutrophic estuaries globally (Douglas et al., 2016). Despite the increase in porewater NH_4^+ and NO_3^- concentration, no changes in DNF rates were observed (Figure 4.2). While it was expected N enrichment may enhance MPB biomass and thus C availability in N limited systems (Smith and Underwood,

2000), both C supply and degradation (OC, humic-like DOM and CD_S,) did not increase with enrichment suggesting DNF was likely to be C limited. However, increases in the correlation strength of DNF to porewater concentration, and reductions in strength to chlorophyll *a* and macrofaunal abundances with increasing enrichment suggests a potential switch from tightly coupled NTR- DNF to direct DNF. The facilitation of direct DNF is likely a consequence of the increase in nitrate concentration reducing the competition between primary producers and nitrifying and denitrifying bacteria (Cornwell et al., 1999).

Sediment nutrient enrichment resulted in significant increases of NH_4^+ effluxed into the water column. This is consistent with rates of DNF remaining constant and no substantial increases in MPB assimilation (i.e., no change in MPB biomass). There was, however, a significant reduction in effluxes during winter compared to summer periods (Figure 4.2). This may be a product of reduced activity by key bioturbators and thus the advection of solutes (Herbert, 1999, Glud, 2008), which is supported by a similar reduction in SOC and macrofaunal abundance under increasing nutrient enrichment (Figure 4.4), and lower rates of SOC in winter compared to summer (Figure 4.2, Table 4.3) further supporting evidence of the importance of biodiversity-ecosystem relationships in influencing biogeochemical cycling (Douglas et al., 2017).

DNF is an important service in removing excess N, but perhaps even more important as an indicator of change is the percentage of total DIN removed as N_2, expressed as DNF efficiency (DE) (Eyre and Ferguson, 2009). Under no nutrient enrichment, DE averaged 86 % with maximum values of 220 %, highlighting the dominance of DNF over N regeneration in low nutrient estuaries, such that more N was removed as N_2 than remained as bioavailable N within the system (>100 %) (Figure 4.2). DE was most strongly correlated to carbon decomposition (CD_S), a relationship previously reported within the literature (Eyre and Ferguson, 2002, 2009). Although CD_S cannot be directly compared to that calculated previously (ΣCO_2), the positive relationship (Pearson's $r = 0.77$, $p < 0.001$; Figure 4.3) observed in this study is likely to correspond to the beginning of the parabolic relationship

found by Eyre and Ferguson (2009) for relationships established between oligotrophic to hypertrophic estuaries. The control of C on DE is further supported by the strong positive correlation to PR, and thus increasing net autotrophy. A higher PR value has previously been shown to correspond to higher rates of gross primary production and thus C production, a consequence associated with reduced water column turbidity (Mangan et al., 2020b).

DE was additionally positively correlated to the abundance of bioturbating macrofaunal (*M. liliana*; Pearson's r = 0.46, $p < 0.001$) which promotes a higher degree of biocomplexity within the sediment and facilitates the overlapping of aerobic and anaerobic zones, enhancing the supply of NO_3^- and the movement of C into sub-oxic sediment layers (Volkenborn et al., 2012). However, under increasing nutrient enrichment DE was significantly reduced, averaging 7 and 2 % in medium and high treatments, respectively. The low rates of DE reflects both the absence of a response from DNF and the substantial increase in NH_4^+ efflux, increasing the potential for a shift towards pelagic dominated primary production.

Increasing nutrient enrichment considerably altered the relationships and interactions between N and C cycling, environmental variables and macrofaunal communities. However, many relationships appeared to be non-linear, as evidenced by the changes in correlation direction under increasing nutrient enrichment. This has important implications for ecosystem functioning considering a small increase in cumulative stress can result in an abrupt ecological shift if thresholds are crossed (Scheffer et al., 2012). Surface (0 – 2 cm) porewater NH_4^+ concentration was used as a proxy for nutrient enrichment treatment to identify changes in response and thus critical transitions using factor-ceiling relationships.

The similarity in response between SOC and total macrofaunal abundance suggests benthic metabolism was dominated by macrofaunal activity, and in particular adult *A. stutchburyi* (Figure 4.4). However, the unimodal response highlights the sensitivity of macrofaunal communities to increasing N enrichment, as evidenced by a change in response and reductions in total abundance under a

medium level of nutrient enrichment. The sensitivity of *M. liliana* was significantly greater than *A. stutchburyi*, with linear declines observed with increasing enrichment. While initial increases in adult *A. stutchburyi* may facilitate coupled NTR-DNF through increased bioturbation activity (Volkenborn et al., 2012), eventually, reductions in the abundance of both key bioturbating species will reduce the spatial and temporal heterogeneity of sedimentary redox zones and thus suppress NTR under increased sediment anoxia (Thrush et al., 2006, Woodin et al., 2010, Volkenborn et al., 2012, Foster and Fulweiler, 2014).

The reduction in the vertical movement of solutes within the sediment with increasing nutrient enrichment was evidenced by comparing the difference between surface and deep porewater DOM under different nutrient enrichment treatments (Figure A3.1). Humic-like DOM at the sediment surface was 6 % lower than at depth in both control and medium nutrient enrichment treatments but 33 % lower in response to high enrichment. The larger difference at high N enrichment indicates a more stratified sediment layer and thus lower mixing and bioturbation activity. In addition, the higher intensity of humic-like DOM at depth has been suggested to represent the accumulation of refractory, low molecular weight DOM during sediment OM diagenesis in addition to increased sediment anoxia (Burdige et al., 2004). These increases in sediment anoxia may have resulted in further reductions in macrofauna abundances and thus bioturbation activity in the high nutrient enrichment treatments. However, any changes in bioturbation activity did not directly translate into changes in DNF, a possible consequence of DNF becoming uncoupled with increasing nutrient enrichment and C supply limiting DNF (as shown by no change in carbon decomposition rate).

A unimodal relationship was additionally observed for the trophic status of the system (as indicated using PR), where a critical transition in response occurred between medium and high nutrient enrichment (Figure 4.4). The modification of PR is an important indicator of benthic nutrient fluxes in shallow coastal ecosystems because increasing net heterotrophy can lead to an increase in the release of inorganic nutrients through respiration (Eyre and Ferguson, 2002).

While it is important to recognise that these patterns are correlative and there are other factors which can influence sediment biogeochemical cycling, the transition to increasing net heterotrophy has important implications for overall ecosystem functioning owing to the potential intensification of pelagic production and the start of a cascade towards a more eutrophic state.

4.5 Conclusions

It is evident that both C and N cycling within estuarine sediments are tightly coupled and embedded within a complex network of ecosystem interactions. However, anthropogenic pressure on coastal ecosystems is intensifying which is impeding the capacity to moderate intensifying pollutant loads. By coupling measurements of N and C cycling within low-nutrient estuaries, an area currently underrepresented (Vieillard et al., 2020), this study highlights the limited capacity for DNF to mitigate large increases in N availability, as evidenced through the reductions in DE. Increases in porewater N concentrations along with subsequent changes in macrofaunal communities resulted in the potential uncoupling of NTR-DNF to direct DNF. However, it should be recognised that these responses may differ depending on the quality and quantity of any accompanying C inputs (Eyre et al., 2013) in addition to the stimulation of hypoxia which often occurs simultaneously with coastal eutrophication (Gray et al., 2002). Macrofaunal communities and the degree of net autotrophy/ heterotrophy (PR) were shown to have important influences on N processing. Factor-ceiling relationships revealed, that in general, optimum abundances corresponded to lower N enrichment, highlighting the vulnerability of estuaries to increasing stressor loads. The appearance of these transitions can signify changes to the interactions of intrinsic dynamics and drivers which can fundamentally alter biogeochemical cycling within soft sediments and increase the likelihood of abrupt non-linear shifts in ecosystem functioning (Cloern et al., 2016, Thrush et al., 2020). Consequently, current stress-response management approaches to increasing N enrichment may not be suitable in preventing a shift towards a more eutrophied state as dynamic changes dominate ecosystem interactions.

Chapter Five: General Discussion

Throughout this thesis I have investigated how two prevalent stressors; increased sediment loading and nutrient enrichment, can interact and influence microphytobenthic primary production and biogeochemical cycling within coastal ecosystems. In addition, I have considered the ecological implications when coupled with a global scale stressor; sea level rise and the subsequent loss of intertidal area. To achieve this, I employed a combination of monitoring techniques, literature review and experimental field studies over a large spatial and temporal extent, that collectively highlight that the interaction of multiple local scale stressors can lead to significant ecological degradation and the increased reliance on emerged tidal periods is likely to predispose soft sediment ecosystems to increasing vulnerability when coupled with future global change.

5.1 Summary of major findings and implications

5.1.1 Benthic productivity

While it is well known that high water column turbidity can directly reduce the rate and efficiency of benthic primary production (Pratt et al., 2014, Du et al., 2018) and ultimately restrict MPB producitivty to emerged tidal periods (Migné et al., 2004, Spilmont et al., 2006), before this thesis the extent to which this may occur across New Zealand was largely unknown. In Chapter 2 I aimed to characterise the light climate reaching intertidal MPB across multiple New Zealand estuaries during emerged and submerged tidal periods. To achieve this I deployed light sensors at 22 sites situated within 14 estuaries that covered 11 degrees of latitude. I demonstrated that light availability was highly spatially and temporally variable and was driven by opposing factors depending on tidal stage. Such that, during emerged periods variability was attributed to latitude (i.e. sun angle) and geographic characteristics, compared to water column turbidity during submerged periods.

Changes in light availability become ecologically important when phototrophic organisms become light limited. However, before this thesis, a global summary of the relationship between light and MPB production within intact communities was missing, and therefore general estimations of light limitation across large temporal and spatial scales were difficult. To overcome this, I conducted a literature search of *in situ* MPB photosynthesis-irradiance curves with a focus on natural, intact communities that integrated the effects of environmental and behavioural responses (Chapter 2). This analysis revealed the limited knowledge of the functional relationship between light and MPB primary production; only 18 studies. However, by using a globally relevant value of light saturation, I was able to estimate that water column turbidity may limit MPB productivity across my study estuaries between a median of 55 – 100 % of the time. Consequently, I suggest some sites and estuaries (e.g. Manukau harbour) within New Zealand may not support MPB productivity during submerged periods and therefore water column turbidity is likely to be a chronic stressor within several estuaries across New Zealand.

The considerable influence of water column turbidity on MPB productivity was confirmed by *in situ* measurements taken within Chapter 3, where up to 40 % of the variability in submerged primary production estimates were explained by water column turbidity alone. Over the long term, increasing water column turbidity and the associated increase in net heterotrophy and negative net primary production (Chapter 3) can directly reduce the supply of labile carbon to coastal food webs (Serôdio and Catarino, 1999, Middelburg et al., 2000, Christianen et al., 2017). In addition, reduced MPB productivity can alter sediment stability and erosion thresholds through reductions in the secretion of extracellular polymeric substances (which is an additional source of organic material to bacteria) (Tobias et al., 2003, Underwood and Paterson, 2003, Tolhurst et al., 2008) and modify the transformation and recycling of nutrients (Longphuirt et al., 2009, Hochard et al., 2010, Benelli et al., 2018) which can be further influenced by changes to macrofaunal communites (Lever and Valiela, 2005). Therefore, persistent water column turbidity both in New Zealand and globally can negatively influence the

ecosystem functions and services delivered by MPB, and thus have cascading ecological consequences.

A unique characteristic of Chapter 3 was the coupling of submerged and emerged MPB primary productivity estimates *in situ*, over a large environmental gradient and across two seasons. This empirically showed net autotrophic emerged tidal periods where MPB production becomes unconstrained by light limitation, are likely be an important initial mechanism of resilience through sustaining MPB benthic productivity. This is already estimated to occur within New Zealand (Drylie et al., 2018, Chapter 2) as well as globally (Spilmont et al., 2006, Denis et al., 2012, Migné et al., 2018). However, by taking measurements across a gradient of water column turbidity I was able to show that emerged tidal periods are unlikely to fully compensate the reductions in productivity lost during submergence. For example, MPB productivity was significantly lower at high turbidity sites during emergence than at low turbidity sites during submergence (Chapter 3). In addition, other ecosystems functions are likely to be reduced or lost such as a reduced uptake of nitrogen by MPB which can lead to an increase in ammonium efflux into the water column (Thornton et al., 1999, Longphuirt et al., 2009, Pratt et al., 2014) and the increasing likelihood of pelagic algal blooms. This is turn can further increase light attenuation to the benthos, creating positive feedback loops which can ultimately promote coastal eutrophication (Vahtera et al., 2007).

Anthropogenic stressors, however, rarely occur in isolation. Both in New Zealand and globally, increases in nutrient availability are often accompanied by sedimentation inputs (which frequently leads to high water column turbidity) (Thrush et al., 2004), which can alter rates of benthic primary production and favour increases in pelagic dominated production (Nixon, 1995, Cloern, 2001, Rabalais et al., 2005). Therefore, Chapter 3 uniquely included the investigation of the potential interactive effects of an additional stressor, increased nitrogen availability, on MPB productivity over a full tidal cycle. To achieve this, I enriched the sediment with nitrogen for up to 20 months at the 6 sites situated over a gradient in water column turbidity. Experimental enrichment of the sediment

successfully resulted in porewater ammonium concentrations comparable to those in eutrophic estuaries globally, however, nutrient enrichment had no significant influence on MPB productivity after 8, 15 or 20 months. This was unexpected considering calculated N:P porewater ratios within the control plots suggested all sites were nitrogen limited (Chapter 3). These results highlight the multifaceted response of MPB to increasing stressor loads, where simple linear increases are rarely observed *in situ*. Instead, the limited response of MPB productivity to increasing nutrient enrichment is likely to be moderated by a combination of factors which include bedload transport, carbon supply, light availability, phosphorus limitation and/or grazing activity (Barranguet et al., 1998, Meyercordt and Meyer-Reil, 1999, Hillebrand et al., 2000, Stutes et al., 2006).

Further complicating the effects of multiple stressors at a local scale, is the interacting effect with global stressors such as climate change. In particular, the effects of climate change are expected to be greater for communities already experiencing a high level of existing stress (Harley et al., 2006, Hewitt et al., 2016) and therefore the ecosystem functions and services delivered by MPB in highly turbid estuaries may be further compromised when considering future global change. My research considers how the vulnerability of estuaries characterised by high water column turbidity will change in response to reductions in intertidal areas owing to increasing sea-level rise (Chapter 2). When considering a 1.4 m increase in sea-level predicted for the end of the century (Rahmstorf, 2007, Turner et al., 2009), I estimated the intertidal area of my study estuaries could decline by 27 – 94 %. When large decreases in intertidal area are coupled with measurements of high water column turbidity (and thus light limitation), I highlight how the vulnerability to the loss and degradation of ecosystem functioning will increase, as emersion periods, which were providing a level of resilience to estuarine ecosystems, become restricted. Furthermore, under predicted increases in the intensity and severity of storm events (Seneviratne et al., 2012), this is likely to be exacerbated, further reducing the delivery of ecosystem services by MPB. Overall, this thesis has been able to contribute to the existing literature by considering and evaluating many of the interactions proposed at the beginning of this thesis in

Chapter 1 (Figure 5.1), and collectively highlight how coastal habitats may become increasingly vulnerable to collapse when considering both local stressors and future global change.

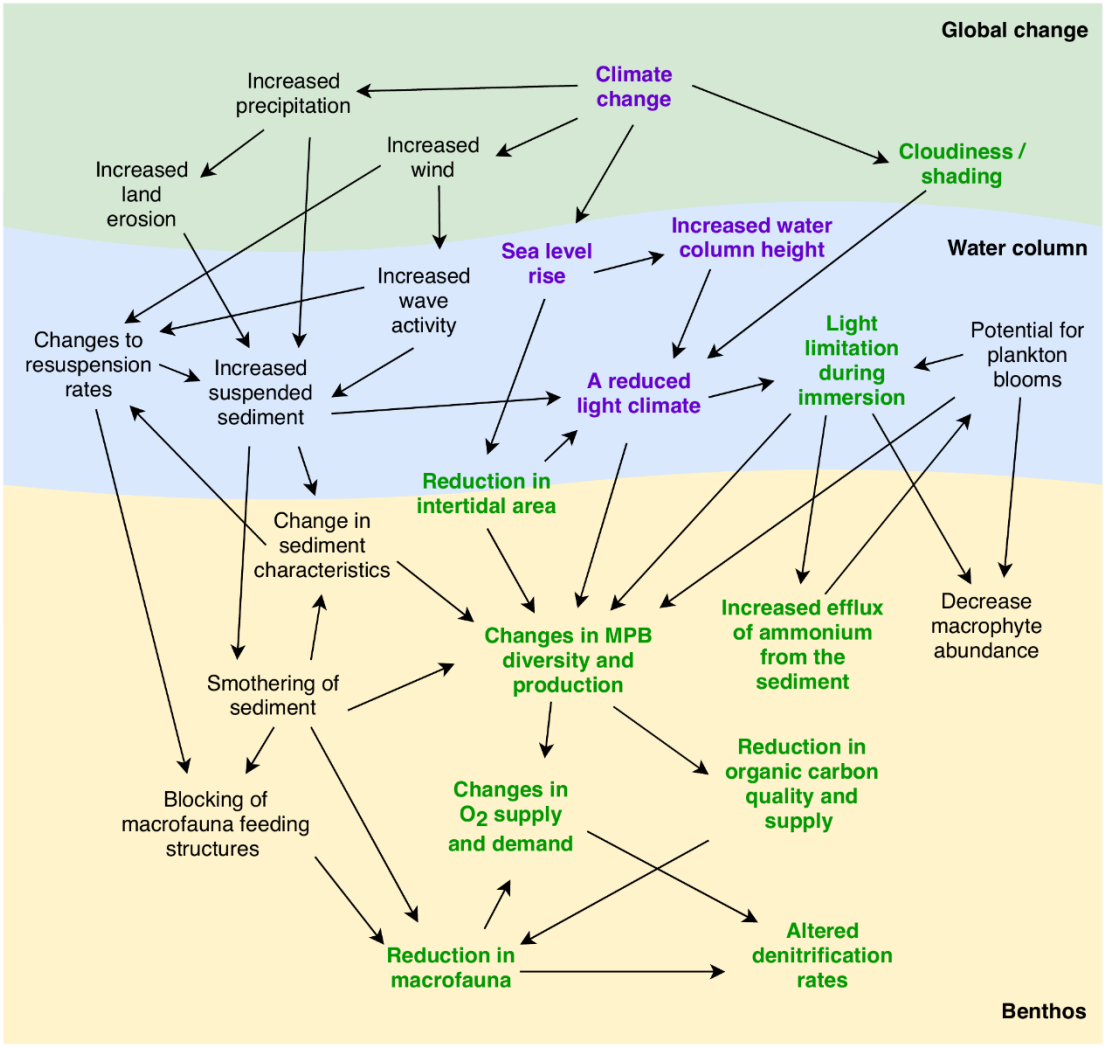

Figure 5.1: The main pathways which alter water column light climate and the subsequent alterations to ecosystem functioning and service delivery in intertidal habitats dominated by MPB. Adapted from Thrush et al. (2004). Purple and green text highlight the factors considered and assessed during this thesis, respectively.

5.1.2 Nutrient cycling

Soft sediment intertidal habitats are not only hot spots for benthic productivity, but they also play a fundamental role in global biogeochemical cycling (Crossland et al., 2005, Huettel et al., 2014, Hope et al., 2020). The intensification of nutrient loading within coastal areas can significantly alter the transport, processing and recycling of nutrients which can ultimately lead to coastal eutrophication (Cooper and Brush, 1993, Scheffer and Carpenter, 2003). Therefore, in Chapter 4 I aimed to investigate the influence of increased nitrogen availability on the coupling between nitrogen and carbon cycling and identify any alterations in biodiversity-ecosystem relationships which can regulate nutrient processing in soft sediment habitats (Stief, 2013, Douglas et al., 2017). This was accomplished by combining measurements of nutrient and gas fluxes with the nutrient enrichment experiment described in Chapter 3. This study demonstrated tight coupling between nitrogen and carbon cycling across multiple different estuaries under no nutrient enrichment, further supporting the importance of including measurements of both carbon quality and quantity when investigating nitrogen cycling (Brettar and Rheinheimer, 1992, Fulweiler et al., 2008, Eyre et al., 2013). Nutrient cycling additionally appeared to be regulated by macrofaunal communities and the trophic status of the system. The latter highlights the influence of water column turbidity, whereby net heterotrophic, turbid systems were characterised by lower rates of denitrification and higher ammonium effluxes, potentially facilitating the enhancement of pelagic over benthic primary production through alterations in the ability to process nitrogen.

Under increasing nutrient inputs, denitrification is often characterised as an important mechanism which can increase the resilience of coastal ecosystems owing to the removal of bioavailable nitrogen (Seitzinger et al., 2006, Teixeira et al., 2010). Net denitrification rate was not augmented by increasing nitrogen availability, resulting in the proportions of nitrogen denitrified compared to returned to the water column as ammonium significantly reducing from an average of 86 % to 7 % and 2 % under control, medium and high nutrient

enrichment, respectively. Alternatively, denitrification was largely regulated by carbon supply, the trophic state of the system and biodiversity-ecosystem relationships (Chapter 4). In estuaries with low water column nitrate such as those within New Zealand (Lohrer et al., 2010, Santos et al., 2014), denitrification is likely to be tightly coupled to nitrification and therefore organic matter is important in permitting denitrification to proceed, and supplying the ammonium needed for nitrification (during organic matter mineralisation) (Seitzinger et al., 2006, Devol, 2015). However, as porewater nitrogen concentrations increased, I suggested a decoupling between nitrification-denitrification may have occurred, leading to an increase in direct denitrification (Chapter 4). While having no direct influence on overall net denitrification rate, changes in biogeochemical relationships can fundamentally alter the architecture of ecosystem interaction networks, which has implications for the robustness of a system to self-regulate against increasing stress (Biggs et al., 2012, Selkoe et al., 2015).

Carbon supply and trophic status are inherently linked, considering net heterotrophic systems (which dominate highly turbid intertidal habitats) were shown to have lower rates of gross primary production (Chapter 3) and therefore reductions in the quantity of autochthonous carbon produced. These reductions in carbon supply are not only likely to lead to the suppression of denitrification but may alter competition between benthic primary producers and nitrifying/ denitrifying bacteria (Risgaard-Petersen et al., 2004a, Risgaard-Petersen et al., 2004b), resulting in the observed increase in ammonium released from the water column in increasingly net heterotrophic systems (Chapter 4). These increases in ammonium effluxes coupled with the limited capacity for denitrification to mitigate increase in nitrogen enrichment may therefore indicate a shift towards a more eutrophied state (Eyre and Ferguson, 2002).

Despite the negligible influence on net dentification rate, increasing nutrient enrichment significantly altered relationships and interactions between nitrogen and carbon cycling, environmental variables and macrofaunal communities (Chapter 4). In particular, a decrease and unimodal response of adult *M. liliana*

and *A. stutchburyi* abundance, respectively, highlights the sensitivity of important bivalve species to increasing stressors loads. This can have a significant influence on biogeochemical cycling through reductions in the mediation of sediment mixing and thus the vertical distribution of solutes, oxygen and carbon (Sandwell et al., 2009, Laverock et al., 2011, Stief, 2013). For example, diminished bioturbation activity as evidenced by increases in the difference of DOM intensity between the sediment surface and at depth (Chapter 4), suggests reductions in the spatial and temporal heterogeneity of sedimentary redox zones (Volkenborn et al., 2012, Woodin et al., 2016). The large increase in nitrogen availability and the potential switch to direct denitrification was likely to diminish the importance of macrofaunal communities on sediment biogeochemical cycling. However, the potential simplification of the interactions of intrinsic dynamics and drivers and the presence of nonlinearities can fundamentally alter biogeochemical cycling within soft sediments and increase the likelihood of abrupt non-linear shifts in ecosystem functioning (Cloern et al., 2016, Thrush et al., 2020). Overall, this study highlights the limited capacity for denitrification to mitigate large increases in nitrogen enrichment, and the increased likelihood of abrupt non-linear shifts in ecosystem functioning under increasing nitrogen enrichment.

5.1.3 Stressor thresholds

The co-occurrence of multiple anthropogenic stressors in both time and space highlights the necessity of multi-stressor studies to further our understanding of the potential interactive effects which can manifest into additive, multiplicative, synergistic or antagonistic pathways (Folt et al., 1999, Todgham and Stillman, 2013). In particular, the detection of nonlinearities and step changes are important in understanding the influence of increasing stressor loads on the interactions between ecosystem components (Hewitt et al., 2016, Thrush et al., 2020). This is particularly important considering coastal ecosystems experiencing a high degree of anthropogenic disturbance can be predisposed to abrupt and non-linear shifts in ecosystem functioning (Lotze et al., 2006, Cloern et al., 2016). My research suggests both increasing water column turbidity and nutrient

enrichment of sediment porewaters may reduce the robustness of intertidal coastal habitats to future global change. This can occur through the loss of benthic productivity during tidal submergence, which cascades to alterations in the delivery of other ecosystem services, such as the capacity to process increasing nitrogen loads (O'Meara et al., 2017, Hope et al., 2020). While partial resilience to increasing water column turbidity can be afforded by emerged tidal periods, this will become increasingly eroded as sea-level rise inundates coastal areas. Considering stress induced tipping points are not only a consequence of large changes in external factors but can occur through subtle and gradual changes (Scheffer and Carpenter, 2003), it is possible both increasing water column turbidity and nutrient enrichment may increase the predisposition of intertidal habitats to threshold changes which can fundamentally move a system to an alternative, often irreversible state owing to strong intrinsic feedbacks (Carpenter et al., 2001).

Identifying the limits and thresholds in ecosystem functionality where these changes may occur is integral to preventing ecosystem degradation and the loss of ecosystem services. For estuaries in particular, knowing the thresholds of factors which can fundamentally influence benthic productivity and nutrient recycling will be important in managing sedimentation and nutrient inputs to prevent eutrophication and the loss of ecosystem services. By using a gradient in water column turbidity, I showed a switch from positive to negative net primary production at sites which experienced maximum PAR below 295 µmol m^{-2} s^{-1} (Chapter 3). This is in agreement with a recent study which showed a breakpoint in ecosystem functionality in highly turbid estuaries receiving an average PAR of < 350 µmol m^{-2} s^{-1} (Thrush et al., 2020), which resulted in reduced productivity by MPB and affected rates of organic matter and nutrient processing. In addition, I highlight a change in response in the maximum abundances of key bioturbating macrofaunal species (Chapter 4), which can reduce the heterogeneity of sedimentary redox zones, significantly altering organic matter processing and nutrient transformations (Welsh, 2003, Jones et al., 2011). However, to increase confidence in predicting stressor thresholds and increase our understanding of the

breaks in feedback loops which can facilitate ecological tipping points, conducting further gradient based experimental designs aimed to target potential boundaries in ecosystem functionality will help to elucidate the presence of potential thresholds and the vulnerability of estuarine ecosystems to tipping points. This will additionally help to identify any context dependency and aid a proactive approach to tipping points management, by identifying any loss of resilience before a regime shift occurs (Lindegren et al., 2012, Kelly et al., 2015).

5.2 Future research

Within the three research chapters of my thesis, I have investigated the response of benthic intertidal ecosystems to two prevalent coastal stressors; increased sedimentation and nutrient inputs and discussed the interaction with a global scale stressor; sea-level rise and the subsequent loss of intertidal area. As a product of these chapters, several limitations and key questions for future research have emerged.

The direct measurements of time-dependent insolation made in Chapter 2 are relatively uncommon within the literature, most likely a consequence of time and budget constraints associated with the deployment and maintenance of PAR/ light loggers. Other methods to estimate PAR over large spatial and temporal scales is to use satellite imagery. For example, Gattuso et al. (2006) estimated global scale irradiance reaching the seafloor over a 10 year period. However, they highlight that the limited spectral resolution in coastal areas and the conversion of reflectance to PAR can constrain extrapolations to benthic primary producers in specific areas of interest. Therefore, future research incorporating direct measurements of PAR to ground truth and increase the resolution and applicability of satellite estimations may provide an interesting avenue to gain more accurate and long-term estimations of the extent of water column turbidity over large spatial scales.

It was clear from Chapter 2 that the number of photosynthesis-irradiance curves on which MPB production was estimated was severely limited. This prevented the

inclusion of potential adaptations to low light availability, global comparisons to local MPB communities and the differentiation between emerged and submerged saturation values which has the potential to differ over large temporal scales. Therefore, it would be useful to develop photosynthesis-irradiance on local MPB communities, and develop these over a large gradient in water column turbidity during both submerged and emerged tidal periods to improve our understanding of the thresholds at which water column turbidity can limit benthic productivity by MPB.

Within the two experimental chapters of my thesis (Chapters 3 and 4), I explored the multi-stressor impacts of increasing water column turbidity and nutrient enrichment on benthic productivity by MPB and biogeochemical cycling. While multi-stressor research is imperative in understanding the combined effects of prevalent coastal pressures and thus the interaction between them, the influence of nutrient enrichment within this thesis was impaired by the use of a nitrogen only fertiliser. This switched the system to phosphate limited while omitting the enhancement of carbon supply, which is often associated with increasing eutrophication (Rabalais et al., 2009). Further research that includes a eutrophication gradient and therefore incorporates the modifications in both carbon and nutrient supply is likely to reveal if benthic productivity and biogeochemical cycling will be resilient to environmental change and increasing stressors, providing information of potential thresholds in functionality which would have direct relevance and applications for environmental managers.

To fully understand biogeochemical cycling within low nutrient estuaries, and then begin to identify any threshold changes in response to increasing anthropogenic stress, other pathways of nitrogen cycling need to be investigated. For example, nitrification, biomass assimilation, dissimilatory nitrate reduction to ammonium (DNRA), and the contribution of additional forms of denitrification; anaerobic ammonium oxidation (anammox), iron-driven denitrification and sulphur-driven denitrification. Within Chapter 4, I suggest denitrification was driven by tightly coupled nitrification-denitrification, but this potentially switched to direct

denitrification with increasing nutrient enrichment. However, measurements of nitrification would remove the need for such assumptions. In addition, increases in sediment nutrient concentrations may facilitate the growth of slow-growing anammox bacteria which require both nitrate and ammonium (Devol, 2015). While the high oxygenation of the water column and low nitrate concentrations (Lohrer et al., 2010) are likely to occlude anammox production in the estuaries included within this thesis, research along stressor gradients may alter the importance of different pathways, which has consequences for concentrations of biologically available nitrogen considering one unit of both ammonium and nitrate forms one unit of N_2 during anammox compared to one unit of nitrate during heterotrophic denitrification. Further work which includes other nitrogen cycling pathways along a stressor gradient are therefore essential in understanding the potential dominance of other nitrogen cycling processes over denitrification, and thus identify potential thresholds which will become necessary in order to manage for environmental change.

It is evident both from my results in Chapter 4 and other studies (e.g. Ferguson and Eyre, 2010, Eyre et al., 2013) that nitrogen and carbon cycling within soft sediment ecosystems are inherently linked. However, cost and time constraints can impede the ability to measure the quality and quantity of carbon in addition to dissolved inorganic nutrient fluxes and dinitrogen gas. I therefore used a rapid and cost-effective fluorescence method to attain information on the biochemical characteristics of dissolved organic matter. While this method has previously been used to describe organic matter within sediment porewaters (Burdige et al., 2004), to my knowledge this is the first time this method has been applied to estuarine porewaters within New Zealand whilst also providing links to nitrogen cycling. However, within the framework of my thesis it was not possible to fully explore the potential for this method to be a proxy for other carbon related parameters. For example, fluorescence has been used as a proxy for total dissolved organic carbon, a water quality indicator, microbial activity, and an indicator of dissolved organic nitrogen (Baker and Inverarity, 2004, Burdige et al., 2004, Hansen et al., 2016, Clark et al., 2017). In particular, the potential to build a calibration to

calculate both total dissolved organic carbon and nitrogen concentrations would result in significant additions to understanding biogeochemical cycling within estuarine ecosystems.

Finally, interactions between local and global scale stressors and the implications to benthic communities have been inferred or suggested within this thesis. While Chapter 2 highlights the potential for sea-level rise to significantly alter benthic ecosystem functioning, much of these ecological implications to climatic changes were speculative. Future research encompassing a space for time approach (Blois et al., 2013), or in the context of sea-level rise, comparing shallow subtidal and intertidal habitats would vastly improve our ability to predict how benthic ecosystem functioning may change in the future. Furthermore, the multifaceted and dynamic nature of coastal ecosystems results in multiple combinations of stressor types which will influence ecosystem functionality (Gunderson et al., 2016). Therefore, the inclusion of additional stressors such as marine heatwaves which can rapidly influence the structure of benthic communities (Jones et al., 2017, Oliver et al., 2017, Smale et al., 2017) will further improve our predictive understanding of the biological responses to increasing anthropogenic stress, which is essential to make informed decisions about the future management of marine systems (Bernhardt and Leslie, 2013).

5.3 Concluding remarks

Despite the relatively recent arrival of humans (McWethy et al., 2010), the results from my research chapters and the extrapolation of their findings support previous evidence that the health and functioning of New Zealand's estuaries are being significantly degraded by anthropogenic activities (Thrush et al., 2004, Drylie et al., 2018, Douglas et al., 2019). In particular, by using a combination of observation-based, literature review, experimental and statistical approaches which vitally incorporated large gradients in environmental variability, the research within this thesis underscores the potential for water column turbidity to significantly influence several estuaries across New Zealand. The effects of this

dominant stressor are likely to increasingly predispose soft sediment intertidal ecosystems to breaching ecological thresholds when coupled with the cumulative effects of additional local stressors, such as increasing nitrogen loading and the subsequent alterations in the ability to process excess nutrients. The interactions between multiple local stressors will however fundamentally change as global scale stressors increase in prevalence. For example, climatic changes are likely to increase the intensity and severity of storm events, further increasing the delivery of land derived sediment (Seneviratne et al., 2012), in addition to other significant stressors such as marine heat waves (Frölicher et al., 2018) and ocean acidification (Feely et al., 2009). At this crucial period, the resilience originally provided by intertidal areas will begin to erode as sea-level rise inundates coastal areas. Under future global change therefore, the degradation of ecosystem functions and services delivered by MPB will further push these valuable habitats closer towards tipping points. Increasing our understanding of how multiple stressors can influence benthic ecosystems is therefore essential in order to inform a precautionary environmental management approach which targets the effective management of local scale stressors in order to optimise ecosystem resilience to global scale stressors and thus maintain the healthy functioning of soft sediment estuarine ecosystems.

References

Ackleson, S. G. 2003. Light in shallow waters: A brief research review. *Limnology and Oceanography,* 48**,** 323-328.

Airoldi, L. 2003. The effects of sedimentation on rocky coast assemblages. *Oceanography and Marine Biology, An Annual Review.* CRC Press.

Airoldi, L. & Beck, M. W. 2007. Loss, status and trends for coastal marine habitats of Europe. *Oceanography and Marine Biology,* 45**,** 345-407.

Aller, R. C. & Aller, J. Y. 1998. The effect of biogenic irrigation intensity and solute exchange on diagenetic reaction rates in marine sediments. *Journal of Marine Research,* 56**,** 905-936.

An, S. & Joye, S. B. 2001. Enhancement of coupled nitrification-denitrification by benthic photosynthesis in shallow estuarine sediments. *Limnology and Oceanography,* 46**,** 62-74.

Anderson, I. C., Brush, M. J., Piehler, M. F., Currin, C. A., Stanhope, J. W., Smyth, A. R., Maxey, J. D. & Whitehead, M. L. 2014. Impacts of Climate-Related Drivers on the Benthic Nutrient Filter in a Shallow Photic Estuary. *Estuaries and Coasts,* 37**,** 46-62.

Andersson, C. A. & Bro, R. 2000. The N-way Toolbox for MATLAB. *Chemometrics and Intelligent Laboratory Systems,* 52**,** 1-4.

Anthony, K. R. N., Ridd, P. V., Orpin, A. R., Larcombe, P. & Lough, J. 2004. Temporal variation of light availability in coastal benthic habitats: Effects of clouds, turbidity, and tides. *Limnology and Oceanography,* 49**,** 2201-2211.

Arar, E. J. & Collins, G. B. 1997. *Method 445.0: In vitro determination of chlorophyll a and pheophytin a in marine and freshwater algae by fluorescence,* Washington, DC, United States Environmental Protection Agency.

Arkema, K. K., Guannel, G., Verutes, G., Wood, S. A., Guerry, A., Ruckelshaus, M., Kareiva, P., Lacayo, M. & Silver, J. M. 2013. Coastal habitats shield people and property from sea-level rise and storms. *Nature Climate Change,* 3**,** 913-918.

Baker, A. & Inverarity, R. 2004. Protein-like fluorescence intensity as a possible tool for determining river water quality. *Hydrological Processes,* 18**,** 2927-2945.

Barranguet, C., Kromkamp, J. & Peene, J. 1998. Factors controlling primary production and photosynthetic characteristics of intertidal microphytobenthos. *Marine Ecology Progress Series,* 173**,** 117-126.

Bauer, J. E., Cai, W.-J., Raymond, P. A., Bianchi, T. S., Hopkinson, C. S. & Regnier, P. a. G. 2013. The changing carbon cycle of the coastal ocean. *Nature,* 504**,** 61-70.

Benelli, S., Bartoli, M., Zilius, M., Vybernaite-Lubiene, I., Ruginis, T., Petkuviene, J. & Fano, E. A. 2018. Microphytobenthos and chironomid larvae attenuate nutrient recycling in shallow-water sediments. *Freshwater Biology,* 63**,** 187-201.

Bernhardt, J. R. & Leslie, H. M. 2013. Resilience to Climate Change in Coastal Marine Ecosystems. *Annual Review of Marine Science,* 5**,** 371-392.

Biggs, R., Schlüter, M., Biggs, D., Bohensky, E. L., Burnsilver, S., Cundill, G., Dakos, V., Daw, T. M., Evans, L. S., Kotschy, K., Leitch, A. M., Meek, C., Quinlan, A., Raudsepp-Hearne, C., Robards, M. D., Schoon, M. L., Schultz, L. & West, P. C. 2012. Toward Principles for Enhancing the Resilience of Ecosystem Services. *Annual Review of Environment and Resources,* 37**,** 421-448.

Billerbeck, M., Røy, H., Bosselmann, K. & Huettel, M. 2007. Benthic photosynthesis in submerged Wadden Sea intertidal flats. *Estuarine, Coastal and Shelf Science,* 71**,** 704-716.

Blackburn, T. M., Lawton, J. H. & Perry, J. N. 1992. A Method of Estimating the Slope of Upper Bounds of Plots of Body Size and Abundance in Natural Animal Assemblages. *Oikos,* 65**,** 107-112.

Blanchard, G. F., Guarini, J.-M., Gros, P. & Richard, P. 1997. Seasonal effect on the relationship between the photosynthetic capacity of intertidal microphytobenthos and temperature. *Journal of Phycology,* 33**,** 723-728.

Blois, J. L., Williams, J. W., Fitzpatrick, M. C., Jackson, S. T. & Ferrier, S. 2013. Space can substitute for time in predicting climate-change effects on biodiversity. *Proceedings of the National Academy of Sciences,* 110**,** 9374-9379.

Blum, M. D. & Roberts, H. H. 2009. Drowning of the Mississippi Delta due to insufficient sediment supply and global sea-level rise. *Nature Geoscience,* 2**,** 488-491.

Borum, J. & Sand-Jensen, K. 1996. Is Total Primary Production in Shallow Coastal Marine Waters Stimulated by Nitrogen Loading? *Oikos,* 76**,** 406-410.

Boucher, G., Clavier, J. & Garrigue, C. 1994. Oxygen and carbon dioxide fluxes at the watersediment interface of a tropical lagoon. *Marine Ecology Progress Series,* 107**,** 185-193.

Braeckman, U., Provoost, P., Gribsholt, B., Van Gansbeke, D., Middelburg, J. J., Soetaert, K., Vincx, M. & Vanaverbeke, J. 2010. Role of macrofauna functional traits and density in biogeochemical fluxes and bioturbation. *Marine Ecology Progress Series,* 399**,** 173-186.

Brettar, I. & Rheinheimer, G. 1992. Influence of carbon availability on dentrification in the central Baltic Sea. *Limnology and Oceanography,* 37**,** 1146-1163.

Burdige, D. J., Kline, S. W. & Chen, W. 2004. Fluorescent dissolved organic matter in marine sediment pore waters. *Marine Chemistry,* 89**,** 289-311.

Burnham, K. P. & Anderson, D. R. 2002. *A practical information-theoretic approach*, Springer, New York.

Cahoon, L. 1999. The role of benthic microalgae in neritic ecosystems. *Oceanography and marine biology,* 37**,** 47-86.

Cahoon, L. B. 2006. Upscaling primary production estimates : regional and global scale estimates of microphytobenthos production. *Functioning of Microphytobenthos in Estuaries.* Royal Netherlands Academy of Arts and Science.

Cahoon, L. B., Nearhoof, J. E. & Tilton, C. L. 1999. Sediment grain size effect on benthic microalgal biomass in shallow aquatic ecosystems. *Estuaries,* 22**,** 735-741.

Carpenter, S., Walker, B., Anderies, J. M. & Abel, N. 2001. From Metaphor to Measurement: Resilience of What to What? *Ecosystems,* 4**,** 765-781.

Carrier-Belleau, C., Drolet, D., Mckindsey, C. W. & Archambault, P. 2021. Environmental stressors, complex interactions and marine benthic communities' responses. *Scientific Reports,* 11**,** 4194.

Cebrián, J. 2004. Grazing On Benthic Primary Producers. *In:* Nielsen, S. L., Banta, G. T. & Pedersen, M. F. (eds.) *Estuarine Nutrient Cycling: The Influence of Primary Producers: The Fate of Nutrients and Biomass.* Dordrecht: Springer Netherlands.

Charpy-Roubaud, C. & Sournia, A. 1990. The comparative estimation of phytoplanktonic, microphytobenthic and macrophytobenthic primary production in the oceans. *Marine Microbial Food Webs,* 4**,** 31-57.

Christianen, M. J. A., Middelburg, J. J., Holthuijsen, S. J., Jouta, J., Compton, T. J., Van Der Heide, T., Piersma, T., Sinninghe Damsté, J. S., Van Der Veer, H. W., Schouten, S. & Olff, H. 2017. Benthic primary producers are key to sustain the Wadden Sea food web: stable carbon isotope analysis at landscape scale. *Ecology,* 98**,** 1498-1512.

Clark, D. E., Pilditch, C. A., Pearman, J. K., Ellis, J. I. & Zaiko, A. 2020. Environmental DNA metabarcoding reveals estuarine benthic community response to nutrient enrichment – evidence from an in-situ experiment. *Environmental Pollution,* 267**,** 115472.

Clark, J. B., Long, W. & Hood, R. R. 2017. Estuarine Sediment Dissolved Organic Matter Dynamics in an Enhanced Sediment Flux Model. *Journal of Geophysical Research: Biogeosciences,* 122**,** 2669-2682.

Cloern, J. E. 1987. Turbidity as a control on phytoplankton biomass and productivity in estuaries. *Continental Shelf Research,* 7**,** 1367-1381.

Cloern, J. E. 2001. Our evolving conceptual model of the coastal eutrophication problem. *Marine ecology progress series,* 210**,** 223-253.

Cloern, J. E., Abreu, P. C., Carstensen, J., Chauvaud, L., Elmgren, R., Grall, J., Greening, H., Johansson, J. O. R., Kahru, M., Sherwood, E. T., Xu, J. & Yin, K. 2016. Human activities and climate variability drive fast-paced change across the world's estuarine–coastal ecosystems. *Global Change Biology,* 22**,** 513-529.

Coble, P. G. 2007. Marine Optical Biogeochemistry: The Chemistry of Ocean Color. *Chemical Reviews,* 107**,** 402-418.

Coelho, H., Vieira, S. & Serôdio, J. 2009. Effects of desiccation on the photosynthetic activity of intertidal microphytobenthos biofilms as studied by optical methods. *Journal of Experimental Marine Biology and Ecology,* 381**,** 98-104.

Consalvey, M., Paterson, D. M. & Underwood, G. J. C. 2004. The ups and downs of life in a benthic biofilm: Migration of benthic diatoms. *Diatom Research,* 19**,** 181-202.

Consalvey, M., Perkins, R. G., Paterson, D. M. & Underwood, G. J. C. 2005. PAM fluorescence: a beginners guide for benthic diatomists. *Diatom Research,* 20**,** 1-22.

Cooper, S. R. & Brush, G. S. 1993. A 2,500-year history of anoxia and eutrophication in Chesapeake Bay. *Estuaries,* 16**,** 617-626.

Cornwell, J. C., Kemp, W. M. & Kana, T. M. 1999. Denitrification in coastal ecosystems: methods, environmental controls, and ecosystem level controls, a review. *Aquatic Ecology,* 33**,** 41-54.

Crossland, C. J., Kremer, H. H., Lindeboom, H., Crossland, J. I. M. & Le Tissier, M. D. 2005. *Coastal fluxes in the Anthropocene: the land-ocean interactions in the coastal zone project of the International Geosphere-Biosphere Programme*, Springer Science & Business Media.

Cussioli, M. C., Bryan, K. R., Pilditch, C. A., De Lange, W. P. & Bischof, K. 2019. Light penetration in a temperate meso-tidal lagoon: Implications for seagrass growth and dredging in Tauranga Harbour, New Zealand. *Ocean & Coastal Management,* 174**,** 25-37.

D'alpaos, A., Lanzoni, S., Marani, M. & Rinaldo, A. 2007. Landscape evolution in tidal embayments: Modeling the interplay of erosion, sedimentation, and vegetation dynamics. *Journal of Geophysical Research,* 112.

Dalsgaard, T., Thamdrup, B. & Canfield, D. E. 2005. Anaerobic ammonium oxidation (anammox) in the marine environment. *Research in Microbiology,* 156**,** 457-464.

Dame, R. F. 2008. Estuaries. *In:* Jørgensen, S. E. & Fath, B. D. (eds.) *Encyclopedia of Ecology.* Oxford: Academic Press.

De Jonge, V. N., De Boer, W. F., De Jong, D. J. & Brauer, V. S. 2012. Long-term mean annual microphytobenthos chlorophyll a variation correlates with air temperature. *Marine Ecology Progress Series,* 468**,** 43-56.

Denis, L. & Desreumaux, P.-E. 2009. Short-term variability of intertidal microphytobenthic production using an oxygen microprofiling system. *Marine and Freshwater Research,* 60**,** 712-726.

Denis, L., Gevaert, F. & Spilmont, N. 2012. Microphytobenthic production estimated by in situ oxygen microprofiling: short-term dynamics and carbon budget implications. *Journal of Soils Sediments,* 12**,** 1517-1529.

Devol, A. H. 2015. Denitrification, Anammox, and N2 Production in Marine Sediments. *Annual Review of Marine Science,* 7**,** 403-423.

Dong, L., Thornton, D. C. O., Nedwell, D. B. & Underwood, G. 2000. Denitrification in sediments of the River Colne estuary, England. *Marine Ecology Progress Series,* 203**,** 109-122.

Douglas, E. J., Lohrer, A. M. & Pilditch, C. A. 2019. Biodiversity breakpoints along stress gradients in estuaries and associated shifts in ecosystem interactions. *Scientific Reports,* 9**,** 17567.

Douglas, E. J., Pilditch, C. A., Hines, L. V., Kraan, C. & Thrush, S. F. 2016. In situ soft sediment nutrient enrichment: A unified approach to eutrophication field experiments. *Marine Pollution Bulletin,* 111**,** 287-294.

Douglas, E. J., Pilditch, C. A., Kraan, C., Schipper, L. A., Lohrer, A. M. & Thrush, S. F. 2017. Macrofaunal Functional Diversity Provides Resilience to Nutrient Enrichment in Coastal Sediments. *Ecosystems,* 20**,** 1324-1336.

Douglas, E. J., Pilditch, C. A., Lohrer, A. M., Savage, C., Schipper, L. A. & Thrush, S. F. 2018. Sedimentary Environment Influences Ecosystem Response to Nutrient Enrichment. *Estuaries and Coasts,* 41**,** 1994-2008.

Drylie, T. P., Lohrer, A. M., Needham, H. R., Bulmer, R. H. & Pilditch, C. A. 2018. Benthic primary production in emerged intertidal habitats provides resilience to high water column turbidity. *Journal of Sea Research,* 142**,** 101-112.

Du, G., Yan, H., Liu, C. & Mao, Y. 2018. Behavioral and physiological photoresponses to light intensity by intertidal microphytobenthos. *Journal of Oceanology and Limnology,* 36**,** 293-304.

Duarte, C. M. 1995. Submerged aquatic vegetation in relation to different nutrient regimes. *Ophelia,* 41**,** 87-112.

Duarte, C. M., Middelburg, J. J. & Caraco, N. 2005. Major role of marine vegetation on the oceanic carbon cycle. *Biogeosciences,* 2**,** 1-8.

Dugan, J. E., Emery, K. A., Alber, M., Alexander, C. R., Byers, J. E., Gehman, A. M., Mclenaghan, N. & Sojka, S. E. 2018. Generalizing Ecological Effects of Shoreline Armoring Across Soft Sediment Environments. *Estuaries and Coasts,* 41**,** 180-196.

Dürr, H. H., Laruelle, G. G., Van Kempen, C. M., Slomp, C. P., Meybeck, M. & Middelkoop, H. 2011. Worldwide Typology of Nearshore Coastal Systems: Defining the Estuarine Filter of River Inputs to the Oceans. *Estuaries and Coasts,* 34**,** 441-458.

Eklund, B. 1992. Practical Guidance for Flux Chamber Measurements of Fugitive Volatile Organic Emission Rates. *Journal of the Air & Waste Management Association,* 42**,** 1583-1591.

Ellis, J., Cummings, V., Hewitt, J., Thrush, S. & Norkko, A. 2002. Determining effects of suspended sediment on condition of a suspension feeding bivalve (Atrina zelandica): results of a survey, a laboratory experiment and a field

transplant experiment. *Journal of Experimental Marine Biology and Ecology,* 267**,** 147-174.

Eyre, B., D. & Ferguson, A., J. P. 2002. Comparison of carbon production and decomposition, benthic nutrient fluxes and denitrification in seagrass, phytoplankton, benthic microalgae- and macroalgae-dominated warm-temperate Australian lagoons. *Marine Ecology Progress Series,* 229**,** 43-59.

Eyre, B., D. & Ferguson, A., J. P. 2009. Denitrification efficiency for defining critical loads of carbon in shallow coastal ecosystems. *In:* Andersen, J. H. & Conley, D. J. (eds.) *Eutrophication in Coastal Ecosystems: Towards better understanding and management strategies Selected Papers from the Second International Symposium on Research and Management of Eutrophication in Coastal Ecosystems, 20–23 June 2006, Nyborg, Denmark.* Dordrecht: Springer Netherlands.

Eyre, B. D. & Ferguson, A. J. P. 2005. Benthic metabolism and nitrogen cycling in a subtropical east Australian estuary (Brunswick): Temporal variability and controlling factors. *Limnology and Oceanography,* 50**,** 81-96.

Eyre, B. D., Maher, D. T. & Squire, P. 2013. Quantity and quality of organic matter (detritus) drives N2 effluxes (net denitrification) across seasons, benthic habitats, and estuaries. *Global Biogeochemical Cycles,* 27**,** 1083-1095.

Eyre, B. D., Rysgaard, S., Dalsgaard, T. & Christensen, P. B. 2002. Comparison of isotope pairing and N2:Ar methods for measuring sediment denitrification—Assumption, modifications, and implications. *Estuaries,* 25**,** 1077-1087.

Feely, R. A., Doney, S. C. & Cooley, S. R. 2009. Ocean Acidification: Present Conditions and Future Changes in a High-CO_2 World. *Oceanography,* 22**,** 36-47.

Fenchel, T. M. & Riedl, R. J. 1970. The sulfide system: a new biotic community underneath the oxidized layer of marine sand bottoms. *Marine Biology,* 7**,** 255-268.

Ferguson, A. J. P. & Eyre, B. D. 2010. Carbon and Nitrogen Cycling in a Shallow Productive Sub-Tropical Coastal Embayment (Western Moreton Bay, Australia): The Importance of Pelagic-Benthic Coupling. *Ecosystems,* 13**,** 1127-1144.

Field, C. B., Barros, V. R., Dokken, D. J., Mach, K. J., Mastrandrea, M. D., Bilir, T. E., Chatterjee, M., Ebi, K. L., Estrada, Y. O., Genova, R. C., Girma, B., Kissel, E. S., Levy, A. N., Maccracken, S., Mastrandrea, P. R. & L.L., W. 2014. IPCC Climate Change 2014: Impacts, Adaptation, and Vulnerability. Part A: Global and Sectoral Aspects. Contribution of Working Group II to the Fifth Assessment Report of the Intergovernmental Panel on Climate Change Cambridge, United Kingdom and New York, NY, USA: Cambridge University Press.

Folt, C. L., Chen, C. Y., Moore, M. V. & Burnaford, J. 1999. Synergism and antagonism among multiple stressors. *Limnology and Oceanography,* 44**,** 864-877.

Foster, S. Q. & Fulweiler, R. W. 2014. Spatial and historic variability of benthic nitrogen cycling in an anthropogenically impacted estuary. *Frontiers in Marine Science,* 1.

Fowler, D., Coyle, M., Skiba, U., Sutton, M. A., Cape, J. N., Reis, S., Sheppard, L. J., Jenkins, A., Grizzetti, B., Galloway, J. N., Vitousek, P., Leach, A., Bouwman, A. F., Butterbach-Bahl, K., Dentener, F., Stevenson, D., Amann, M. & Voss, M. 2013. The global nitrogen cycle in the twenty-first century. *Philosophical Transactions of the Royal Society B: Biological Sciences,* 368**,** 20130164.

Friedrichs, C. T. & Aubrey, D. G. 1996. Uniform Bottom Shear Stress and Equilibrium Hyposometry of Intertidal Flats. *In:* Washington, D. A. (ed.) *Pattiaratchi, C. B. (ed.) Mixing in Estuaries and Coastal Seas.*

Frölicher, T. L., Fischer, E. M. & Gruber, N. 2018. Marine heatwaves under global warming. *Nature,* 560**,** 360-364.

Fulweiler, R. W., Nixon, S. W., Buckley, B. A. & Granger, S. L. 2008. Net Sediment N2 Fluxes in a Coastal Marine System—Experimental Manipulations and a Conceptual Model. *Ecosystems,* 11**,** 1168-1180.

Gattuso, J. P., Gentili, B., Duarte, C. M., Kleypas, J. A., Middelburg, J. J. & Antoine, D. 2006. Light availability in the coastal ocean: impact on the distribution of benthic photosynthetic organisms and their contribution to primary production. *Biogeosciences,* 3**,** 489-513.

Glud, R. N. 2008. Oxygen dynamics of marine sediments. *Marine Biology Research,* 4**,** 243-289.

Gonçalves, W. F. O., Luiz-Silva, W., Machado, W., Nizoli, E. C. & Santelli, R. E. 2012. Geochemistry of intertidal sediment pore waters from the industrialized Santos-Cubatão Estuarine System, SE Brazil. *Anais da Academia Brasileira de Ciências,* 84**,** 427-442.

Gongol, C. & Savage, C. 2016. Spatial variation in rates of benthic denitrification and environmental controls in four New Zealand estuaries. *Marine Ecology Progress Series,* 556**,** 59-77.

Gray, J. S., Wu, R. S.-S. & Or, Y. Y. 2002. Effects of hypoxia and organic enrichment on the coastal marine environment. *Marine Ecology Progress Series,* 238**,** 249-279.

Griffiths, J. R., Kadin, M., Nascimento, F. J. A., Tamelander, T., Törnroos, A., Bonaglia, S., Bonsdorff, E., Brüchert, V., Gårdmark, A., Järnström, M., Kotta, J., Lindegren, M., Nordström, M. C., Norkko, A., Olsson, J., Weigel, B., Žydelis, R., Blenckner, T., Niiranen, S. & Winder, M. 2017. The importance of benthic–pelagic coupling for marine ecosystem functioning in a changing world. *Global Change Biology,* 23**,** 2179-2196.

Gruber, N. & Galloway, J. N. 2008. An Earth-system perspective of the global nitrogen cycle. *Nature,* 451**,** 293-296.

Guarini, J.-M., Cloern, J. E., Edmunds, J. & Gros, P. 2002. Microphytobenthic potential productivity estimated in three tidal embayments of the San Francisco Bay: A comparative study. *Estuaries,* 25**,** 409-417.

Gunderson, A. R., Armstrong, E. J. & Stillman, J. H. 2016. Multiple Stressors in a Changing World: The Need for an Improved Perspective on Physiological Responses to the Dynamic Marine Environment. *Annual Review of Marine Science,* 8**,** 357-378.

Hallegatte, S., Green, C., Nicholls, R. J. & Corfee-Morlot, J. 2013. Future flood losses in major coastal cities. *Nature Climate Change,* 3**,** 802.

Halpern, B. S., Frazier, M., Afflerbach, J., Lowndes, J. S., Micheli, F., O'hara, C., Scarborough, C. & Selkoe, K. A. 2019. Recent pace of change in human impact on the world's ocean. *Scientific Reports,* 9**,** 11609.

Halpern, B. S., Walbridge, S., Selkoe, K. A., Kappel, C. V., Micheli, F., D'agrosa, C., Bruno, J. F., Casey, K. S., Ebert, C., Fox, H. E., Fujita, R., Heinemann, D., Lenihan, H. S., Madin, E. M. P., Perry, M. T., Selig, E. R., Spalding, M., Steneck, R. & Watson, R. 2008. A Global Map of Human Impact on Marine Ecosystems. *Science,* 319**,** 948-952.

Hamme, R. C. & Emerson, S. R. 2004. The solubility of neon, nitrogen and argon in distilled water and seawater. *Deep Sea Research Part I: Oceanographic Research Papers,* 51**,** 1517-1528.

Hansen, A. M., Kraus, T. E. C., Pellerin, B. A., Fleck, J. A., Downing, B. D. & Bergamaschi, B. A. 2016. Optical properties of dissolved organic matter (DOM): Effects of biological and photolytic degradation. *Limnology and Oceanography,* 61**,** 1015-1032.

Harley, C. D. G., Randall Hughes, A., Hultgren, K. M., Miner, B. G., Sorte, C. J. B., Thornber, C. S., Rodriguez, L. F., Tomanek, L. & Williams, S. L. 2006. The impacts of climate change in coastal marine systems. *Ecology Letters,* 9**,** 228-241.

Herbert, R. 1999. Nitrogen cycling in coastal marine ecosystems. *FEMS microbiology reviews,* 23**,** 563-590.

Hewitt, J. E., Ellis, J. I. & Thrush, S. F. 2016. Multiple stressors, nonlinear effects and the implications of climate change impacts on marine coastal ecosystems. *Global Change Biology,* 22**,** 2665-75.

Hewitt, J. E. & Norkko, J. 2007. Incorporating temporal variability of stressors into studies: An example using suspension-feeding bivalves and elevated suspended sediment concentrations. *Journal of Experimental Marine Biology and Ecology,* 341**,** 131-141.

Hewitt, J. E., Thrush, S. F., Cummings, V. J. & Pridmore, R. D. 1996. Matching patterns with processes: predicting the effect of size and mobility on the

spatial distributions of the bivalves Macomona liliana and Austrovenus stutchburyi. *Marine Ecology Progress Series,* 135**,** 57-67.

Hicks, D. M., Shankar, U., Mckerchar, A. I., Basher, L., Lynn, I., Page, M. & Jessen, M. 2011. Suspended sediment yields from New Zealand rivers. *Journal of Hydrology (New Zealand),* 50**,** 81-142.

Hillebrand, H., Worm, B. & Lotze, H. K. 2000. Marine microbenthic community structure regulated by nitrogen loading and grazing pressure. *Marine Ecology Progress Series,* 204**,** 27-38.

Hochard, S., Pinazo, C., Grenz, C., Evans, J. L. B. & Pringault, O. 2010. Impact of microphytobenthos on the sediment biogeochemical cycles: A modeling approach. *Ecological Modelling,* 221**,** 1687-1701.

Hope, J. A., Paterson, D. M. & Thrush, S. F. 2020. The role of microphytobenthos in soft-sediment ecological networks and their contribution to the delivery of multiple ecosystem services. *Journal of Ecology,* 108**,** 815-830.

Howarth, R. W. & Marino, R. 2006. Nitrogen as the limiting nutrient for eutrophication in coastal marine ecosystems: Evolving views over three decades. *Limnology and Oceanography,* 51**,** 364-376.

Huettel, M., Berg, P. & Kostka, J. E. 2014. Benthic Exchange and Biogeochemical Cycling in Permeable Sediments. *Annual Review of Marine Science,* 6**,** 23-51.

Huettel, M., Ziebis, W., Forster, S. & Luther Iii, G. 1998. Advective transport affecting metal and nutrient distributions and interfacial fluxes in permeable sediments. *Geochimica et Cosmochimica Acta,* 62**,** 613-631.

Hume, T. M., Snelder, T., Weatherhead, M. & Liefting, R. 2007. A controlling factor approach to estuary classification. *Ocean & Coastal Management,* 50**,** 905-929.

Jenkins, M. C. & Kemp, W. M. 1984. The coupling of nitrification and denitrification in two estuarine sediments1,2. *Limnology and Oceanography,* 29**,** 609-619.

Jesus, B., Perkins, R. G., Consalvey, M., Brotas, V. & Paterson, D. M. 2006. Effects of vertical migrations by benthic microalgae on fluorescence measurements of photophysiology. *Marine Ecology Progress Series,* 315**,** 55-66.

Jickells, T. D., Andrews, J. E. & Parkes, D. J. 2016. Direct and Indirect Effects of Estuarine Reclamation on Nutrient and Metal Fluxes in the Global Coastal Zone. *Aquatic Geochemistry,* 22**,** 337-348.

Joensuu, M., Pilditch, C. A., Harris, R., Hietanen, S., Pettersson, H. & Norkko, A. 2018. Sediment properties, biota, and local habitat structure explain variation in the erodibility of coastal sediments. *Limnology and Oceanography,* 63**,** 173-186.

Jones, H. F., Pilditch, C. A., Hamilton, D. P. & Bryan, K. R. 2017. Impacts of a bivalve mass mortality event on an estuarine food web and bivalve grazing

pressure. *New Zealand journal of marine and freshwater research,* 51**,** 370-392.

Jones, H. F. E., Pilditch, C. A., Bruesewitz, D. A. & Lohrer, A. M. 2011. Sedimentary Environment Influences the Effect of an Infaunal Suspension Feeding Bivalve on Estuarine Ecosystem Function. *PLOS ONE,* 6**,** e27065.

Kelly, R. P., Erickson, A. L., Mease, L. A., Battista, W., Kittinger, J. N. & Fujita, R. 2015. Embracing thresholds for better environmental management. *Philosophical Transactions of the Royal Society B: Biological Sciences,* 370**,** 20130276.

Kemp, W. M., Boynton, W. R., Adolf, J. E., Boesch, D. F., Boicourt, W. C., Brush, G., Cornwell, J. C., Fisher, T. R., Glibert, P. M., Hagy, J. D., Harding, L. W., Houde, E. D., Kimmel, D. G., Miller, W. D., Newell, R. I. E., Roman, M. R., Smith, E. M. & Stevenson, J. C. 2005. Eutrophication of Chesapeake Bay: historical trends and ecological interactions. *Marine Ecology Progress Series,* 303**,** 1-29.

Kemp, W. M., Sampou, P., Caffrey, J., Mayer, M., Henriksen, K. & Boynton, W. R. 1990. Ammonium recycling versus denitrification in Chesapeake Bay sediments. *Limnology and Oceanography,* 35**,** 1545-1563.

Kingston, M. B. 1999. Wave effects on the vertical migration of two benthic microalgae: Hantzschia virgata var. intermedia and Euglena proxima. *Estuaries,* 22**,** 81-91.

Kirk, J. T. O. 1994. *Light and photosynthesis in aquatic ecosystems,* Cambridge [England] ; Melbourne, Cambridge University Press.

Kopp, R. E., Deconto, R. M., Bader, D. A., Hay, C. C., Horton, R. M., Kulp, S., Oppenheimer, M., Pollard, D. & Strauss, B. H. 2017. Evolving understanding of Antarctic ice-sheet physics and ambiguity in probabilistic sea-level projections. *Earth's Future,* 5**,** 1217-1233.

Kowalski, N., Dellwig, O., Beck, M., Grunwald, M., Fischer, S., Piepho, M., Riedel, T., Freund, H., Brumsack, H.-J. & Böttcher, M. E. 2009. Trace metal dynamics in the water column and pore waters in a temperate tidal system: response to the fate of algae-derived organic matter. *Ocean Dynamics,* 59**,** 333-350.

Kromkamp, J., Peene, J., Van Rijswijk, P., Sandee, A. & Goosen, N. 1995. Nutrients, light and primary production by phytoplankton and microphytobenthos in the eutrophic, turbid Westerschelde estuary (The Netherlands). *Hydrobiologia,* 311**,** 9-19.

Kwon, B.-O., Kim, H.-C., Koh, C.-H., Ryu, J., Son, S., Kim, Y. H. & Khim, J. S. 2018. Development of temperature-based algorithms for the estimation of microphytobenthic primary production in a tidal flat: A case study in Daebu mudflat, Korea. *Environmental Pollution,* 241**,** 115-123.

Laverock, B., Gilbert, J. A., Tait, K., Osborn, A. M. & Widdicombe, S. 2011. Bioturbation: impact on the marine nitrogen cycle. Portland Press Ltd.

Lever, M., A. & Valiela, I. 2005. Response of microphytobenthic biomass to experimental nutrient enrichment and grazer exclusion at different land-derived nitrogen loads. *Marine Ecology Progress Series,* 294**,** 117-129.

Levin, L. A., Boesch, D. F., Covich, A., Dahm, C., Erséus, C., Ewel, K. C., Kneib, R. T., Moldenke, A., Palmer, M. A., Snelgrove, P., Strayer, D. & Weslawski, J. M. 2001. The Function of Marine Critical Transition Zones and the Importance of Sediment Biodiversity. *Ecosystems,* 4**,** 430-451.

Lindegren, M., Dakos, V., Gröger, J. P., Gårdmark, A., Kornilovs, G., Otto, S. A. & Möllmann, C. 2012. Early Detection of Ecosystem Regime Shifts: A Multiple Method Evaluation for Management Application. *PLOS ONE,* 7**,** e38410.

Lohrer, A. M., Halliday, N. J., Thrush, S. F., Hewitt, J. E. & Rodil, I. F. 2010. Ecosystem functioning in a disturbance-recovery context: Contribution of macrofauna to primary production and nutrient release on intertidal sandflats. *Journal of Experimental Marine Biology and Ecology,* 390**,** 6-13.

Longphuirt, S. N., Lim, J.-H., Leynaert, A., Claquin, P., Choy, E.-J., Kang, C.-K. & An, S. 2009. Dissolved inorganic nitrogen uptake by intertidal microphytobenthos: nutrient concentrations, light availability and migration. *Marine Ecology Progress Series,* 379**,** 33-44.

Lotze, H. K., Lenihan, H. S., Bourque, B. J., Bradbury, R. H., Cooke, R. G., Kay, M. C., Kidwell, S. M., Kirby, M. X., Peterson, C. H. & Jackson, J. B. C. 2006. Depletion, Degradation, and Recovery Potential of Estuaries and Coastal Seas. *Science,* 312**,** 1806-1809.

Macintyre, H. L., Geider, R. J. & Miller, D. C. 1996. Microphytobenthos: The ecological role of the "secret garden" of unvegetated, shallow-water marine habitats. I. Distribution, abundance and primary production. *Estuaries,* 19**,** 186-201.

Magalhães, C. M., Joye, S. B., Moreira, R. M., Wiebe, W. J. & Bordalo, A. A. 2005. Effect of salinity and inorganic nitrogen concentrations on nitrification and denitrification rates in intertidal sediments and rocky biofilms of the Douro River estuary, Portugal. *Water Research,* 39**,** 1783-1794.

Maher, D. T. & Eyre, B. D. 2012. Carbon budgets for three autotrophic Australian estuaries: Implications for global estimates of the coastal air-water CO2 flux. *Global Biogeochemical Cycles,* 26**,** GB1032.

Mangan, S., Bryan, K. R., Thrush, S. F., Gladstone-Gallagher, R. V., Lohrer, A. M. & Pilditch, C. A. 2020a. Shady business: the darkening of estuaries constrains benthic ecosystem function. *Marine Ecology Progress Series,* 647**,** 33-48.

Mangan, S., Lohrer, A. M., Thrush, S. F. & Pilditch, C. A. 2020b. Water Column Turbidity Not Sediment Nutrient Enrichment Moderates Microphytobenthic Primary Production. *Journal of Marine Science and Engineering,* 8**,** 732.

Mcwethy, D. B., Whitlock, C., Wilmshurst, J. M., Mcglone, M. S., Fromont, M., Li, X., Dieffenbacher-Krall, A., Hobbs, W. O., Fritz, S. C. & Cook, E. R. 2010.

Rapid landscape transformation in South Island, New Zealand, following initial Polynesian settlement. *PNAS,* 107**,** 21343-21348.

Meyercordt, J. & Meyer-Reil, L.-A. 1999. Primary production of benthic microalgae in two shallow coastal lagoons of different trophic status in the southern Baltic Sea. *Marine Ecology Progress Series,* 178**,** 179-191.

Middelburg, J. J., Barranguet, C., Boschker, H. T. S., Herman, P. M. J., Moens, T. & Heip, C. H. R. 2000. The fate of intertidal microphytobenthos carbon: An in situ 13C-labeling study. *Limnology and Oceanography,* 45**,** 1224-1234.

Middelburg, J. J., Soetaert, K., Herman, P. M. J. & Heip, C. H. R. 1996. Denitrification in marine sediments: A model study. *Global Biogeochemical Cycles,* 10**,** 661-673.

Migné, A., Davoult, D., Bourrand, J.-J. & Boucher, G. 2005. Benthic primary production, respiration and remineralisation: in situ measurements in the soft-bottom Abra alba community of the western English Channel (North Brittany). *Journal of Sea Research,* 53**,** 223-229.

Migné, A., Davoult, D., Spilmont, N., Menu, D., Boucher, G., Gattuso, J.-P. & Rybarczyk, H. J. M. B. 2002. A closed-chamber CO2-flux method for estimating intertidal primary production and respiration under emersed conditions. 140**,** 865-869.

Migné, A., Spilmont, N. & Davoult, D. 2004. In situ measurements of benthic primary production during emersion: seasonal variations and annual production in the Bay of Somme (eastern English Channel, France). *Continental Shelf Research,* 24**,** 1437-1449.

Migné, A., Trigui, R. J., Davoult, D. & Desroy, N. 2018. Benthic metabolism over the emersion - immersion alternation in sands colonized by the invasive Manila clam Ruditapes philippinarum. *Estuarine, Coastal and Shelf Science,* 200**,** 371-379.

Millennium Ecosystem Assessment 2005. Current state and trends. Washington, DC.

Miller, D. C., Geider, R. J. & Macintyre, H. L. 1996. Microphytobenthos: The ecological role of the "secret garden" of unvegetated, shallow-water marine habitats. II. role in sediment stability and shallow-water food webs. *Estuaries,* 19**,** 202-212.

Mills, D. K. & Wilkinson, M. 1986. Photosynthesis and Light in Estuarine Benthic Microalgae. *Botanica Marina,* 29**,** 125.

Moller, H., Macleod, C. J., Haggerty, J., Rosin, C., Blackwell, G., Perley, C., Meadows, S., Weller, F. & Gradwohl, M. 2008. Intensification of New Zealand agriculture: Implications for biodiversity. *New Zealand Journal of Agricultural Research,* 51**,** 253-263.

Montani, S., Magni, P. & Abe, N. 2003. Seasonal and interannual patterns of intertidal microphytobenthos in combination with laboratory and areal production estimates. *Marine Ecology Progress Series,* 249**,** 79-91.

Morris, L. & Keough, M., J. 2003. Variation in the response of intertidal infaunal invertebrates to nutrient additions: field manipulations at two sites within Port Phillip Bay, Australia. *Marine Ecology Progress Series,* 250**,** 35-49.

Murphy, K. R., Stedmon, C. A., Graeber, D. & Bro, R. 2013. Fluorescence spectroscopy and multi-way techniques. PARAFAC. *Analytical Methods,* 5**,** 6557-6566.

Murray, N. J., Phinn, S. R., Dewitt, M., Ferrari, R., Johnston, R., Lyons, M. B., Clinton, N., Thau, D. & Fuller, R. A. 2019. The global distribution and trajectory of tidal flats. *Nature,* 565**,** 222-225.

National Research Council 2007. Mitigating Shore Erosion along Sheltered Coasts. National Academies Press, Washington, DC, USA.

National Research Council 2012. *Sea-level rise for the coasts of California, Oregon, and Washington: past, present, and future*, National Academies Press.

Nicholls, R. J. & Cazenave, A. 2010. Sea-Level Rise and Its Impact on Coastal Zones. *Science,* 328**,** 1517-1520.

Nielsen, S. L., Sand-Jensen, K., Borum, J. & Geertz-Hansen, O. 2002. Phytoplankton, Nutrients, and Transparency in Danish Coastal Waters. *Estuaries,* 25**,** 930-937.

Nixon, S. W. 1995. Coastal marine eutrophication: A definition, social causes, and future concerns. *Ophelia,* 41**,** 199-219.

Noss, R. F. 2011. Between the devil and the deep blue sea: Florida's unenviable position with respect to sea level rise. *Climatic Change,* 107**,** 1-16.

O'meara, T., Gibbs, E. & Thrush, S. F. 2018. Rapid organic matter assay of organic matter degradation across depth gradients within marine sediments. *Methods in Ecology and Evolution,* 9**,** 245-253.

O'meara, T. A., Hewitt, J. E., Thrush, S. F., Douglas, E. J. & Lohrer, A. M. 2020. Denitrification and the Role of Macrofauna Across Estuarine Gradients in Nutrient and Sediment Loading. *Estuaries and Coasts,* 43**,** 1394–1405.

O'meara, T. A., Hillman, J. R. & Thrush, S. F. 2017. Rising tides, cumulative impacts and cascading changes to estuarine ecosystem functions. *Scientific Reports,* 7**,** 10218.

Oakes, J. M., Eyre, B. D. & Ross, D. J. 2011. Short-Term Enhancement and Long-Term Suppression of Denitrification in Estuarine Sediments Receiving Primary- and Secondary-Treated Paper and Pulp Mill Discharge. *Environmental Science & Technology,* 45**,** 3400-3406.

OECD 2020. Agri-Environmental indicators: Nutrients.

Oliver, E. C. J., Benthuysen, J. A., Bindoff, N. L., Hobday, A. J., Holbrook, N. J., Mundy, C. N. & Perkins-Kirkpatrick, S. E. 2017. The unprecedented 2015/16 Tasman Sea marine heatwave. *Nature Communications,* 8**,** 16101.

Passeri, D. L., Hagen, S. C., Medeiros, S. C., Bilskie, M. V., Alizad, K. & Wang, D. 2015. The dynamic effects of sea level rise on low-gradient coastal landscapes: A review. *Earth's Future,* 3**,** 159-181.

Percuoco, V. P., Kalnejais, L. H. & Officer, L. V. 2015. Nutrient release from the sediments of the Great Bay Estuary, N.H. USA. *Estuarine, Coastal and Shelf Science,* 161**,** 76-87.

Perkins, M. J., Ng, T. P. T., Dudgeon, D., Bonebrake, T. C. & Leung, K. M. Y. 2015. Conserving intertidal habitats: What is the potential of ecological engineering to mitigate impacts of coastal structures? *Estuarine, Coastal and Shelf Science,* 167**,** 504-515.

Perkins, R. G., Underwood, G. J. C., Brotas, V., Snow, G. C., Jesus, B. & Ribeiro, L. 2001. Responses of microphytobenthos to light: primary production and carbohydrate allocation over an emersion period. *Marine Ecology Progress Series,* 223**,** 101-112.

Piehler, M. F. & Smyth, A. R. 2011. Habitat-specific distinctions in estuarine denitrification affect both ecosystem function and services. *Ecosphere,* 2**,** art12.

Pivato, M., Carniello, L., Moro, I. & D'odorico, P. 2019. On the feedback between water turbidity and microphytobenthos growth in shallow tidal environments. *Earth Surface Processes and Landforms* 44**,** 1192-1206.

Pörtner, H.-O., Roberts, D. C., Masson-Delmotte, V., Zhai, P., Tignor, M., Poloczanska, E., Mintenbeck, K., Nicolai, M., Okem, A., Petzold, J., Rama, B. & (Eds.), W. N. 2019. IPCC, 2019: Summary for Policymakers. *IPCC Special Report on the Ocean and Cryosphere in a Changing Climate*

Posey, M. H., Alphin, T. D. & Cahoon, L. 2006. Benthic community responses to nutrient enrichment and predator exclusion: Influence of background nutrient concentrations and interactive effects. *Journal of Experimental Marine Biology and Ecology,* 330**,** 105-118.

Pratt, D. R., Pilditch, C. A., Lohrer, A. M. & Thrush, S. F. 2014. The effects of short-term increases in turbidity on sandflat microphytobenthic productivity and nutrient fluxes. *Journal of Sea Research,* 92**,** 170-177.

Rabalais, N. N., Norse, E. & Crowder, L. 2005. The potential for nutrient overenrichment to diminish marine biodiversity. *Marine conservation biology: the science of maintaining the sea's biodiversity.*: Island Press, Washington, DC.

Rabalais, N. N., Turner, R. E., Díaz, R. J. & Justić, D. 2009. Global change and eutrophication of coastal waters. *ICES Journal of Marine Science,* 66**,** 1528-1537.

Rahmstorf, S. 2007. A Semi-Empirical Approach to Projecting Future Sea-Level Rise. 315**,** 368-370.

Redfield, A. C. 1963. The influence of organisms on the composition of seawater. *The sea,* 2**,** 26-77.

Rice, J., Arvanitidis, C., Borja, A., Frid, C., Hiddink, J. G., Krause, J., Lorance, P., Ragnarsson, S. Á., Sköld, M., Trabucco, B., Enserink, L. & Norkko, A. 2012. Indicators for Sea-floor Integrity under the European Marine Strategy Framework Directive. *Ecological Indicators,* 12**,** 174-184.

Rijstenbil, J. 2003. Effects of UVB radiation and salt stress on growth, pigments and antioxidative defence of the marine diatom Cylindrotheca closterium. *Marine Ecology Progress Series,* 254**,** 37-48.

Risgaard-Petersen, N. 2003. Coupled nitrification-denitrification in autotrophic and heterotrophic estuarine sediments: On the influence of benthic microalgae. *Limnology and Oceanography,* 48**,** 93-105.

Risgaard-Petersen, N., Meyer, R. L., Schmid, M., Jetten, M. S., Enrich-Prast, A., Rysgaard, S. & Revsbech, N. P. 2004a. Anaerobic ammonium oxidation in an estuarine sediment. *Aquatic Microbial Ecology,* 36**,** 293-304.

Risgaard-Petersen, N., Nicolaisen, M. H., Revsbech, N. P. & Lomstein, B. A. 2004b. Competition between Ammonia-Oxidizing Bacteria and Benthic Microalgae. *Applied and Environmental Microbiology,* 70**,** 5528-5537.

Rysgaard, S., Christensen, P. B. & Nielsen, L. P. 1995. Seasonal variation in nitrification and denitrification in estuarine sediment colonized by benthic microalgae and bioturbating infauna. *Marine Ecology Progress Series,* 126**,** 111-121.

Saburova, M., A. & Polikarpov, I., G. 2003. Diatom activity within soft sediments: behavioural and physiological processes. *Marine Ecology Progress Series,* 251**,** 115-126.

Sandwell, D. R., Pilditch, C. A. & Lohrer, A. M. 2009. Density dependent effects of an infaunal suspension-feeding bivalve (Austrovenus stutchburyi) on sandflat nutrient fluxes and microphytobenthic productivity. *Journal of Experimental Marine Biology and Ecology,* 373**,** 16-25.

Santos, I. R., Bryan, K. R., Pilditch, C. A. & Tait, D. R. 2014. Influence of porewater exchange on nutrient dynamics in two New Zealand estuarine intertidal flats. *Marine Chemistry,* 167**,** 57-70.

Scheffer, M. & Carpenter, S. R. 2003. Catastrophic regime shifts in ecosystems: linking theory to observation. *Trends in Ecology & Evolution,* 18**,** 648-656.

Scheffer, M., Carpenter, S. R., Lenton, T. M., Bascompte, J., Brock, W., Dakos, V., Van De Koppel, J., Van De Leemput, I. A., Levin, S. A., Van Nes, E. H., Pascual, M. & Vandermeer, J. 2012. Anticipating Critical Transitions. *Science,* 338**,** 344-348.

Seitzinger, S., Harrison, J. A., Böhlke, J. K., Bouwman, A. F., Lowrance, R., Peterson, B., Tobias, C. & Drecht, G. V. 2006. Denitrification across landscapes and waterscapes: a synthesis. *Ecological Applications,* 16**,** 2064-2090.

Seitzinger, S. P. 1987. Nitrogen biogeochemistry in an unpolluted estuary: the importance of benthic denitrification. *Marine ecology progress series. Oldendorf,* 41**,** 177-186.

Seitzinger, S. P. 1988. Denitrification in freshwater and coastal marine ecosystems: ecological and geochemical significance. *Limnology and oceanography,* 33**,** 702-724.

Selkoe, K. A., Blenckner, T., Caldwell, M. R., Crowder, L. B., Erickson, A. L., Essington, T. E., Estes, J. A., Fujita, R. M., Halpern, B. S., Hunsicker, M. E., Kappel, C. V., Kelly, R. P., Kittinger, J. N., Levin, P. S., Lynham, J. M., Mach, M. E., Martone, R. G., Mease, L. A., Salomon, A. K., Samhouri, J. F., Scarborough, C., Stier, A. C., White, C. & Zedler, J. 2015. Principles for managing marine ecosystems prone to tipping points. *Ecosystem Health and Sustainability,* 1**,** 1-18.

Seneviratne, S. I., Nicholls, N., Easterling, D., Goodess, C. M., Kanae, S., Kossin, J., Luo, Y., Marengo, J., Mcinnes, K., Rahimi, M., Reichstein, M., Sorteberg, A., Vera, C. & Zhang, X. 2012. Changes in climate extremes and their impacts on the natural physical environment. *Managing the Risks of Extreme Events and Disasters to Advance Climate Change Adaptation.* Cambridge University Press, Cambridge, United Kingdom and New York, NY, USA: A Special Report of Working Groups I and II of the Intergovernmental Panel on Climate Change.

Serôdio, J. & Catarino, F. 1999. Fortnightly light and temperature variability in estuarine intertidal sediments and implications for microphytobenthos primary productivity. *Aquatic Ecology,* 33**,** 235-241.

Sierra, M. M. D., Donard, O. F. X., Etcheber, H., Soriano-Sierra, E. J. & Ewald, M. 2001. Fluorescence and DOC contents of pore waters from coastal and deep-sea sediments in the Gulf of Biscay. *Organic Geochemistry,* 32**,** 1319-1328.

Smale, D. A., Wernberg, T. & Vanderklift, M. A. 2017. Regional-scale variability in the response of benthic macroinvertebrate assemblages to a marine heatwave. *Marine Ecology Progress Series,* 568**,** 17-30.

Smith, D. J. & Underwood, G. J. C. 2000. The production of extracellular carbohydrates by estuarine benthic diatoms: the effects of growth phase and light and dark treatment. *Journal of Phycology,* 36**,** 321-333.

Smith, V. H. 2003. Eutrophication of freshwater and coastal marine ecosystems a global problem. *Environmental Science and Pollution Research,* 10**,** 126-139.

Snelgrove, P. V. R., Thrush, S. F., Wall, D. H. & Norkko, A. 2014. Real world biodiversity–ecosystem functioning: a seafloor perspective. *Trends in Ecology & Evolution,* 29**,** 398-405.

Spilmont, N., Davoult, D. & Migné, A. 2006. Benthic primary production during emersion: In situ measurements and potential primary production in the Seine Estuary (English Channel, France). *Marine Pollution Bulletin,* 53**,** 49-55.

Stedmon, C. A. & Bro, R. 2008. Characterizing dissolved organic matter fluorescence with parallel factor analysis: a tutorial. *Limnology and Oceanography: Methods,* 6**,** 572-579.

Stief, P. 2013. Stimulation of microbial nitrogen cycling in aquatic ecosystems by benthic macrofauna: mechanisms and environmental implications. *Biogeosciences,* 10**,** 7829–7846.

Stutes, A. L., Cebrian, J. & Corcoran, A. A. 2006. Effects of nutrient enrichment and shading on sediment primary production and metabolism in eutrophic estuaries. *Marine Ecology Progress Series,* 312**,** 29-43.

Sundbäck, K., Alison, M. & Eva, G. 2000. Nitrogen fluxes, denitrification and the role of microphytobenthos in microtidal shallow-water sediments: an annual study. *Marine Ecology Progress Series,* 200**,** 59-76.

Sundbäck, K., Linares, F., Larson, F., Wulff, A. & Engelsen, A. 2004. Benthic nitrogen fluxes along a depth gradient in a microtidal fjord: The role of denitrification and microphytobenthos. *Limnology and Oceanography,* 49**,** 1095-1107.

Sundbäck, K., Miles, A., Linares, F. & Coasts 2006. Nitrogen dynamics in nontidal littoral sediments: Role of microphytobenthos and denitrification. *Estuaries,* 29**,** 1196-1211.

Swales, A., Williamson, R. B., Van Dam, L. F., Stroud, M. J. & Mcglone, M. S. 2002. Reconstruction of urban stormwater contamination of an estuary using catchment history and sediment profile dating. *Estuaries,* 25**,** 43-56.

Tay, H. W., Bryan, K. R. & Pilditch, C. A. 2013. Dissolved inorganic nitrogen concentrations in an estuarine tidal flat. *Journal of Coastal Research,* 65**,** 135-140.

Teixeira, C., Magalhães, C., Boaventura, R. a. R. & Bordalo, A. A. 2010. Potential rates and environmental controls of denitrification and nitrous oxide production in a temperate urbanized estuary. *Marine Environmental Research,* 70**,** 336-342.

Thomson, J. D., Weiblen, G., Thomson, B. A., Alfaro, S. & Legendre, P. 1996. Untangling Multiple Factors in Spatial Distributions: Lilies, Gophers, and Rocks. *Ecology,* 77**,** 1698-1715.

Thornton, D. C., Dong, L. F., Underwood, G. J. & Nedwell, D. B. 2002. Factors affecting microphytobenthic biomass, species composition and production in the Colne Estuary (UK). *Aquatic Microbial Ecology,* 27**,** 285-300.

Thornton, D. C., Underwood, G. J. & Nedwell, D. B. 1999. Effect of illumination and emersion period on the exchange of ammonium across the estuarine sediment-water interface. *Marine Ecology Progress Series,* 184**,** 11-20.

Thrush, S., Pridmore, R., Hewitt, J. & Cummings, V. 1994. The importance of predators on a sandflat: interplay between seasonal changes in prey densities and predator effects. *Marine Ecology Progress Series,* 107**,** 211-222.

Thrush, S. F., Hewitt, J. E., Cummings, V. J., Ellis, J. I., Hatton, C., Lohrer, A. & Norkko, A. 2004. Muddy Waters: Elevating Sediment Input to Coastal and Estuarine Habitats. *Frontiers in Ecology and the Environment,* 2**,** 299-306.

Thrush, S. F., Hewitt, J. E., Gibbs, M., Lundquist, C. & Norkko, A. 2006. Functional Role of Large Organisms in Intertidal Communities: Community Effects and Ecosystem Function. *Ecosystems,* 9**,** 1029-1040.

Thrush, S. F., Hewitt, J. E., Gladstone-Gallagher, R. V., Savage, C., Lundquist, C., O'meara, T., Vieillard, A., Hillman, J. R., Mangan, S., Douglas, E. J., Clark, D. E., Lohrer, A. M. & Pilditch, C. 2020. Cumulative stressors reduce the self-regulating capacity of coastal ecosystems. *Ecological Applications,* 31**,** e2223.

Thrush, S. F., Hewitt, J. E. & Lohrer, A. M. 2012. Interaction networks in coastal soft-sediments highlight the potential for change in ecological resilience. *Ecological Applications,* 22**,** 1213-1223.

Thrush, S. F., Hewitt, J. E., Parkes, S., Lohrer, A. M., Pilditch, C., Woodin, S. A., Wethey, D. S., Chiantore, M., Asnaghi, V., De Juan, S., Kraan, C., Rodil, I., Savage, C. & Van Colen, C. 2014. Experimenting with ecosystem interaction networks in search of threshold potentials in real-world marine ecosystems. *Ecology,* 95**,** 1451-1457.

Tobias, C., Giblin, A., Mcclelland, J., Tucker, J. & Peterson, B. 2003. Sediment DIN fluxes and preferential recycling of benthic microalgal nitrogen in a shallow macrotidal estuary. *Marine Ecology Progress Series,* 257**,** 25-36.

Todgham, A. E. & Stillman, J. H. 2013. Physiological Responses to Shifts in Multiple Environmental Stressors: Relevance in a Changing World. *Integrative and Comparative Biology,* 53**,** 539-544.

Tolhurst, T. J., Consalvey, M. & Paterson, D. M. 2008. Changes in cohesive sediment properties associated with the growth of a diatom biofilm. *Hydrobiologia,* 596**,** 225-239.

Turner, J., Bindschadler, R., Convey, P., Di Prisco, G., Fahrbach, E., Gutt, J., Hodgson, D., Mayewski, P. & Summerhayes, C. 2009. *Antarctic climate change and the environment*, SCAR, Cambridge.

Underwood, G. J. C. 2001. Microphytobenthos. *In:* Steele, J. H. (ed.) *Encyclopedia of Ocean Sciences (Second Edition).* Oxford: Academic Press.

Underwood, G. J. C. & Kromkamp, J. 1999. Primary Production by Phytoplankton and Microphytobenthos in Estuaries. *Advances in Ecological Research,* 29**,** 93-153.

Underwood, G. J. C. & Paterson, D. M. 2003. The importance of extracellular carbohydrate productionby marine epipelic diatoms. *Advances in Botanical Research.* Academic Press.

Underwood, G. J. C., Perkins, R. G., Consalvey, M. C., Hanlon, A. R. M., Oxborough, K., Baker, N. R. & Paterson, D. M. 2005. Patterns in microphytobenthic primary productivity: Species-specific variation in migratory rhythms and

photosynthetic efficiency in mixed-species biofilms. *Limnology and Oceanography,* 50**,** 755-767.

Vahtera, E., Conley, D. J., Gustafsson, B. G., Kuosa, H., Pitkänen, H., Savchuk, O. P., Tamminen, T., Viitasalo, M., Voss, M., Wasmund, N. & Wulff, F. 2007. Internal ecosystem feedbacks enhance nitrogen-fixing cyanobacteria blooms and complicate management in the Baltic Sea. *Ambio,* 36**,** 186-94.

Valiela, I. & Bowen, J. L. 2002. Nitrogen sources to watersheds and estuaries: role of land cover mosaics and losses within watersheds. *Environmental Pollution,* 118**,** 239-248.

Van Der Wal, D., Herman, P., Forster, R., Ysebaert, T., Rossi, F., Knaeps, E., Plancke, Y. & Ides, S. 2008. Distribution and dynamics of intertidal macrobenthos predicted from remote sensing: response to microphytobenthos and environment. *Marine Ecology Progress Series,* 367**,** 57-72.

Vieillard, A. M., Newell, S. E. & Thrush, S. F. 2020. Recovering From Bias: A Call for Further Study of Underrepresented Tropical and Low-Nutrient Estuaries. *Journal of Geophysical Research: Biogeosciences,* 125**,** e2020JG005766.

Vitousek, P. M., Aber, J. D., Howarth, R. W., Likens, G. E., Matson, P. A., Schindler, D. W., Schlesinger, W. H. & Tilman, D. G. 1997. Human alteration of the global nitrogen cycle: sources and consequences. *Ecological Applications,* 7**,** 737-750.

Volkenborn, N., Hedtkamp, S. I. C., Van Beusekom, J. E. E. & Reise, K. 2007. Effects of bioturbation and bioirrigation by lugworms (Arenicola marina) on physical and chemical sediment properties and implications for intertidal habitat succession. *Estuarine, Coastal and Shelf Science,* 74**,** 331-343.

Volkenborn, N., Meile, C., Polerecky, L., Pilditch, C. A., Norkko, A., Norkko, J., Hewitt, J., Thrush, S., Wethey, D. S. & Woodin, S. 2012. Intermittent bioirrigation and oxygen dynamics in permeable sediments: An experimental and modeling study of three tellinid bivalves. *Journal of Marine Research,* 70**,** 794-823.

Walpersdorf, E., Kühl, M., Elberling, B., Andersen, T., Hansen, B., Pejrup, M. & Glud, R. 2016. In situ oxygen dynamics and carbon turnover in an intertidal sediment (Skallingen, Denmark). *Marine Ecology Progress Series,* 566**,** 49-65.

Welsh, D. T. 2003. It's a dirty job but someone has to do it: The role of marine benthic macrofauna in organic matter turnover and nutrient recycling to the water column. *Chemistry and Ecology,* 19**,** 321-342.

Woodin, S. A., Volkenborn, N., Pilditch, C. A., Lohrer, A. M., Wethey, D. S., Hewitt, J. E. & Thrush, S. F. 2016. Same pattern, different mechanism: Locking onto the role of key species in seafloor ecosystem process. *Scientific Reports,* 6**,** 26678.

Woodin, S. A., Wethey, D. S. & Volkenborn, N. 2010. Infaunal Hydraulic Ecosystem Engineers: Cast of Characters and Impacts. *Integrative and Comparative Biology,* 50**,** 176-187.

Yamochi, S., Tanaka, T., Otani, Y. & Endo, T. 2017. Effects of light, temperature and ground water level on the CO2 flux of the sediment in the high water temperature seasons at the artificial north salt marsh of Osaka Nanko bird sanctuary, Japan. *Ecological Engineering,* 98**,** 330-338.

Yim, J., Kwon, B.-O., Nam, J., Hwang, J. H., Choi, K. & Khim, J. S. 2018. Analysis of forty years long changes in coastal land use and land cover of the Yellow Sea: The gains or losses in ecosystem services. *Environmental Pollution,* 241**,** 74-84.

Appendices

Appendix One: Chapter Two

Table A1.1: Coordinates of sensor deployment locations.

Estuary	Site code	Latitude (decimal)	Longitude (decimal)
Akaroa	AKA	-43.7514	172.9355
Avon-Heathcote	AVO	-43.5508	172.7378
Delaware	DEL	-41.1639	173.4609
Jacobs River	JAC 1	-46.345	167.9914
	JAC 2	-46.3483	167.9999
Mahurangi	MAH 1	-36.4942	174.7375
	MAH 2	-36.4836	174.7131
	MAH 3	-36.4492	174.7306
Manukau	MNK 1	-37.1325	174.6931
	MNK 2	-37.1314	174.6969
New River	NEW	-46.4881	168.3094
Raglan	RAG	-37.8039	174.8672
Tauranga	TAU 1	-37.6486	176.0414
	TAU 2	-37.4914	175.9519
Whangārei	WGR 1	-35.7651	174.3569
	WGR 2	-35.9625	174.5372
Whitianga	WHI 1	-36.8411	175.7117
	WHI 2	-36.8744	175.6936
Waikawa	WKW 1	-46.6256	169.1431
	WKW 2	-46.6253	169.1383
Waimea	WMA	-41.2925	173.185
Whangateau	WTA	-36.3171	174.7697

Table A1.2: Summary of benthic photosynthesis-irradiance curves of unvegetated sediment found within published literature. NS = not specified.

Location	% mud	Method	Light saturation (I_K)	Reference
Subtidal				
Southern Baltic Sea	5-10, 30-90	*In situ* and lab cores, O_2 by titration	300	(Meyercordt & Meyer-Reil, 1999)
Lake Illawarra, Australia	< 25	Lab core, O_2 probe	19, 117	(Qu et al. 2004)
Bodden estuary, South Baltic sea	NS	Lab core O_2 microprofile	10, 22, 32, 54, 86, 106, 116, 152	(Gerbersdorf et al. 2005)
Bay of Brest, France	29	*In situ* benthic chambers, O_2 probe	57, 74, 83	(Longphuirt et al. 2007)
Intertidal: Emersion				
Tagus estuary, Portugal	NS - mudflat	*In situ* ^{14}C radiotracer	750	(Perkins et al. 2001)
Bay of Somme, France	2	*In situ* benthic chambers, CO_2 infrared gas analysis	102, 102, 131, 151, 198, 246, 310	(Migné et al. 2004)
Roscoff Aber Bay, France	NS - fine sand	*In situ* benthic chambers, CO_2 infrared gas analysis	341, 389, 443, 495, 553, 639, 901	(Hubas & Davoult 2006)
Seine estuary, France	15, 50	*In situ* benthic chambers, CO_2 infrared gas analysis	199, 204, 498	(Spilmont et al. 2006)
Eastern English Channel	NS	*In situ* benthic chambers, CO_2 infrared gas analysis	91, 125, 146, 202, 217, 218, 405, 580	(Migné et al. 2007)
Bay of Somme, France	2	*In situ* benthic chambers, CO_2 infrared gas analysis	131, 309, 402, 414	(Spilmont et al. 2007)
Canche estuary, English Channel	88 – 92	*In situ* O_2 microprofile	575	(Denis & Desreumaux, 2009)
Mont Saint-Michel Bay, France	80	*In situ* benthic chamber, CO_2 infrared gas analysis	129, 266, 283, 314, 754	(Migné et al. 2009)
Tachia estuary, Taiwan	9, 28	*In situ* benthic chamber, CO_2 infrared gas analysis	~ 200	(Lee et al. 2011)
Daebu Island, Korea	88	Lab core O_2 microprofile	161, 233, 244, 250, 333	(Kwon et al. 2014)
Daebu Island, Korea	88	Lab core O_2 microprofile	7 – 1666 mean 504	(Kwon et al. 2018)
Intertidal: Immersion and emersion				
Canche estuary, English Channel	NS-sandy	*In situ* O_2 microprofile	315, 427	(Denis et al. 2012)
Skallingen, Denmark	5	*In situ* O_2 microprofile	220	(Walpersdorf et al. 2016)
Rance estuary, France	0	*In situ* benthic chambers: immersion DIC, emersion CO_2 infrared gas analysis	100, 130	(Migné et al. 2018)

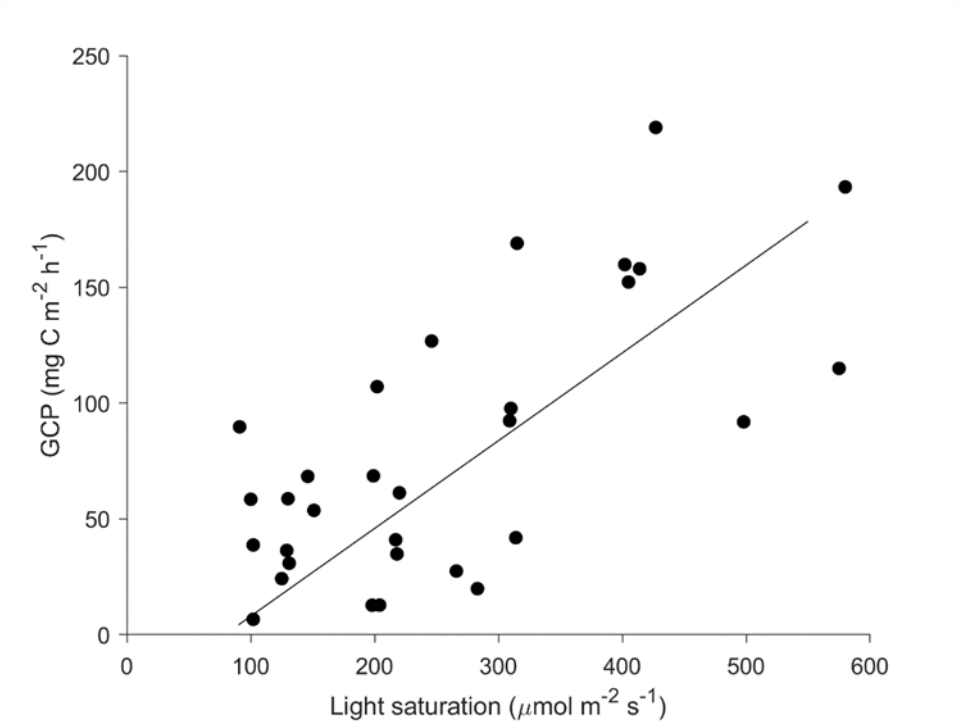

Figure A1.1: Correlation between literature derived intertidal MPB light saturation values and maximum rate of gross community primary production (GCP) (Pearson's r = 0.7, p< 0.001).

Text A1.1. Hypsometry curves

Hypsometry curves are calculated using bathymetric grids and show the total area within each estuary occurring below a given depth relative to mean sea level. Bathymetry data for DEL and WMA were provided by the Sustainable Seas - Forecasting Contamination project (Ben Knight, Cawthron) and for the three Southland estuaries (NEW, JAC, WKW) by Environment Southland (Keryn Roberts). For these five estuaries, a hypsometry curve was constructed by calculating the cumulative distribution of surface area at a given depth. Hypsometry curves from seven of the study estuaries (AVO, MAH, RAG, TAU, WGR, WHI and WTA) were taken directly from Dejeans (2015). MNK (insufficient data) and AKA (low percentage of intertidal area within (3 %)) were omitted from this analysis.

Appendix One References

Dejeans, B. (2015). *Hypsometry of New Zealand estuaries.* (Master of Science (MSc) Masters), University of Waikato, Hamilton, New Zealand. Retrieved from https://hdl.handle.net/10289/10533

Denis, L., & Desreumaux, P.-E. (2009). Short-term variability of intertidal microphytobenthic production using an oxygen microprofiling system. *Marine and Freshwater Research, 60*(7), 712-726. doi:10.1071/mf08070

Denis, L., Gevaert, F., & Spilmont, N. (2012). Microphytobenthic production estimated by in situ oxygen microprofiling: short-term dynamics and carbon budget implications. *Journal of Soils Sediments, 12*(10), 1517-1529. doi:10.1007/s11368-012-0588-8

Gerbersdorf, S. U., Meyercordt, & Meyer-Reil, L.-A. (2005). Microphytobenthic primary production in the Bodden estuaries, southern Baltic Sea, at two study sites differing in trophic status. *Aquatic Microbial Ecology, 41*(2), 181-198.

Hubas, C., & Davoult, D. (2006). Does seasonal proliferation of Enteromorpha sp. affect the annual benthic metabolism of a small macrotidal estuary? (Roscoff Aber Bay, France). *Estuarine, Coastal and Shelf Science, 70*(1), 287-296. doi: 10.1016/j.ecss.2006.06.019

Kwon, B.-O., Kim, H.-C., Koh, C.-H., Ryu, J., Son, S., Kim, Y. H., & Khim, J. S. (2018). Development of temperature-based algorithms for the estimation of microphytobenthic primary production in a tidal flat: A case study in Daebu mudflat, Korea. *Environmental Pollution, 241*, 115-123. doi: 10.1016/j.envpol.2018.05.032

Kwon, B.-O., Koh, C.-H., Khim, J. S., Park, J., Kang, S.-G., & Hwang, J. H. (2014). The Relationship between Primary Production of Microphytobenthos and Tidal Cycle on the Hwaseong Mudflat, West Coast of Korea. *Journal of Coastal Research, 30*(9), 1188-1196.

Lee, L. H., Hsieh, L. Y., & Lin, H. J. (2011). In situ production and respiration of the benthic community during emersion on subtropical intertidal sandflats. *Marine Ecology Progress Series, 441*, 33-47. doi:10.3354/meps09362

Longphuirt, Clavier, J., Grall, J., Chauvaud, L., Le Loc'h, F., Le Berre, I., . . . Leynaert, A. (2007). Primary production and spatial distribution of subtidal microphytobenthos in a temperate coastal system, the Bay of Brest, France. *Estuarine, Coastal and Shelf Science, 74*(3), 367-380. doi: 10.1016/j.ecss.2007.04.025

Meyercordt, J., & Meyer-Reil, L.-A. (1999). Primary production of benthic microalgae in two shallow coastal lagoons of different trophic status in the southern Baltic Sea. *Marine Ecology Progress Series, 178*, 179-191.

Migné, A., Gévaert, F., Créach, A., Spilmont, N., Chevalier, E., & Davoult, D. (2007). Photosynthetic activity of intertidal microphytobenthic communities during emersion: in situ measurements of chlorophyll fluorescence (PAM) and CO2 flux (IRGA)1. *Journal of Phycology, 43*(5), 864-873. doi:10.1111/j.1529-8817.2007.00379.x

Migné, A., Spilmont, N., Boucher, G., Denis, L., Hubas, C., Janquin, M., . . . Davoult, D. (2009). Annual budget of benthic production in Mont Saint-Michel Bay considering cloudiness, microphytobenthos migration, and variability of respiration rates with tidal conditions. *Continental Shelf Research, 29*(19), 2280-2285.

Migné, A., Spilmont, N., & Davoult, D. (2004). In situ measurements of benthic primary production during emersion: seasonal variations and annual production in the Bay of Somme (eastern English Channel, France). *Continental Shelf Research, 24*(13), 1437-1449. doi: 10.1016/j.csr.2004.06.002

Migné, A., Trigui, R. J., Davoult, D., & Desroy, N. (2018). Benthic metabolism over the emersion - immersion alternation in sands colonized by the invasive Manila clam Ruditapes philippinarum. *Estuarine, Coastal and Shelf Science, 200*, 371-379. doi: 10.1016/j.ecss.2017.11.030

Perkins, R. G., Underwood, G. J. C., Brotas, V., Snow, G. C., Jesus, B., & Ribeiro, L. (2001). Responses of microphytobenthos to light: primary production and carbohydrate allocation over an emersion period. *Marine Ecology Progress Series, 223*, 101-112. doi:10.3354/meps223101

Qu, W., Su, C., West, R. J., & Morrison, R. J. (2004). Photosynthetic characteristics of benthic microalgae and seagrass in Lake Illawarra, Australia. *Hydrobiologia, 515*(1), 147-159. doi:10.1023/B:HYDR.0000027326.46856.0a

Spilmont, N., Davoult, D., & Migné, A. (2006). Benthic primary production during emersion: In situ measurements and potential primary production in the Seine Estuary (English Channel, France). *Marine Pollution Bulletin, 53*(1), 49-55. doi: 10.1016/j.marpolbul.2005.09.016

Spilmont, N., Migné, A., Seuront, L., & Davoult, D. (2007). Short-term variability of intertidal benthic community production during emersion and the implication in annual budget calculation. *Marine Ecology Progress Series, 333*, 95-101.

Walpersdorf, E., Kühl, M., Elberling, B., Andersen, T., Hansen, B., Pejrup, M., & Glud, R. (2016). In situ oxygen dynamics and carbon turnover in an intertidal sediment (Skallingen, Denmark). *Marine Ecology Progress Series, 566,* 49-65. doi:10.3354/meps12016

Appendix Two: Chapter Three

Table A2.1: Coordinates of site locations.

Estuary	Site code	Latitude (decimal)	Longitude (decimal)
Manukau	MNK-L	-37.1325	174.6931
	MNK-R	-37.1314	174.6969
Raglan	RAG	-37.8039	174.8672
Tauranga	TAU-T	-37.4914	175.9519
	TAU-O	-37.6486	176.0414
Whangateau	WTA	-36.3171	174.7697

Table A2.2: Summary of sediment properties and univariate macrofaunal community indices as a function of site and nutrient enrichment treatment in November 2017 (T1) and November 2018 (T3). Data are displayed as mean ± SD. * indicates significant difference from control ($p < 0.05$). Differences were tested using ANOVA with treatment as a fixed factor (3 levels) and Tukey post-hoc test, or for data not meeting the assumption of normality, a Kruskal-Wallis test followed by a Dunn post hoc test in R studio.

			Sediment properties			MPB biomass		Porosity		Porewater NH_4^+		Macrofaunal community			
Site	**Time**	**Treat-ment**	**OC**	**Mud**	**MGS**	**Chl *a***	**Phaeo**	**0-2 cm**	**5-7 cm**	**0-2 cm**	**5-7 cm**	**N**	**S**	**AS**	**ML**
		g N m^{-2}	%	%	µm	µg DW g^{-1}	µg DW g^{-1}	%	%	µmol N L^{-1}	µmol N L^{-1}	n $core^{-1}$	n $core^{-1}$	n $core^{-1}$	n $core^{-1}$
MNK-L	T1	0	2.1 ± 0.1	10 ± 1.7	201 ± 8	15 ± 2.6	7.4 ± 1.8	49 ± 1.8	54 ± 6.4	579 ± 273	649 ± 587	222 ± 77	19 ± 3	16 ± 6	15 ± 6
		150	2.2 ± 0.1	10 ± 1.8	202 ± 7	22 ± 2.1	5.3 ± 2.7	51 ± 1.4	48 ± 2.7	1285 ± 642	4238 ± 2639	223 ± 57	20 ± 3	22 ± 7	11 ± 5
		600	2.2 ± 0.1	12 ± 1.9	200 ± 6	13 ± 5.9	14 ± 6.2*	51 ± 3.0	49 ± 7.9	2481 ± 2219	8043 ± 5037	142 ± 49	17 ± 3	19 ± 15	6 ± 4*
	T3	0	3.0 ± 0.2	12 ± 1.6	197 ± 4	15 ± 0.4	11 ± 0.9	44 ± 3.7	45 ± 2.3	40 ± 14	129 ± 9	289 ± 58	22 ± 2	80 ± 20	11 ± 2
		150	3.1 ± 0.2	11 ± 1.3	196 ± 9	17 ± 1.6	12 ± 2.2	51 ± 4.2	50 ± 1.5	671 ± 186	21637 ± 7495	226 ± 22	18 ± 2	91 ± 11	5 ± 3
		600	2.7 ± 0.2	11 ± 0.9	199 ± 7	11 ± 3.3*	12 ± 6.0	57 ± 8.0*	47 ± 12*	5581 ± 2634	51757 ± 9349	104 ± 3*	14 ± 2*	57 ± 2	0 ± 0*
MNK-R	T1	0	1.2 ± 0.1	0.9 ± 0.4	199 ± 2	7.7 ± 2.0	6.0 ± 5.0	55 ± 1.4	66 ± 4.7	576 ± 503	2975 ± 4008	75 ± 9	19 ± 2	3 ± 2	12 ± 4
		150	1.2 ± 0.1	1.4 ± 0.5	198 ± 2	11 ± 2.4	2.7 ± 2.0	48 ± 7.5	65 ± 5.5	977 ± 575	2867 ± 872	74 ± 21	18 ± 3	7 ± 6	15 ± 4
		600	1.2 ± 0.1	1.6 ± 0.8	197 ± 3	11 ± 1.8	3.2 ± 1.7	56 ± 1.9	68 ± 9.0	3893 ± 2405	10662 ± 9897	38 ± 27*	11 ± 3*	4 ± 4	7 ± 6
	T3	0	1.1 ± 0.1	2.3 ± 1.1	200 ± 2	6.0 ± 1.1	4.4 ± 0.8	40 ± 1.2	40 ± 0.5	7.9 ± 4.1	21 ± 10	94 ± 29	22 ± 3	9 ± 2	15 ± 3
		150	1.3 ± 0.2	3.6 ± 1.6	196 ± 3	11 ± 3.0*	6.1 ± 1.1*	42 ± 1.7	39 ± 3.0	35 ± 10	658 ± 595	82 ± 24	17 ± 4	10 ± 1	16 ± 11
		600	1.4 ± 0.3	6.0 ± 3.1	192 ± 7	8.8 ± 1.1	6.5 ± 1.7	42 ± 0.0	39 ± 0.7	19391 ± 7468*	40195 ± 11332*	39 ± 11	11 ± 1*	10 ± 4	4 ± 1
RAG	T1	0	3.8 ± 0.2	16 ± 1.9	130 ± 4	17 ± 4.6	8.7 ± 2.7	53 ± 2.8	52 ± 1.5	45 ± 29	98 ± 33	182 ± 46	21 ± 3	56 ± 18	2 ± 1
		150	3.9 ± 0.2	18 ± 2.6	128 ± 6	19 ± 5.0	7.6 ± 4.4	53 ± 1.7	52 ± 2.6	658 ± 228	7938 ± 3481*	183 ± 26	21 ± 2	56 ± 15	3 ± 2
		600	4.0 ± 0.2	18 ± 1.7	132 ± 4	15 ± 6.5	11 ± 6.1	55 ± 3.5	52 ± 0.7	10029 ± 8245*	49690 ± 20569*	167 ± 27	17 ± 2*	54 ± 10	1 ± 1*
	T3	0	4.2 ± 0.1	24 ± 1.9	118 ± 5	16 ± 2.5	10 ± 1.4	62 ± 2.4	47 ± 6.5	19 ± 7.6	105 ± 21	148 ± 27	17 ± 2	71 ± 6	4 ± 1
		150	4.1 ± 0.1	24 ± 2.5	119 ± 6	17 ± 0.7	9.0 ± 0.6	55 ± 4.7	43 ± 7.9	4975 ± 3963*	9510 ± 1049*	105 ± 31	11 ± 3	60 ± 18	0 ± 1
		600	4.2 ± 0.5	23 ± 3.7	124 ± 8	14 ± 1.4	9.1 ± 0.8	53 ± 3.2	47 ± 4.0	80456 ± 27924*	58705 ± 42316*	140 ± 66	15 ± 5	67 ± 23	3 ± 4

			Sediment properties			MPB biomass		Porosity		Porewater NH_4^+		Macrofaunal community			
Site	**Time**	**Treat-ment**	**OC**	**Mud**	**MGS**	**Chl *a***	**Phaeo**	**0-2 cm**	**5-7 cm**	**0-2 cm**	**5-7 cm**	**N**	**S**	**AS**	**ML**
		g N m^{-2}	%	%	µm	µg DW g^{-1}	µg DW g^{-1}	%	%	µmol N L^{-1}	µmol N L^{-1}	n $core^{-1}$	n $core^{-1}$	n $core^{-1}$	n $core^{-1}$
TAU-O	T1	0	2.6 ± 0.1	14 ± 2.0	157 ± 6	15 ± 0.3	3.2 ± 0.5	47 ± 2.3	47 ± 4.8	9.7 ± 1.5	43 ± 28	74 ± 7	15 ± 2	2 ± 1	6 ± 1
		150	2.7 ± 0.1	13 ± 1.6	168 ± 8	22 ± 4.6*	6.8 ± 1.7*	48 ± 4.9	46 ± 3.7	509 ± 115	4534 ± 349	66 ± 14	15 ± 4	2 ± 1	4 ± 3*
		600	2.5 ± 0.1	11 ± 1.8*	173 ± 15	18 ± 1.4*	4.0 ± 0.5	47 ± 1.7	49 ± 3.3	2570 ± 740*	10090 ± 1312	51 ± 15*	11 ± 1	1 ± 1	0 ± 0*
	T3	0	2.7 ± 0.1	11 ± 1.0	158 ± 5	11 ± 1.1	4.1 ± 0.6	47 ± 0.7	45 ± 9.7	9.0 ± 4.5	16 ± 5.7	36 ± 7	11 ± 1	1 ± 1	5 ± 2
		150	2.9 ± 0.3	12 ± 1.1	158 ± 6	23 ± 2.1*	5.9 ± 1.8	48 ± 0.7	53 ± 2.5	243 ± 26	3950 ± 1766	34 ± 7	9 ± 1	1 ± 1	1 ± 1
		600	2.9 ± 0.0	13 ± 1.0	153 ± 3	12 ± 1.3	5.6 ± 0.5	45 ± 1.8	57 ± 10	8037 ± 4278*	50569 ± 30127*	9 ± 7*	4 ± 2*	0 ± 1	0 ± 0*
TAU-T	T1	0	1.4 ± 0.1	4.4 ± 0.3	200 ± 4	9.9 ± 1.6	2.8 ± 0.9	42 ± 1.8	40 ± 2.3	10 ± 2.3	386 ± 276	105 ± 14	18 ± 3	8 ± 1	5 ± 2
		150	1.3 ± 0.1	4.1 ± 0.8	202 ± 5	9.1 ± 1.5	2.8 ± 0.4	44 ± 2.0	42 ± 2.3	439 ± 150	1276 ± 1057	73 ± 27	15 ± 3	5 ± 3	3 ± 2
		600	1.1 ± 0.1*	3.1 ± 1.0	205 ± 4	6.2 ± 1.3*	1.8 ± 0.3*	43 ± 0.9	40 ± 2.2	3342 ± 2441*	4803 ± 1637*	64 ± 35	14 ± 3	3 ± 2*	1 ± 2*
	T3	0	1.4 ± 0.1	3.1 ± 0.3	201 ± 6	6.6 ± 0.8	2.7 ± 0.4	43 ± 2.1	39 ± 0.9	8.5 ± 2.6	78 ± 70	70 ± 9	15 ± 1	8 ± 1	5 ± 1
		150	1.7 ± 0.2*	2.9 ± 0.4	197 ± 6	11 ± 1.3*	3.8 ± 0.5*	41 ± 1.7	38 ± 2.1	401 ± 247	2013 ± 501	54 ± 7	13 ± 1	4 ± 1*	4 ± 2
		600	1.6 ± 0.1*	3.4 ± 0.5	201 ± 7	8.7 ± 1.4*	3.2 ± 0.3	41 ± 1.9	39 ± 2.8	10304 ± 11237*	8305 ± 1169*	38 ± 12*	9 ± 2*	1 ± 1*	1 ± 1
WTA	T1	0	1.4 ± 0.1	3.4 ± 0.8	255 ± 8	7.7 ± 0.9	2.4 ± 0.9	46 ± 1.2	44 ± 1.2	584 ± 135	496 ± 235	252 ± 55	23 ± 3	52 ± 16	6 ± 2
		150	1.4 ± 0.1	3.6 ± 1.0	248 ± 5	13 ± 1.5*	3.5 ± 0.4	47 ± 1.3	45 ± 2.9	950 ± 82	1358 ± 886	262 ± 44	25 ± 3	37 ± 11	3 ± 1
		600	1.4 ± 0.1	3.5 ± 0.7	252 ± 5	13 ± 2.2*	4.4 ± 0.8*	48 ± 0.8	48 ± 1.2	2608 ± 3459	5048 ± 2621*	166 ± 42*	23 ± 2	23 ± 13*	1 ± 1*
	T3	0	1.4 ± 0.1	2.1 ± 0.4	249 ± 7	6.1 ± 0.8	3.0 ± 0.4	35 ± 2.4	23 ± 11	47 ± 61	20 ± 14	211 ± 42	23 ± 1	37 ± 11	6 ± 1
		150	1.8 ± 0.5*	3.5 ± 1.0*	244 ± 2	13 ± 3.1*	8.6 ± 3.9*	34 ± 3.9	33 ± 1.1	50 ± 45	732 ± 861	268 ± 20	26 ± 1	32 ± 2	1 ± 1*
		600	1.7 ± 0.2*	5.2 ± 1.8*	236 ± 8*	16 ± 6.5*	10 ± 4.1*	40 ± 1.6	33 ± 3.4	1002 ± 700*	11936 ± 16229*	137 ± 34	17 ± 3*	18 ± 6	0 ± 1*

OC = organic content; Mud = mud content; MGS = median grain size; Chl *a* = chlorophyll *a*; DW = dry weight; Phaeo = phaeopigment; 0-2, 5-7 cm = sediment depth; N = total abundance; S = taxa richness; AS = *Austrovenus stutchburyi*; ML = *Macomona liliana*

Table A2.3: Average abundance (n core^{-1}) of taxa as a function of nutrient enrichment treatment in November 2017 (T1; n = 6). Treatments have been abbreviated to C = control, M = medium, H = high.

	MNK-L			MNK-R			RAG			TAU-O			TAU-T			WTA		
	C	**M**	**H**	**C**	**M**	**H**	**C**	**M**	**H**	**C**	**M**	**H**	**C**	**M**	**H**	**C**	**M**	**H**
Anthozoa																		
Anthopleura aureoradiata	8	7	6	1	1	0	9	7	3	1	0	0	0	0	1	38	36	7
Edwardsia	0	0	0	0	0	0	0	0	0	0	0	0	2	0	1	1	3	1
Bivalvia																		
Arthritica bifurca	1	3	1	0	0	0	6	2	1	0	0	0	1	0	1	0	0	0
Austrovenus stutchburyi	16	22	19	3	7	4	56	56	54	2	2	1	8	5	3	52	37	23
Hiatula siliquens	0	0	0	1	1	1	0	0	0	0	0	0	0	0	0	0	0	0
Lasaea parengaensis	0	0	0	0	0	0	0	0	0	4	1	0	6	1	1	6	4	2
Linucula hartvigiana	5	4	2	0	1	0	16	17	12	0	0	0	0	0	0	7	7	4
Macomona liliana	15	11	6	12	15	7	2	3	1	6	4	0	5	3	1	6	3	1
Nucula nitidula	0	0	0	0	0	0	0	0	0	0	0	0	0	0	0	2	2	1
Clitellata																		
Oligochaeta	0	0	0	0	0	0	2	1	0	1	1	0	1	0	1	0	0	1
Gastropoda																		
Cominella glandiformis	2	0	2	0	0	0	1	1	0	0	1	2	0	0	0	0	2	2
Diloma subrostrata	1	1	1	0	0	0	1	1	1	0	1	1	0	0	0	0	0	1
Notoacmea scapha	11	7	8	1	1	0	4	3	1	0	1	0	0	0	0	0	0	0
Pisinna zosterophila	0	0	0	0	0	0	0	0	0	0	0	0	0	0	0	30	40	34
Zeacumantus lutulentus	2	4	5	0	1	1	1	1	1	0	4	4	1	0	0	2	3	2
Zeacumantus subcarinatus	0	0	0	0	0	0	0	0	0	0	0	0	0	0	0	3	6	5
Holothuroidea																		
Taeniogyrus dendyi	0	0	0	2	1	0	0	0	0	0	0	0	0	0	0	3	4	3
Malacostraca																		
Austrominius modestus	20	24	22	2	8	0	12	13	18	0	0	0	0	0	0	0	0	0
Colurostylis lemurum	2	3	3	2	1	2	1	0	0	1	1	0	1	2	4	4	2	2
Exosphaeroma planulum	0	0	1	0	0	0	0	0	0	0	0	0	0	0	0	0	0	0
Exosphaeroma waitemata	0	0	0	0	1	0	0	0	0	0	0	0	0	0	0	2	0	0
Halicarcinus whitei	0	1	1	0	1	0	0	0	0	0	0	0	0	0	0	2	2	1
Hemiplax hirtipes	1	0	0	0	0	0	1	1	1	0	1	1	0	0	0	0	0	0
Isocladus	0	1	1	1	0	0	0	0	0	0	0	0	0	0	0	0	1	1
Lysianassidae	0	0	0	0	0	0	0	0	0	0	0	0	6	1	0	35	35	19

	MNK-L			MNK-R			RAG			TAU-O			TAU-T			WTA		
	C	**M**	**H**	**C**	**M**	**H**	**C**	**M**	**H**	**C**	**M**	**H**	**C**	**M**	**H**	**C**	**M**	**H**
Paracalliope novizealandiae	2	2	0	2	1	0	3	2	3	0	0	0	0	0	1	1	0	0
Paracorophium excavatum	0	0	0	0	0	0	2	1	1	0	0	0	0	0	0	0	0	0
Paramoera chevreuxi	0	0	0	0	0	0	0	0	0	0	0	0	0	0	0	1	1	1
Phoxocephalidae	1	1	0	0	0	0	0	0	0	5	2	0	1	0	0	23	29	17
Protorchestia sp.	0	0	0	0	0	0	0	0	1	0	0	0	1	0	1	0	0	0
Torridoharpinia hurleyi	0	1	1	1	0	0	1	1	2	0	0	0	0	0	0	0	0	0
Nemertea (phylum)	1	0	0	2	2	2	2	2	1	0	1	0	1	2	1	0	0	0
Polychaeta																		
Aonides trifida	110	91	46	12	13	9	0	0	0	6	3	4	22	10	7	1	0	0
Aricidea	0	0	0	6	1	1	0	0	0	0	0	0	0	0	0	0	0	0
Armandia maculata	0	0	0	0	0	0	0	0	1	0	0	0	0	0	0	0	0	0
Boccardia syrtis	1	0	0	2	1	1	1	1	0	0	0	0	0	0	0	0	0	0
Capitella	0	0	0	0	1	0	0	0	0	0	0	0	0	0	0	0	0	0
Ceratonereis	0	0	0	0	0	0	0	0	0	14	13	6	11	13	3	7	8	4
Glycera ovigera	0	0	0	0	0	0	2	1	0	0	0	0	0	0	0	0	0	0
Heteromastus filiformis	8	12	6	4	3	2	9	9	9	5	2	2	4	3	3	3	4	5
Macroclymenella stewartensis	0	0	0	1	1	0	0	0	0	0	0	0	0	0	0	2	1	1
Magelona dakini	1	1	1	15	8	5	0	0	0	0	0	0	0	0	0	0	0	0
Microspio maori	0	0	0	1	0	0	0	0	0	4	3	0	15	7	6	4	3	15
Naineris	0	0	0	0	0	0	0	0	0	0	0	0	0	0	1	0	0	0
Nicon aestuariensis	1	1	1	0	0	0	4	2	1	0	0	0	0	0	0	0	0	0
Orbinia papillosa	0	0	0	1	1	1	0	0	0	0	0	0	1	1	4	0	1	0
Pectinaria australis	0	0	0	0	0	0	0	1	1	0	0	0	0	0	0	0	0	0
Perinereis vallata	1	0	0	0	0	0	0	0	0	1	0	1	2	0	1	0	1	1
Prionospio aucklandica	10	23	8	1	1	1	40	56	53	13	10	12	9	9	8	17	23	14
Scolecolepides benhami	1	1	0	0	1	0	1	1	1	3	2	2	2	2	6	0	0	0
Scoloplos cylindrifer	0	0	0	0	0	0	1	1	0	7	14	14	5	10	11	1	1	0
Sphaerosyllis semiverrucosa	2	1	1	0	0	0	3	2	0	0	0	0	0	0	0	0	0	0
Syllinae	0	0	0	1	0	0	0	0	0	0	0	0	0	0	0	0	0	0

Table A2.4: Average abundance (n core^{-1}) of taxa as a function of nutrient enrichment treatment in November 2018 (T3; n = 3). Treatments have been abbreviated to C = control, M = medium, H = high.

	MNK-L			MNK-R			RAG			TAU-O			TAU-T			WTA		
	C	**M**	**H**	**C**	**M**	**H**	**C**	**M**	**H**	**C**	**M**	**H**	**C**	**M**	**H**	**C**	**M**	**H**
Anthozoa																		
Anthopleura aureoradiata	11	10	6	0	0	0	7	5	4	0	0	0	0	0	0	21	16	1
Bivalvia																		
Arthritica bifurca	6	2	1	0	0	0	4	1	2	0	0	0	0	0	0	0	0	0
Austrovenus stutchburyi	80	91	57	9	10	10	71	60	67	1	1	0	8	4	1	37	32	18
Cyclomactra ovata	0	0	0	1	0	0	0	0	0	0	0	0	0	0	0	0	0	0
Hiatula siliquens	0	0	0	4	1	0	0	0	0	0	0	0	0	0	0	0	0	0
Lasaea parengaensis	0	0	0	0	0	0	0	0	0	2	0	0	6	2	0	9	0	0
Linucula hartvigiana	8	5	1	1	0	0	3	1	6	0	0	0	0	0	0	11	9	1
Macomona liliana	11	5	0	15	16	4	4	0	3	5	1	0	5	4	1	6	1	0
Clitellata																		
Oligochaeta	0	0	0	0	0	0	1	0	0	1	0	0	3	0	0	1	1	0
Gastropoda																		
Cominella glandiformis	0	1	0	0	0	0	0	0	0	0	0	0	0	1	0	0	5	0
Diloma subrostrata	0	1	2	0	0	0	0	0	0	0	0	0	0	0	0	1	0	0
Notoacmea scapha	8	7	7	1	0	1	0	0	2	0	0	0	0	0	0	0	0	0
Zeacumantus lutulentus	3	2	4	1	5	3	1	0	0	0	3	0	0	1	0	14	39	28
Holothuroidea																		
Taeniogyrus dendyi	0	0	0	2	0	0	0	0	0	0	0	0	0	0	0	0	0	0
Malacostraca																		
Austrohelice crassa	0	0	0	0	0	0	0	0	1	0	0	0	0	0	0	0	0	0
Austrominius modestus	29	30	10	4	15	4	3	7	17	0	0	0	0	0	0	2	0	0
Colurostylis lemurum	1	0	0	3	1	2	0	0	0	1	0	0	0	2	1	2	6	8
Exosphaeroma planulum	1	0	0	0	0	0	0	0	0	0	0	0	0	0	0	0	0	0
Exosphaeroma waitemata	1	0	0	2	0	0	0	0	0	0	0	0	0	0	0	0	0	0
Halicarcinus whitei	3	3	0	3	2	1	1	0	0	0	0	0	1	0	0	2	4	0
Hemiplax hirtipes	0	0	0	0	0	0	0	1	0	0	1	0	0	0	0	0	0	0
Isocladus	2	0	0	0	0	0	0	0	0	0	0	0	0	0	0	1	2	0
Lysianassidae	0	0	0	0	0	0	0	0	0	0	0	0	2	0	0	35	20	11
Melita awa	0	0	0	0	0	0	0	0	1	0	0	0	0	0	0	0	0	0
Methalimedon	0	0	0	1	0	0	0	0	0	0	0	0	0	0	0	0	0	0

	MNK-L			MNK-R			RAG			TAU-O			TAU-T			WTA		
	C	**M**	**H**	**C**	**M**	**H**	**C**	**M**	**H**	**C**	**M**	**H**	**C**	**M**	**H**	**C**	**M**	**H**
Mysidae	0	0	0	0	0	0	0	0	0	0	0	0	0	0	0	13	27	3
Paracalliope novizealandiae	3	2	0	3	1	0	2	0	1	0	0	0	0	0	0	3	10	12
Paracorophium excavatum	0	0	0	0	0	0	0	0	1	0	0	0	0	0	0	0	0	0
Paramoera chevreuxi	0	0	0	0	0	0	0	0	0	0	0	0	0	0	0	4	10	0
Philocheras australis	0	0	0	0	0	0	0	0	0	0	0	0	0	0	0	1	0	0
Phoxocephalidae	0	0	0	0	0	0	0	0	0	0	0	0	0	0	0	5	6	0
Protohyate	0	0	0	0	0	0	1	0	0	0	0	0	0	0	0	0	0	0
Torridoharpinia hurleyi	0	0	0	0	0	0	0	1	1	0	0	0	0	0	0	0	2	4
Waitangi brevirostris	0	0	0	1	0	0	0	0	0	0	0	0	0	0	0	0	0	0
Nemertea (phylum)	6	2	1	1	1	1	3	0	2	0	0	0	5	2	0	0	2	0
Polychaeta																		
Aonides trifida	79	25	1	14	10	7	0	0	0	4	0	0	8	6	3	2	0	0
Aricidea	0	0	0	8	2	0	0	0	0	0	0	0	0	0	0	0	0	0
Boccardia syrtis	0	0	0	1	0	0	1	0	0	0	0	0	0	0	0	0	1	2
Capitella	0	0	0	0	0	0	0	0	0	0	0	0	1	0	0	1	1	5
Ceratonereis	0	0	7	0	0	0	0	0	0	9	6	0	6	3	1	0	11	5
Glycera ovigera	1	0	0	0	0	0	1	0	1	0	0	0	0	0	0	0	0	0
Heteromastus filiformis	5	4	1	2	2	0	6	0	2	1	0	0	2	1	1	4	4	0
Macroclymenella stewartensis	3	4	0	2	0	0	0	0	0	0	0	0	0	0	0	0	0	0
Magelona dakini	0	0	0	8	4	0	0	0	0	0	0	0	0	0	0	0	0	0
Microspio maori	0	0	0	0	0	0	0	0	0	2	0	0	3	1	1	25	19	11
Nicon aestuariensis	0	0	0	0	0	0	2	0	1	0	1	0	0	0	0	2	2	0
Orbinia papillosa	0	0	0	1	1	0	0	0	0	0	0	0	2	1	3	0	0	0
Owenia petersenae	0	0	0	0	0	0	1	0	0	0	0	0	0	0	0	0	0	0
Paradoneis lyra	0	0	0	2	1	0	0	0	0	0	0	0	0	0	0	0	0	0
Pectinaria australis	0	0	0	0	0	0	0	0	1	0	0	0	0	0	0	0	0	0
Perinereis vallata	0	0	0	0	0	0	0	1	0	2	0	0	1	0	1	0	3	3
Prionospio aucklandica	21	30	5	2	7	2	33	26	26	1	0	0	6	8	6	3	15	7
Scolecolepides benhami	0	1	0	0	1	0	1	1	1	0	1	0	1	1	0	0	0	0
Scoloplos cylindrifer	0	0	0	0	0	0	0	0	1	6	17	6	10	17	18	2	16	15
Sphaerosyllis semiverrucosa	2	1	0	0	0	0	2	0	1	0	0	0	0	0	0	0	0	0

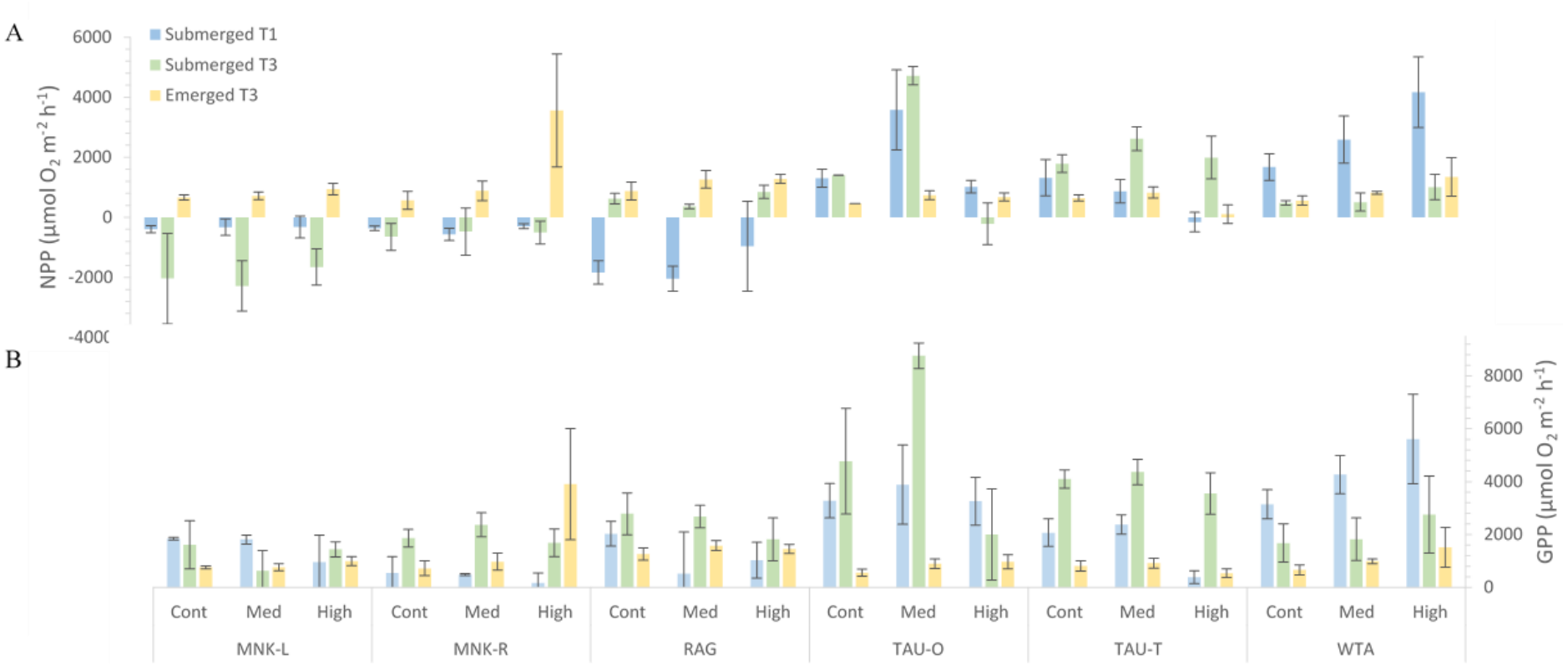

Figure A2.1: Primary production measures A) NPP and B) GPP as a function of site, nutrient enrichment treatment, tidal state and time.

Table A2.5: A repeated measures PERMANOVA using Euclidean distance was used to detect treatment effects on submerged and emerged primary production estimates. The analysis had treatment (3 levels), site (6 levels) and time (2 levels; sub T1 and T3; em T2 and T3) as fixed factors and replicate plot nested within treatment. Significant effects (p<0.05) are given in bold. Main effects were not considered if interaction effects were significant and post hoc pairwise tests were undertaken to identify where differences occurred. For interaction terms Monte-Carlo P-values were used owing to the small number of possible permutations. Site names have been further abbreviated to: M = MNK-L, N = MNK-R, R = RAG, O = TAU-O, T = TAU-T, W = WTA, and control, medium and high nutrient enrichment to c, m and h, respectively.

	Term	df	Pseudo-F	p (perm)	Post-hoc pairwise tests		
					Treatment	Site	Time
Submerged							
NPP	Site	5	45.28	**0.001**			
	Treatment	2	5.63	0.059			
	Time	1	0.01	0.923			
	Site x Treatment	10	6.83	**0.001**	**M, N, R, T,** c=m=h **O,** m≠(c=h) **W,** m=(c≠h)	**c,** M=N,M=R,M=O,M=T,M=W,N=R,N<O, N<T,N<W,R=O,R=T,R=W,O=T,O=W,T=W **m,** M<N,M=R,M<O,M<T,M<W,N=R,N<O, N=T,N=W,R<O,R<T,R<W,O=T,O=W,T=W **h,** M=N,M=R,M=O,M=T,M<W,N=R,N=O, N=T,N<W,R=O,R=T,R<W,O=T,O=W,T=W	
	Site x Time	5	20.68	**0.001**		**T1,** M=N,M>R,M<O,M<T,M<W,N>R,N<O, N<T,N<W,R<O,R<T,R<W,O>T,O=W,T<W **T3,** M<N,M<R,M<O,M<T,M<W,N<R,N<O, N<T,N<W,R<O,R<T,R=W,O=T,O>W,T>W	**M, W,** T1>T3 **N, O,** T1=T3 **R, T,** T1<T3
	Treatment x Time	2	0.54	0.596			
	Site x Treatment x Time	10	1.36	0.229			
GPP	Site	5	20.24	**0.001**			
	Treatment	2	3.38	0.060			
	Time	1	20.78	**0.007**			
	Site x Treatment	10	4.01	**0.002**	**M, N, R,** c=m=h **O, T,** c=(m≠h) **W,** m=(c≠h)	**c,** M=N,M=R,M=O,M=T,M=W,N=R,N=O, N<T,N=W,R=O,R=T,R=W,O=T,O=W,T=W **m,** M=N,M=R,M<O,M<T,M<W,N=R,N<O, N<T,N<W,R<O,R=T,R=W,O>T,O>W,T=W **h,** M=N,M=R,M=O,M=T,M=W,N=R,N=O,	

						N=T,N<W,R=O,R=T,R<W,O=T,O=W,T=W	
	Site x Time	5	6.95	**0.001**		**T1,** M>N,M=R,M<O,M=T,M<W,N=R,N<O, N<T,N<W,R<O,R=T,R<W,O>T,O=W,T<W	**M, R, O,** T1=T3 **N, T,** T1<T3 **W,** T1>T3
						T3, M=N,M=R,M<0,M<T,M=W,N=R,N<O, N<T,N=W,R<O,R<T,R=W,O=T,O>W,T>W	
	Treatment x Time	2	3.23	0.127			
	Site x Treatment x Time	10	1.68	0.139			
Emerged							
NPP	Site	5	5.04	**0.002**			
	Treatment	2	3.55	0.110			
	Time	1	4.84	0.076			
	Site x Treatment	10	2.88	**0.016**	**M,N,R,O,T,W,** c=m=h	**c,** R=O,R≠T,R=M,R≠N,R=W,O=T,O=M,O=N, O=W,T=M,T=N,T=W,M=N,M=W,N=W **m,** R=O,R≠T,R=M,R=N,R=W,O=T,O=M,O=N, O=W,T=M,T=N,T=W,M=N,M=W,N=W **h,** R=O,R≠T,R=M,R=N,R=W,O=T,O=M,O=N, O=W,T=M,T=N,T=W,M=N,M=W,N=W	
	Site x Time	2	1.15	0.342			
	Treatment x Time	2	1.84	0.231			
	Site x Treatment x Time	4	1.35	0.307			
GPP	Site	5	5.93	**0.001**			
	Treatment	2	2.56	0.179			
	Time	1	7.27	**0.033**			
	Site x Treatment	10	2.53	**0.020**	**M,N,R,O,T,W,** c=m=h	**c,** R≠O,R≠T,R=M,R≠N,R=W,M=N=O=T=W **m,** R≠O,R=T,R≠M,R=N,R=W, M=N=O=T=W **h,** R=O,R≠T,R=M,R=N,R=W, M=N=O=T=W	
	Site x Time	2	4.06	**0.048**		**T2,** R≠(O=T) **T3,** R≠O,R≠T,R≠M,R=N,R=W, M=N=O=T=W	**R,** T2≠T3 **O, T,** T2=T3
	Treatment x Time	2	0.70	0.496			
	Site x Treatment x Time	4	1.44	0.272			

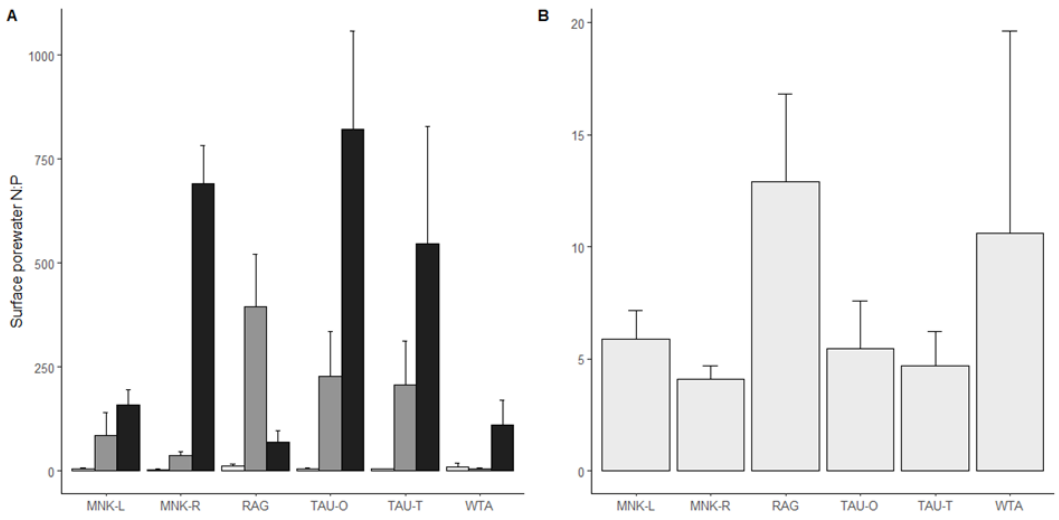

Figure A2.2: Surface (0–2 cm) porewater N:P ratios within A) all sediment nutrient enrichment treatments (control = light grey, medium = dark grey, high = black) and B) within control plots as a function of site (n = 6–9). Data are pooled across all sampling dates and standard error bars displayed.

Appendix Three: Chapter Four

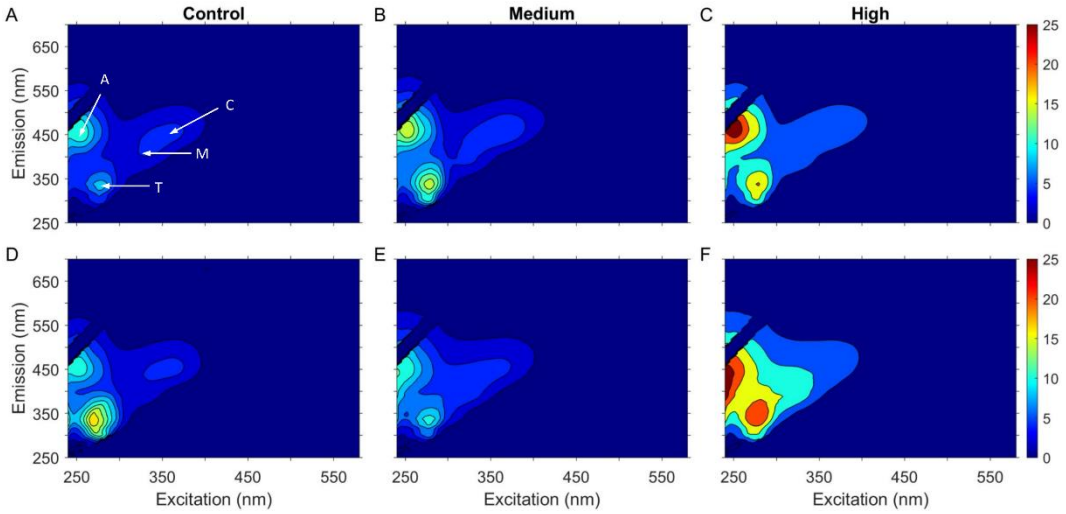

Figure A3.1: 3D excitation-emission matrices (EEM) of porewater DOM at 0 – 2 cm (top row; A, B, C) and 5 – 7 cm sediment depth as a function of nutrient enrichment treatment (A and D = control; B and E = medium; C and F = high). Each EEMs plot represents an average of 3 replicates at 6 sites (n = 18) during the summer sampling period. Peak features have been added to panel A for reference, as described by Coble (2007).

Table A3.1: 3D EEMs fluorescence peaks as described by Coble (2007).

Component	Peak name	Excitation/emission (nm)	Source
Humic-like	A	260 / 400–460	Terrestrial, allochthonous. Bulk of DOM export.
Humic-like	C	320–360 / 420–460	Terrestrial, agriculture.
Marine humic-like	M	290–310 / 370–410	Anthropogenic wastewater and agriculture, marine.
Protein-like (tryptophan)	T	275 / 340	Autochthonous.

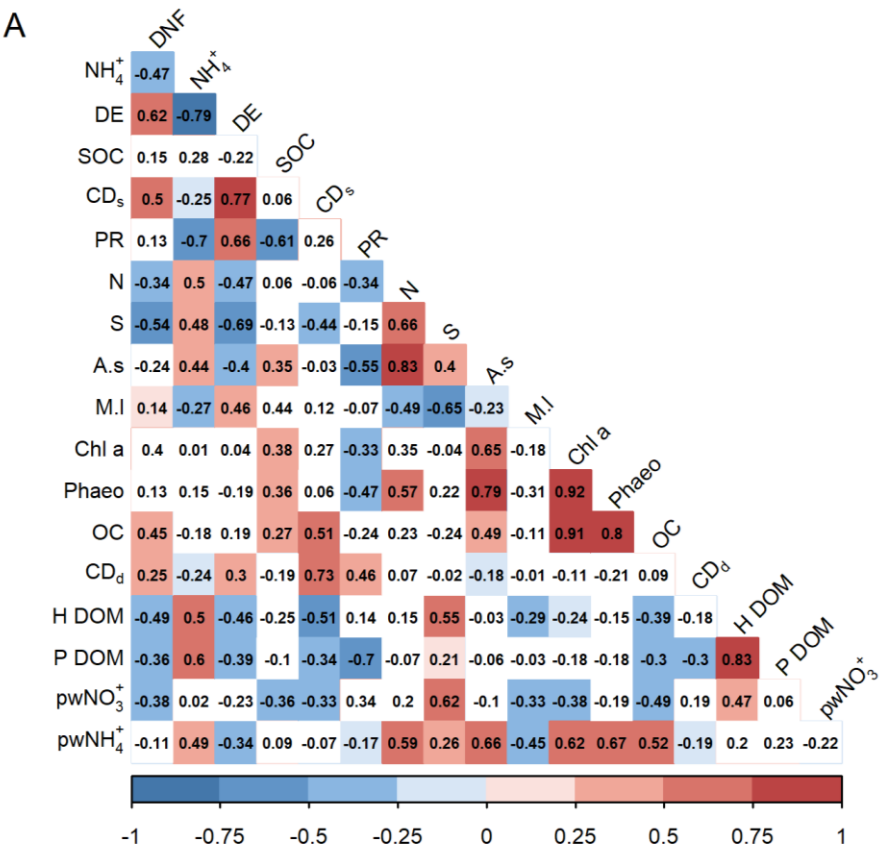
A
DNF
NH_4^+
DE
SOC
CD_s
PR
N
S
A.s
M.I
Chl a
Phaeo
OC
CD_d
H DOM
P DOM
$pwNO_3^-$
$pwNH_4^+$
-1
-0.75
-0.5
-0.25
0
0.25
0.5
0.75
1

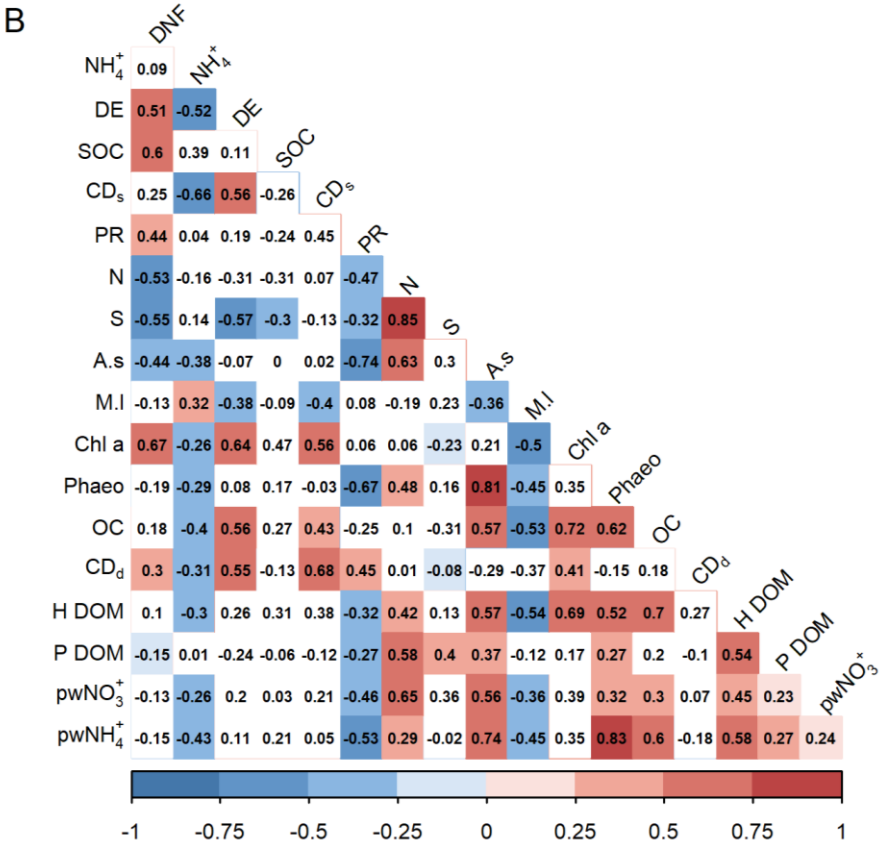
B
DNF
NH_4^+
DE
SOC
CD_s
PR
N
S
A.s
M.I
Chl a
Phaeo
OC
CD_d
H DOM
P DOM
$pwNO_3^-$
$pwNH_4^+$
-1
-0.75
-0.5
-0.25
0
0.25
0.5
0.75
1

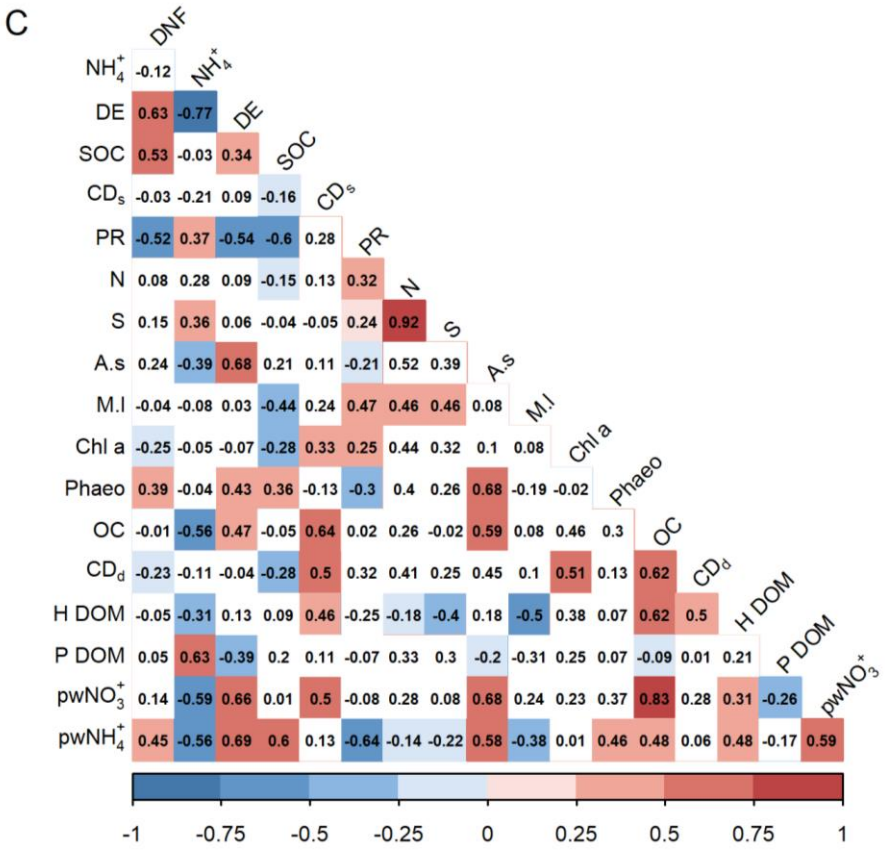

Figure A3.2: Pearson's correlation coefficients between summer N and C cycling parameters, environmental variables and univariate indices of macrofaunal communities under A) no (control), B) medium and C) high nutrient enrichment (n = 18). Correlations with *p*-values < 0.05 are coloured in shades of blue for negative and red for positive correlations. Parameters are ordered as N cycling, C cycling, univariate macrofaunal indices, environmental variables and porewater concentrations. DNF = net denitrification rate; NH_4^+ = NH_4^+ efflux; DE = denitrification efficiency; SOC = sediment oxygen consumption; CD_S = carbon degradation rate at the sediment surface; PR = photosynthesis respiration ratio; N = total abundance; S = species richness; A .s = adult *Austrovenus stutchburyi*; M.l = adult *Macomona liliana*; Chl a = sediment chlorophyll *a*; Phaeo = phaeopigment content; OC = sediment organic content; CD_D = carbon degradation rate at 5 – 7 cm; H DOM = humic-like fluorescence; P DOM = protein-like fluorescence; pw NO_3^- = porewater nitrate concentration; pw NH_4^+ = porewater ammonium concentration. Both fluorescence intensities and porewater concentrations are an averaged of data collected at 0 – 2 cm and 5 – 7 cm sediment depth.

Appendix Three References

Coble, P. G. 2007. Marine Optical Biogeochemistry: The Chemistry of Ocean Color. *Chemical Reviews*, 107, 402-418.